

UNIVERSITY OF CALIFORNIA
SANTA BARBARA

The Analysis of Distributed Spatially Periodic Systems

A Dissertation submitted in partial satisfaction
of the requirements for the degree of

Doctor of Philosophy

in

Mechanical Engineering

by

Makan Fardad

Committee in charge:

Professor Bassam Bamieh, Chairperson

Professor Mihai Putinar

Professor Igor Mezić

Professor Mustafa Khammash

June 2006

The dissertation of Makan Fardad is approved:

Professor Mihai Putinar

Professor Igor Mezić

Professor Mustafa Khammash

Professor Bassam Bamieh, Committee Chairperson

May 2006

The Analysis of Distributed Spatially Periodic Systems

Copyright © 2006

by

Makan Fardad

To Anya, of course

Acknowledgments

I would like to begin by expressing my sincere debt of gratitude to my advisor Professor Bassam Bamieh for providing a fertile academic environment and giving me the freedom to pursue my research interests. Bassam's insightful and thought-provoking questions and comments always indirectly pointed me in the right direction. Above all, I would like to thank Bassam for his infinite patience and flexibility.

My warmest appreciation goes to Professor Mihai Putinar. Mihai always treated me like his own student and gave me endless hours of his time. I always found his mind-boggling knowledge of mathematics absolutely fascinating and a true source of inspiration. My gratitude extends to the other members of my dissertation committee Professor Igor Mezić and Professor Mustafa Khammash, and to Professor Munther Dahleh for kindly arranging for my stay at MIT.

I would like to use this opportunity to acknowledge Professor Mohammad-Ali Massoumnia who first introduced me to the field of controls and inspired me to pursue my graduate studies in this area.

During my years at UCSB, I have had the amazing fortune of having some of the best friends a guy could ask for. First and foremost, I would like to express my deep gratitude to Mihailo Jovanović for his friendship and encouragement, particularly during the last year of my studies. To my dear friends Mike Grebeck, Hana El-Samad, Umesh Vaidya, Symeon Grivopoulos, Maria Napoli, Vasu Salapaka, Ove Storset, George Mathew, Aruna Ranaweera, Thomas John, Zoran Levnjajić, Yonggang Xu, Niklas Karlsson, I will never forget our coffee breaks, walks to the UCen, lunch hours, studying on the office couch, office socials and birthday celebrations, parties and conference trips, and endless discussions and debates about everything and nothing. It has been a privilege knowing each and every one of you.

I would also like to thank my dear friend Payam Naghshtabrizi whom I have come to know as a brother. I will definitely miss our workout sessions in the RecCen, which somehow always ended up being more about rants and jokes than actually getting a sweat going.

Of course, my deepest appreciation goes to my parents and my sister Shima for their unconditional love and support. Unfortunately, with the political situation between Iran and the United States being the way it has been and reentry to the

US having no guarantee, I never got the chance to visit them in all these years.

My stay at UCSB has been a truly fruitful one, but (by many orders-of-magnitude) more because it brought my wife Anya and I together than for any other reason. There is no doubt in my mind that my stay here would have taken a completely different route had I not met Anya and not had her love, devotion, and encouragement with me at all times. And of course, she patiently put up with my rants on PDEs, spatial periodicity, and bi-infinite matrices. But then again, I too got my fair share of her heavy tails, financial risks, and operational losses.

Curriculum Vitae of Makan Fardad

Education

PhD in Mechanical Engineering. University of California at Santa Barbara, June 2006.

MS in Electrical Engineering. Iran University of Science and Technology, Iran, September 2000.

BS in Electrical Engineering. Sharif University of Technology, Iran, September 1998.

Experience

Graduate Researcher. University of California at Santa Barbara, September 2000 – June 2006.

Teaching and Lab Assistant. University of California at Santa Barbara, September 2000 – June 2003.

Graduate Researcher. Iran University of Science and Technology, September 1998 – September 2000.

Awards, Honors, and Recognitions

BEST SESSION PRESENTATION AWARD, American Control Conference, Portland, 2005.

PRESIDENT'S WORK-STUDY AWARD, University of California at Santa Barbara, 2003, 2004, 2005, 2006.

RANKED 1ST IN ELECTRICAL ENGINEERING GRADUATE PROGRAM, Iran University of Science and Technology, Spring 2000.

RANKED TOP 5% OF NATIONAL GRADUATE PROGRAM ENTRANCE EXAM, Iran, 1998.

RANKED TOP 1% OF NATIONAL UNDERGRADUATE ENTRANCE EXAM, Iran, 1994.

SELECTED FOR NATIONAL MATHEMATICS OLYMPIAD, Iran, 1993.

Selected Publications

Work in Progress

1. M. FARDAD, M. R. JOVANOVIĆ & B. BAMIEH, *Frequency Analysis and Norms of Distributed Spatially Periodic Systems*, submitted to IEEE Transactions on Automatic Control, 2005.
2. M. FARDAD & B. BAMIEH, *Perturbation Methods in Stability and Norm Analysis of Spatially Periodic Systems*, submitted to SIAM Journal on Control and Optimization, 2006.
3. M. FARDAD & B. BAMIEH, *The Nyquist Stability Criterion For A Class Of Spatially Periodic Systems*, submitted to Systems and Control Letters, 2006.
4. M. FARDAD & B. BAMIEH, *An Extension of the Argument Principle and Nyquist Criterion to Systems with Unbounded Generators*, submitted to IEEE Transactions on Automatic Control, 2006.
5. M. FARDAD & B. BAMIEH, *On Stability and the Spectrum Determined Growth Condition for Spatially Periodic Systems*, submitted to 45th IEEE Conference on Decision and Control, 2006.

Refereed Proceedings

1. M. FARDAD & B. BAMIEH, *The Nyquist Stability Criterion for a Class of Spatially Periodic Systems*, in Proceedings of the 44th IEEE Conference on Decision and Control, pp. 5275-5280, 2005.
2. M. FARDAD & B. BAMIEH, *A Perturbation Approach to the H^2 Analysis of Spatially Periodic Systems*, in Proceedings of the 2005 American Control Conference, pp. 4838-4843, 2005.
3. M. FARDAD & B. BAMIEH, *A Perturbation Analysis of Parametric Resonance and Periodic Control in Spatially Distributed Systems*, in Proceedings of the 43rd IEEE Conference on Decision and Control, pp. 3786-3791, 2004.
4. M. FARDAD & B. BAMIEH, *A Frequency Domain Analysis and Synthesis of the Passivity of Sampled-Data Systems*, in Proceedings of the 43rd IEEE Conference on Decision and Control, pp. 2358-2363, 2004.
5. B. BAMIEH, I. MEZIĆ & M. FARDAD, *A Framework for Destabilization of Dynamical Systems and Mixing Enhancement*, in Proceedings of the 40th IEEE Conference on Decision and Control, pp. 4980-4983, 2001.

Abstract

The Analysis of Distributed Spatially Periodic Systems

by

Makan Fardad

Spatially periodic systems are of interest in problems of science and engineering and are typically described by partial (integro) differential equations with periodic coefficients. In this work we present tools for the analysis of such systems in the spatial-frequency domain.

In Part I of this dissertation, we describe the basic theory of spatially periodic systems. We use the frequency lifting operation to represent a spatially periodic system as a family of infinitely-many coupled first-order ordinary differential equations. We describe the notions of stability and input-output norms for these systems, and give nonconservative results both for determining stability using the Nyquist criterion and for evaluating system norms.

In Part II of this dissertation, we use perturbation methods to analyze the properties of spatially periodic systems. It is often physically meaningful to regard a spatially periodic system as a spatially invariant one perturbed by spatially periodic operators. We show that this approach leads to a significant reduction in the computational burden of verifying stability and estimating norms.

Although perturbation methods are valid for small ranges of the perturbation parameter and may give conservative results, they can be very beneficial in revealing important trends in system behavior, identifying resonance conditions, and providing guidelines for the design of periodic structures.

Contents

Acknowledgments	v
Curriculum Vitae	vii
Abstract	ix
Contents	x
List of Figures	xiii
Glossary of Symbols	xv
1 Introduction	1
1.1 General Introduction	1
1.2 Contributions of Thesis	3
1.3 Organization of Thesis	6
I Basic Theory of Distributed Spatially Periodic Systems	8
2 Preliminaries: Representation of Spatially Periodic Functions, Operators, and Systems	9
2.1 Introduction	9
2.2 Terminology	9
2.3 Notation	10
2.4 Definitions	11
2.4.1 Spatial Functions	11
2.4.2 Spatial Operators and Spatial Systems	12
2.4.3 Stochastic Processes and Random Fields	12
2.5 Frequency Representation of Periodic Operators	13
2.5.1 Spatially Periodic Operators	13
2.5.2 Spectral-Correlation Density Operators	19

2.6	Representations of Spatially Periodic Systems	22
2.7	Appendix to Chapter 2	27
3	Norms of Spatially Periodic Systems	28
3.1	Introduction	28
3.2	Deterministic Interpretation of the \mathcal{H}^2 -Norm	29
3.2.1	Spatially Periodic Operators	29
3.2.2	Linear Spatially Periodic Systems	30
3.3	Stochastic Interpretation of the \mathcal{H}^2 -Norm	31
3.3.1	Spatially Periodic Operators	31
3.3.2	Linear Spatially Periodic Systems	32
3.4	The \mathcal{H}^∞ -Norm	34
3.4.1	Spatially Periodic Operators	34
3.4.2	Linear Spatially Periodic Systems	35
3.5	Numerical Implementation and Finite Dimensional Truncations	35
3.5.1	\mathcal{H}^∞ -norm	37
3.5.2	\mathcal{H}^2 -norm	38
3.6	Examples	40
3.7	Appendix to Chapter 3	43
4	Stability of Spatially Periodic Systems and the Nyquist Criterion	53
4.1	Introduction	53
4.2	Stability Conditions and Spectrum of the Infinitesimal Generator	53
4.3	Nyquist Stability Problem Formulation	55
4.4	The Nyquist Stability Criterion for Spatially Periodic Systems	57
4.4.1	The Determinant Method	57
4.4.2	The Eigenloci Method	59
4.5	Numerical Implementation	61
4.5.1	Finite Truncations of System Operators	61
4.5.2	Regularity in the θ Parameter	62
4.6	An Illustrative Example	62
4.7	Appendix to Chapter 4	65
4.8	Summary	67

II Perturbation Methods in the Analysis of Spatially Periodic Systems 68

5	Perturbation Analysis of the \mathcal{H}^2 Norm of Spatially Periodic Systems	69
5.1	Introduction	69
5.2	The Perturbation Setup	70

5.3	Perturbation Analysis of the \mathcal{H}^2 -Norm	71
5.4	Examples	75
5.5	Appendix to Chapter 5	80
5.6	Summary	81
6	Stability and the Spectrum Determined Growth Condition for Spatially Periodic Systems	82
6.1	Introduction	82
6.2	Spectrum of Spatially Invariant Operators	83
6.3	Sectorial Operators	83
6.4	Conditions for Infinitesimal Generator to be Sectorial	85
6.5	Conditions for Infinitesimal Generator to have Spectrum in \mathbb{C}^-	87
6.6	Appendix to Chapter 6	90
6.7	Summary	92
7	Conclusions and Future Directions	94
	Bibliography	95

List of Figures

2.1	For $d = 2$, $X = [x_1 x_2]$ where x_1 and x_2 are the dashed 2×1 vectors shown above. In this picture, $x = Xm + \varphi$ where $m = [2 \ 1]^*$ and $\varphi \in \Phi$	11
2.2	Left: The frequency kernel representation of a general spatial operator G for $d = 1$. Right: The frequency kernel representation of a spatially periodic operator G for $d = 1$	14
2.3	The action of the kernel function of a periodic operator for $d = 1$.	16
2.4	Graphical interpretation of \mathcal{G}_θ for $d = 1$ and $\theta \in [0, \Omega)$. Note that θ need only change in $[0, \Omega)$ to fully capture \hat{G}	18
2.5	Graphical interpretation of $\hat{Q}^u(\varkappa, \mu)$ for $d = 1$	21
2.6	Composition of spatially periodic operators in the frequency domain for $d = 1$	21
2.7	Relationship between different representations of the spatio-temporal system G . \mathcal{F}_x is the spatial Fourier transform, and \mathcal{F}_t the temporal Fourier transform. \mathcal{M}_θ is the frequency lifting operator.	24
2.8	Left: A spatially periodic system, as the closed-loop interconnection of a spatially invariant system G° and a spatially periodic operator F . Right: A spatially periodic system can be written as the LFT of a system G° with spatially invariant dynamics and a spatially periodic operator F	25
3.1	Left: All impulses occur at points that are distance Xm apart, $m \in \mathbb{Z}^2$. Right: Spatial impulses applied at different points inside of a primitive cell Φ in \mathbb{R}^2	29
3.2	If a spatially periodic system G is given a stationary input u , the output y is cyclostationary.	32
3.3	The \mathcal{H}^2 -norm of the system (3.10) as a function of amplitude and frequency of the spatially periodic term for $c = 0.1$	41
3.4	The \mathcal{H}^2 -norm of the system (3.10) as a function of amplitude and frequency of the spatially periodic term for $c = -0.1$	41

4.1	Left: The spatially periodic closed-loop system as the feedback interconnection of a spatially invariant system G and a spatially periodic multiplication operator F . Right: The closed-loop system \mathbf{S}^{cl} in the standard form for Nyquist stability analysis.	55
4.2	The closed-loop system $\mathbf{S}_\theta^{\text{cl}}$	56
4.3	The closed contour \mathfrak{D}^θ traversed in the clockwise direction taken as the Nyquist path as $r \rightarrow \infty$. The indentations are arbitrarily made to avoid the eigenvalues of \mathcal{A}_θ (i.e., open-loop modes) on the imaginary axis.	58
4.4	Top: The Nyquist path \mathfrak{D}^0 ; The Nyquist plot for $\theta = 0$. Center: Blown-up version of the center part of the Nyquist plot for $\theta = 0$. Bottom: The Nyquist path $\mathfrak{D}^{0.5}$; The Nyquist plot for $\theta = 0.5$	64
5.1	G° has a spatially invariant infinitesimal generator A° . The LFT of G° and the spatially periodic multiplication operator ϵF yields a system which has a spatially periodic infinitesimal generator A	71
5.2	Above: Plot of $P_0(\cdot)$. Below: Plot of $P_0(\cdot - \Omega)$ and $P_0(\cdot + \Omega)$ (dashed).	76
5.3	Left: Plots of Example 4 for $\varkappa = 1$ and $c = 0.1$. Notice that the first graph is plotted against k and the second against Ω . Right: The plot of \mathcal{H}^2 -norm of the same example, but calculated by taking large truncations of the $\mathcal{A}_\theta, \mathcal{B}_\theta, \mathcal{C}_\theta$ matrices and using Theorem 3.	77
5.4	The plot of Example 4 with $\varkappa = 1$ and $c = 0.1$ and a purely imaginary perturbation.	78
5.5	Plot of Example 5 for $\varkappa = 1$ and $c = 0.1$	79
5.6	Graphs of Example 6 for $R = 6$ and $c = 1$	79
6.1	Top: Representation of the symbol $A_0(\cdot)$ of Example 7 in ‘complex-plane \times spatial-frequency’ space. Center: $\Sigma(A)$ in the complex plane. Bottom: For spatially invariant A , the (diagonal) elements of \mathcal{A}_θ are samples of the Fourier symbol $A_0(\cdot)$	84
6.2	Top: The \mathfrak{B}_{θ_n} regions viewed in the ‘complex-plane \times spatial-frequency’ space (the disks are parallel to the complex plane). Center: $\Sigma(\mathcal{A}_\theta)$ is contained inside the union of the regions \mathfrak{B}_{θ_n} . Bottom: The bold line shows $\Sigma(A^\circ)$ and the dotted region contains $\Sigma(A)$, $A = A^\circ + \epsilon E$	89

Glossary of Symbols

x	Spatial coordinate
k	Spatial-frequency variable
d	Number of spatial dimensions
X	Spatial-period of spatially periodic function/operator
Ω	$2\pi X^{-*}$ ($2\pi/X$ in one spatial dimension)
$\psi(\cdot)$	Spatial function; belongs to L^2
$\hat{\psi}(\cdot)$	Fourier transform of spatial function
ψ_θ	Lifted function; belongs to ℓ^2 for every θ
$\psi(t, \cdot)$	Spatio-temporal function; belongs to L^2 for every t
$\hat{\psi}(t, \cdot)$	Fourier transform of spatio-temporal function
$\psi_\theta(t)$	Lifted spatio-temporal function; belongs to ℓ^2 for every t, θ
A	Spatially periodic operator; acts on L^2
\hat{A}	Fourier transform of spatially periodic operator
\mathcal{A}_θ	Lifted form of spatially periodic operator; acts on ℓ^2
\mathcal{D}	Dense domain of L^2
$\ \cdot\ _F$	Frobenius norm of matrix
$\ \cdot\ _{HS}$	Hilbert-Schmidt norm of operator
$\Sigma(\cdot)$	Spectrum of operator
$\Sigma_p(\cdot)$	Point spectrum of operator or eigenvalues of matrix
$\rho(\cdot)$	Resolvent set of operator/matrix
$\mathcal{E}\{\cdot\}$	Expected value
\mathbb{C}^-	Complex numbers with real part strictly less than zero
\mathbb{C}^+	Complex numbers with real part greater than or equal to zero
j	$\sqrt{-1}$

Chapter 1

Introduction

The last thing one knows when writing a book is what to put first. *B. Pascal*

1.1 General Introduction

Spatially distributed systems are a special class of distributed parameter dynamical systems in which states, inputs, and outputs are spatially distributed fields. The general theory of distributed parameter systems is by now well developed and mature [1–4]. A recent trend has been the exploitation of special system structures in order to derive tighter results than is possible for very general classes of infinite dimensional systems. Examples of this are many, with the most closely related to our work being the class of spatially invariant systems [5]. Although the study of special classes of systems restricts the applicability of the given results, one should interpret these results in a wider context. An analogy might be in how the theory of Linear Time Invariant (LTI) systems is widely used as a starting point in the analysis and control of real world systems that are in effect time varying and nonlinear.

In this thesis we consider a class of systems we term *spatially periodic* systems. These are spatially distributed linear dynamical systems over infinite spatial domains in which the underlying Partial Differential Equations (PDEs) contain spatially periodic coefficients with commensurate periods. This class of systems has rather rich behavior in terms of response characteristics, stability properties and signal amplification as measured by system norms. A particular motivation we have for this study is an analogy with how the introduction of temporally periodic coefficients in Ordinary Differential Equations (ODEs) can change stability properties of initially LTI systems. For example, certain unstable LTI systems can be stabilized by being put in feedback with temporally periodic gains of properly designed amplitudes and frequencies. This can be roughly considered as an example of “vibrational control” [6]. On the other hand, certain stable or neutrally stable

LTI systems can be destabilized by periodic feedback gains. This is sometimes referred to as “parametric resonance” in the dynamical systems literature [7]. In all of the above examples, the periodic terms in the ODE can be considered as a feedback modification of an LTI system. The stabilization/destabilization process depends in subtle ways on “resonances” between the natural modes of the LTI subsystem and the frequency and amplitude of the periodic coefficients.

In this thesis we provide several examples in which changes in system properties occur in PDEs by the introduction of *spatially periodic* coefficients. In a close analogy with the ODE examples listed above, we can consider such systems as spatially invariant systems modified by feedback with spatially periodic gains. The periodicity of the coefficients can occur in a variety of ways. For example, in boundary layer and channel flow problems with corrugated walls (referred to as “Riblets” in the literature), the linearized Navier-Stokes equations in this geometry has periodic coefficients. This periodicity appears to influence flow instabilities and disturbance amplification, and may ultimately explain drag reduction or enhancement in such geometries. Another example comes from nonlinear optics in which wave propagation in periodic media is responsible for a variety of optical switching techniques. These applications represent significant research efforts in themselves and we do not directly address them in this thesis. Instead, we provide simpler examples that illustrate the effects of periodic coefficients in PDEs.

Our aim is to lay the foundations for the study of linear spatially periodic systems and provide more detailed tests for system theoretic properties (such as stability and system norm computations) than can be achieved by considering them as general distributed parameter systems. The main technique used is a spatial frequency representation akin to that used for temporally periodic systems, and alternatively referred to as the *harmonic transfer function* [8], the *frequency response operator* [9], or the *frequency domain lifting* [10] (see also [11]). By using a similar *spatial* frequency representation we reduce the study of linear spatially periodic systems to that of families of matrix-valued LTI systems, where the matrices involved are bi-infinite with a special structure. This is in contrast to spatially invariant systems where the proper frequency representation produces families of finite dimensional LTI systems. This reflects the additional richness of the class of spatially periodic systems as well as the fact that such systems mix frequency components in a special way. We pay special attention to stochastic interpretations of this frequency representation by considering spatially distributed systems driven by random fields. The resulting random fields are not necessarily spatially stationary but rather spatially *cyclo-stationary* (a direct analog of the notion of temporally cyclo-stationary processes [12]). This reflects the fact that frequency components of a cyclo-stationary field are correlated in ways determined by the underlying system’s periodicity. We show how the frequency domain representation of systems clarifies the frequency mixing process in the deterministic case and frequency correlations in the stochastic case.

Finally, we would like to reiterate that our analysis of spatially periodic systems is valid *for all* periods of the periodic coefficients. In the case where the coefficients have very small period (rapidly oscillating coefficients), the *homogenization* process [13] can be used to find an equivalent spatially invariant system that captures the bulk effect of the original system.

1.2 Contributions of Thesis

Part I

We consider systems described by linear, time-invariant, integro partial differential equations defined on an unbounded domain. In general the system can be defined over a domain with arbitrary spatial dimension, but for the sake of describing the main contributions of the thesis here we assume that the spatial dimension is equal to one. We use a standard state-space representation of the form

$$\begin{aligned} [\partial_t \psi](t, x) &= [A \psi](t, x) + [B u](t, x), \\ y(t, x) &= [C \psi](t, x), \end{aligned} \tag{1.1}$$

where $t \in [0, \infty)$ and $x \in \mathbb{R}$, ψ, u, y are spatio-temporal functions, and A, B, C are spatial integro-differential operators with coefficients that are periodic functions with a common period X . We refer to such systems as *spatially periodic*, and to A as the *infinitesimal generator*.

In this thesis our analysis and results are derived using a special frequency representation. We show that the spatial periodicity of the operators A, B and C implies that (1.1) can be rewritten as

$$\begin{aligned} [\partial_t \psi_\theta](t) &= [\mathcal{A}_\theta \psi_\theta](t) + [\mathcal{B}_\theta u_\theta](t), \\ y_\theta(t) &= [\mathcal{C}_\theta \psi_\theta](t), \end{aligned} \tag{1.2}$$

where $\theta \in [0, 2\pi/X)$; for every value of θ , $\psi_\theta, u_\theta, y_\theta$ are bi-infinite vectors, and $\mathcal{A}_\theta, \mathcal{B}_\theta, \mathcal{C}_\theta$ are bi-infinite matrices. The systems (1.2) and (1.1) are related through a unitary transformation, and in particular quadratic forms and norms are preserved by this transformation. Consequently, stability and quadratic norm properties of (1.2) and (1.1) are equivalent. With this transformation, the analysis of the original system (1.1) is reduced to that of the family of systems (1.2) that are *decoupled* in the parameter θ . In particular, as we will see in Part II, perturbation analysis for (1.2) is easier and less technical than that for the original system (1.1).

For a large class of infinite-dimensional systems, computing the \mathcal{H}^2 -norm involves solving an *operator* algebraic Lyapunov equation

$$AP + PA^* = -BB^*.$$

In general this is a difficult task that must be done using appropriate discretization techniques. However, in the case when A and B are spatially periodic operators, then so is the solution P . Thus the frequency representation implies that this operator Lyapunov equation is equivalent to the decoupled (in θ) family of Lyapunov equations

$$\mathcal{A}_\theta \mathcal{P}_\theta + \mathcal{P}_\theta \mathcal{A}_\theta^* = -\mathcal{B}_\theta \mathcal{B}_\theta^*, \quad (1.3)$$

where $\mathcal{A}_\theta, \mathcal{B}_\theta$ and \mathcal{P}_θ are the bi-infinite matrix representations of A, B and P . Once \mathcal{P}_θ is found, the \mathcal{H}^2 -norm of the system can be computed from

$$\frac{1}{2\pi} \int_0^\Omega \text{trace}[\mathcal{C}_\theta \mathcal{P}_\theta \mathcal{C}_\theta^*] d\theta, \quad \Omega = 2\pi/X. \quad (1.4)$$

We also give the \mathcal{H}^2 -norm a stochastic interpretation in terms of spatio-temporal cyclostationary random fields.

Of course to be able to define system norms one has to first verify system stability. When A is an infinite-dimensional operator though, it is possible that its spectrum $\Sigma(A)$ lies inside \mathbb{C}^- and yet $\|e^{At}\|$ grows exponentially [14–16]. In such cases it is said that the *spectrum-determined growth condition* is not satisfied [16]. Assuming that the systems we consider *do* indeed satisfy this condition, then to guarantee exponential stability it is sufficient to show that $\Sigma(A) \subset \mathbb{C}^-$. But as mentioned earlier, systems (1.2) and (1.1) are related through a unitary transformation, which together with an assumption on the continuous dependence of \mathcal{A}_θ on θ yields $\Sigma(A) = \bigcup_{\theta \in [0, \Omega]} \Sigma(\mathcal{A}_\theta)$. Therefore it is sufficient to show that $\Sigma(\mathcal{A}_\theta) \subset \mathbb{C}^-$ for every θ .

One method of checking the condition $\Sigma(\mathcal{A}_\theta) \subset \mathbb{C}^-$ is by the Nyquist stability criterion, where we study the stability of systems as a function of certain gain parameters by decomposing them into an open-loop subsystem and a feedback gain. Then by plotting the eigenloci of the open-loop system a graphical description is found from which it is possible to “read off” the stability of the closed-loop system for a family of feedback gains. In the case of those systems analyzed in this thesis the open-loop system typically has spatially distributed inputs and outputs. Hence the corresponding eigenloci is composed of an infinite number of curves. It is shown that the eigenloci converge uniformly to zero in a way that only a finite number of them need to be found to verify stability for a given feedback gain.

Part II

It is often physically meaningful to regard the spatially periodic operators as additive or multiplicative perturbations of spatially invariant ones [and by spatially invariant we mean those operators that can be described by generalized spatial convolutions, e.g., integro-differential operators with constant coefficients]. For example, the generator in (1.1) can often be decomposed as $A = A^\circ + \epsilon E$, where A°

is a spatially invariant operator and E is an operator that includes multiplication by periodic functions. In some control applications, the operator E is something to be “designed”. Therefore it is desirable to have easily verifiable conditions for stability and norms of such systems. This would then allow for the selection of the spatial period of E to achieve the desired behavior. The perturbation analysis we present, though limited to small values of ϵ , provides useful results for selecting candidate “periods” for E .

We first present the results on perturbation analysis of the \mathcal{H}^2 -norm, and then deal with the issue of stability.

In Part I we discussed how the \mathcal{H}^2 -norm can be found from solving a family of operator Lyapunov equations (1.3). But solving (1.3) is still a difficult problem in general since it involves bi-infinite matrices, and truncations that lead to good enough approximations may become extremely large. Therefore we use perturbation analysis as follows: the generator is expressed as $\mathcal{A}_\theta = \mathcal{A}_\theta^\circ + \epsilon \mathcal{E}_\theta$ where \mathcal{A}_θ° and \mathcal{E}_θ correspond to the spatially invariant and spatially periodic components respectively. It follows that the solution \mathcal{P}_θ is analytic in ϵ and the terms of its power series expansion (denoted by $\mathcal{P}_\theta^{(i)}$) satisfy a sequence of forward coupled Lyapunov equations. Furthermore, the terms $\mathcal{P}_\theta^{(i)}$ are banded matrices, with the number of bands increasing with the index i . These Lyapunov equations can then be solved recursively for $i = 0, 1, 2, \dots$. We give formulae for these representations and the corresponding sequence of Lyapunov equations. And in some examples that we present, these formulae lead to simple “resonance” conditions for stabilization or destabilization of PDEs using spatially periodic feedback.

The second set of results concern the problem of stability. In Part I we discussed the issue of spectrum-determined growth condition not necessarily being satisfied for infinite-dimensional systems. Yet there exists a wide range of infinite-dimensional systems for which the spectrum-determined growth condition *is* satisfied. These include (but are not limited to) systems for which the A -operator is *sectorial* (also known as an operator which generates a *holomorphic* or *analytic* semigroup) [17–19] or is a *Riesz-spectral* operator [3]. In this thesis we focus on sectorial operators.

Thus to establish exponential stability of a system, one possibility would be to show simultaneously that

- (i) A is sectorial,
- (ii) $\Sigma(A)$ lies in \mathbb{C}^- .

But this still does not make the problem trivial. In fact proving that an infinite-dimensional operator is sectorial, and then finding its spectrum, can in general be extremely difficult.

Once again we use perturbation methods to show (i) and (ii). We consider A to have the form $A = A^\circ + \epsilon E$ where A° is a spatially invariant operator,

E is a spatially periodic operator, and ϵ is a small complex scalar. Using the (matrix-valued) Fourier symbol of the spatially invariant operator A° , we first find conditions on A° such that (i) and (ii) are satisfied. We then show that (i) and (ii) will *remain* satisfied if ϵ is small enough and if the spatially periodic operator E is “weaker” than A° (in the sense that E is *relatively bounded* with respect to A°). The utility of this approach is that (i) and (ii) are much easier to check for a spatially invariant operator than they are for a spatially periodic one.

1.3 Organization of Thesis

This thesis is organized as follows:

Part I

- In Chapter 2 we develop a mathematical framework for analysis of spatially periodic systems. We exploit the special structure of spatially periodic operators to convert spatially periodic systems into parameterized families of matrix-valued first-order systems.
- In Chapter 3 we introduce the notions of \mathcal{H}^∞ and \mathcal{H}^2 norms for spatially periodic operators and systems, and give both stochastic and deterministic interpretations of the \mathcal{H}^2 norm. We derive a sufficient condition for finiteness of the \mathcal{H}^2 norm in system with arbitrary spatial dimensions. We give sufficient and easy-to-check conditions for the convergence of truncations as required for numerical computation of the \mathcal{H}^2 and \mathcal{H}^∞ norms of spatially periodic systems. We finish by providing examples that demonstrate how norms of spatially invariant PDEs can be changed when spatially periodic coefficients are introduced.
- In Chapter 4 we describe the general stability conditions for spatially distributed systems. We extend the Nyquist stability criterion to spatially periodic systems with unbounded infinitesimal generators and distributed input-output spaces. We do this by first deriving a new version of the argument principle applicable to such systems. We establish that only a finite number of (the infinite number of) eigenloci need to be computed. We prove the convergence of the eigenloci of a truncated system to those of the original system, thus showing that computation of eigenloci and checking the Nyquist stability criterion are numerically feasible.

Part II

- In Chapter 5 we consider the important scenario where a spatially invariant PDE is perturbed by the introduction of small spatially periodic functions

in its coefficients. We prove that to compute the \mathcal{H}^2 norm of the perturbed system it is sufficient to solve a family of Lyapunov/Sylvester equations of dimension equal to the Euclidean dimension of the original system. The developed framework can be used to choose the frequency of the periodic coefficients to most significantly affect the value of the system norm, reveal important trends in system behavior, and provide valuable guidelines for design.

- In Chapter 6 we use perturbation theory of unbounded operators to derive sufficient conditions for a spatially periodic operator to be the infinitesimal generator of a holomorphic semigroup. This is important because such semigroups satisfy the spectrum-determined growth condition. Thus, together with the spectrum of the infinitesimal generator belonging to the left-half of the complex plane, holomorphicity proves exponential stability. We use a generalized notion of Geršgorin circles for infinite-dimensional operators to estimate the location of the spectrum of a spatially periodic infinitesimal generator, and find sufficient conditions for exponential stability.

Note: In general, one can not speak of system norms before one has settled the issue of stability. We are aware of this, but have chosen to discuss input-output norms before stability in both parts of the thesis. This has been done to make for easier reading, as the chapters on stability are slightly more involved.

Part I

Basic Theory of Distributed Spatially Periodic Systems

Chapter 2

Preliminaries: Representation of Spatially Periodic Functions, Operators, and Systems

Fourier is a mathematical poem.

Lord Kelvin

2.1 Introduction

In this chapter we briefly review some definitions and mathematical preliminaries. Sections 2.2 and 2.3 introduce the terminology and notational conventions that will be used throughout this thesis. Section 2.4 reviews the definitions of spatially periodic functions, spatially periodic operators, and spatially periodic systems [see Section 2.2 regarding terminology]. Section 2.5 reviews the (spatial-) frequency representation of spatially periodic operators, and Section 2.6 that of spatially periodic systems.

2.2 Terminology

Throughout the thesis, we use the terms *spatial ‘operators’* and *spatial ‘systems’*. By the former, we mean a *purely spatial* system with no temporal dynamics (i.e. a memoryless operator that acts on a spatial function and yields a spatial function), whereas the latter refers to a *spatio-temporal* system (a system where the state evolves on some spatial domain, i.e., for every time t the state is a function on a spatial domain). Also, spatial and spatio-temporal stochastic processes will be called *random fields*, to differentiate them from purely temporal stochastic process. The $\mathcal{H}_{\text{sp}}^2$ and $\mathcal{H}_{\text{sp}}^\infty$ -norms are extensions of the well-known \mathcal{H}^2 and \mathcal{H}^∞ -norms of stable linear systems to purely spatial operators, and will be defined in the thesis.

We use the term ‘pure point spectrum’ (or ‘discrete spectrum’) to mean that the spectrum of an operator consists entirely of *isolated* eigenvalues [17].

2.3 Notation

The dimension of the spatial coordinates is denoted by d , and the spatial variable by $x \in \mathbb{R}^d$. We use $k \in \mathbb{R}^d$ to characterize the spatial-frequency variable, also known as the *wave-vector* (or *wave-number* when $d = 1$). \mathbb{C}^- denotes all complex numbers with real part less than zero, \mathbb{C}^+ denotes all complex numbers with real part greater than or equal to zero, and $j := \sqrt{-1}$. $\overline{\mathfrak{S}}$ is the closure of the set $\mathfrak{S} \subset \mathbb{C}$. $C(z_0; \mathfrak{P})$ is the number of counter-clockwise encirclements of the point $z_0 \in \mathbb{C}$ by the closed path \mathfrak{P} . $\|\cdot\|$ for vectors (and matrices) is the standard Euclidean norm (Euclidean induced-norm), and may also be used to denote the induced norm on operator spaces when there is no chance of confusion. $\Sigma(T)$ is the spectrum of the operator T , and $\Sigma_p(T)$ its point spectrum, $\rho(T)$ its resolvent set, and $R(\zeta, T)$ its resolvent operator $(\zeta - T)^{-1}$. $\sigma_n(T)$ is the n^{th} singular-value of T . $\mathcal{B}(\ell^2)$ denotes the bounded operators on ℓ^2 , $\mathcal{B}_0(\ell^2)$ the compact operators on ℓ^2 , $\mathcal{B}_2(\ell^2)$ the Hilbert-Schmidt operators on ℓ^2 , and $\mathcal{B}_1(\ell^2)$ the trace class operators on ℓ^2 ; $\mathcal{B}_1(\ell^2) \subset \mathcal{B}_2(\ell^2) \subset \mathcal{B}_0(\ell^2) \subset \mathcal{B}(\ell^2)$ [20]. ‘*’ denotes the complex-conjugate transpose for vectors and matrices, and also the adjoint of a linear operator. We will use the same notation G for a system/operator and it’s kernel representation. The spatio-temporal function $u(t, x)$ (operator G) is denoted by $\hat{u}(t, k)$ (respectively \hat{G}) after the application of a Fourier transform on the spatial variable x , and by $u(\omega, x)$ (respectively G) after the application of a Fourier transform on the time variable t . Similarly $\hat{u}(\omega, k)$ (respectively \hat{G}) is used when Fourier transforms have been applied in both the spatial and temporal domains. $\mathcal{E}\{u(t, x)\}$ denotes the expected value of $u(t, x)$.

Throughout the thesis we use functions $\psi(\cdot)$ that are square integrable on $x \in \mathbb{R}^d$. In dealing with these functions (and operators that act on them) we often choose to ignore their Euclidean dimensions and treat them as scalars. For example if for every x , $\psi(x)$ is a vector in \mathbb{C}^q and $\|\psi\|$ is square integrable, we simply write $\psi \in L^2(\mathbb{R}^d)$ [rather than $\psi \in L^2_{\mathbb{C}^q}(\mathbb{R}^d)$]. The same applies to ℓ^2 vectors, i.e., each element of an ℓ^2 vector can have Euclidean dimension greater than one even though it is not explicitly stated. This is done only for the sake of notational clarity and to avoid clutter.

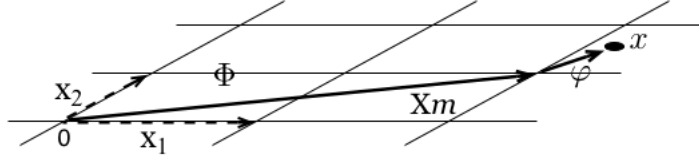


Figure 2.1: For $d = 2$, $X = [x_1 | x_2]$ where x_1 and x_2 are the dashed 2×1 vectors shown above. In this picture, $x = Xm + \varphi$ where $m = [2 \ 1]^*$ and $\varphi \in \Phi$.

2.4 Definitions

2.4.1 Spatial Functions

The Fourier transform of the function $u(x) \in L^2(\mathbb{R}^d)$, $d = 1, 2, \dots$, is defined as

$$\hat{u}(k) := \int_{\mathbb{R}^d} e^{-jk^*x} u(x) dx, \quad (2.1)$$

where $k \in \mathbb{R}^d$ and $dx = dx_1 dx_2 \cdots dx_d$ is the differential volume element in \mathbb{R}^d .

A function $u(x)$, $x \in \mathbb{R}^d$ is *periodic* if and only if there exists an invertible matrix $X \in \mathbb{R}^{d \times d}$ such that

$$u(x + Xm) = u(x), \quad (2.2)$$

for any $m \in \mathbb{Z}^d$. Suppose that for every other invertible matrix $X' \in \mathbb{R}^{d \times d}$ which satisfies (2.2), and for every $m' \in \mathbb{Z}^d$, we have $X'm' = Xm$ for some $m \in \mathbb{Z}^d$. Then we refer to the matrix X as the (spatial) *period* of $u(\cdot)$. X can be thought of as a generalization of the notion of the period of a periodic function on \mathbb{R} .

Let \mathbb{U}^d denote all vectors $\eta \in \mathbb{R}^d$ with elements $0 \leq \eta_i < 1$, $i = 1, 2, \dots, d$. The spatial region $\Phi := \{X\eta, \eta \in \mathbb{U}^d\}$ is called a *primitive cell* of the periodic function u , and has volume $V(\Phi) = |\det X|$. Notice that any $x \in \mathbb{R}^d$ can be written as $x = Xm + \varphi$ where $m \in \mathbb{Z}^d$ and $\varphi \in \Phi$. See Figure 2.1 for a demonstration in $d = 2$.

We call the matrix $\Omega := 2\pi X^{-*}$ the (spatial) *frequency* of u . The functions $e^{j(\Omega l)^*x}$, $l \in \mathbb{Z}^d$, are periodic in x with period X . It can be shown that these functions form a basis of $L^2(\Phi)$ and one can write a Fourier series expansion of $u \in L^2(\Phi)$

$$u(x) := \sum_{l \in \mathbb{Z}^d} u_l e^{j(\Omega l)^*x}, \quad (2.3)$$

where u_l are the Fourier series coefficients of $u(\cdot)$.

Finally, the primitive cell in the frequency domain is defined as $\Theta := \{\Omega\eta, \eta \in \mathbb{U}^d\}$ and is also known as the *reciprocal primitive cell*. Notice again that any $k \in \mathbb{R}^d$ can be written as $k = \Omega l + \theta$ where $l \in \mathbb{Z}^d$ and $\theta \in \Theta$.

2.4.2 Spatial Operators and Spatial Systems

If $u(x)$ and $y(x)$ are two spatial functions related by a linear operator, it is in general possible to write the relation between them as

$$y(x) = \int_{\mathbb{R}^d} G(x, \chi) u(\chi) d\chi,$$

where the function G is termed the *kernel function* of the operator. A linear *spatially periodic operator* G with period X is one whose kernel has the property

$$G(x + Xm, \chi + Xm) = G(x, \chi),$$

for all $x, \chi \in \mathbb{R}^d$ and $m \in \mathbb{Z}^d$.

If $u(t, x)$ and $y(t, x)$ are the spatio-temporal input and output of a linear causal spatio-temporal system, then it is possible to write

$$y(t, x) = \int_0^t \int_{\mathbb{R}^d} G(t, \tau; x, \chi) u(\tau, \chi) d\chi d\tau, \quad (2.4)$$

and G is the kernel function of the linear system. A linear *spatially periodic* (time-invariant) *system* G with spatial period X , is one whose kernel satisfies

$$G(t + s, \tau + s; x + Xm, \chi + Xm) = G(t, \tau; x, \chi),$$

for all $t, \tau, s \in [0, \infty)$, $t \geq \tau$, $x, \chi \in \mathbb{R}^d$ and $m \in \mathbb{Z}^d$. From time-invariance it follows that

$$G(t, \tau; x, \chi) = H(t - \tau; x, \chi),$$

for all $x, \chi \in \mathbb{R}^d$, where H is the temporal (and operator-valued) ‘impulse response’ of the system, i.e., (2.4) can be expressed as the temporal convolution $y(t, x) = \int_0^t \int_{\mathbb{R}^d} H(t - \tau; x, \chi) u(\tau, \chi) d\chi d\tau$.

2.4.3 Stochastic Processes and Random Fields

A random field $v(x)$ is called *wide-sense cyclostationary* if its autocorrelation $R^v(x, \chi) := \mathcal{E}\{v(x) v^*(\chi)\}$ satisfies

$$R^v(x + Xm, \chi + Xm) = R^v(x, \chi), \quad (2.5)$$

for all $x, \chi \in \mathbb{R}^d$, $m \in \mathbb{Z}^d$, and some $X \in \mathbb{R}^{d \times d}$.

If $u(t, x)$ is a spatio-temporal random field, then its autocorrelation function can be defined as $R^u(t, \tau; x, \chi) := \mathcal{E}\{u(t, x) u^*(\tau, \chi)\}$. If $u(t, x)$ is wide-sense

stationary in both the temporal and spatial directions, then

$$R^u(t, \tau; x, \chi) = \bar{R}(t - \tau; x - \chi),$$

for all $t, \tau, s \in [0, \infty)$, $x, \chi \in \mathbb{R}^d$ and some function \bar{R} . If $u(t, x)$ is wide-sense stationary in the temporal direction but wide-sense cyclostationary in the spatial direction, then

$$R^u(t + s, \tau + s; x + Xm, \chi + Xm) = R^u(t, \tau; x, \chi),$$

for all $t, \tau, s \in [0, \infty)$, $x, \chi \in \mathbb{R}^d$ and $m \in \mathbb{Z}^d$. As a result, it can be shown that

$$R^u(t, \tau; x, \chi) = \tilde{R}(t - \tau; x, \chi),$$

for some function \tilde{R} . In the following, we abuse notation by writing $R^u(t - \tau; x, \chi)$ instead of $\tilde{R}(t - \tau; x, \chi)$.

Finally, $R^u(t, t; x, x) = R^u(0; x, x)$ is the variance of u at spatial location x . It may also be of interest to observe quantities such as $R^u(\Delta t; x, x)$ or $R^u(0; x, x + \Delta x)$ known as *two-point correlations*, the former being a two-point correlation in time, the latter in space.

2.5 Frequency Representation of Periodic Operators

In this section we review the representation of spatially periodic operators in the Fourier (frequency) domain. We show that it is possible to exploit the particular structure of spatially periodic operators in the frequency domain to yield a representation of these operators that is more amenable to numerical computations.

2.5.1 Spatially Periodic Operators

Let $\hat{u}(k)$ and $\hat{y}(k)$ denote the Fourier transforms of two spatial functions $u(x)$ and $y(x)$ respectively. If u and y are related by a linear operator,

$$y(x) = \int_{\mathbb{R}^d} G(x, \chi) u(\chi) d\chi,$$

then so are their Fourier transforms, and it is in general possible to write the relation between \hat{u} and \hat{y} as

$$\hat{y}(k) = \int_{\mathbb{R}^d} \hat{G}(k, \kappa) \hat{u}(\kappa) d\kappa. \quad (2.6)$$

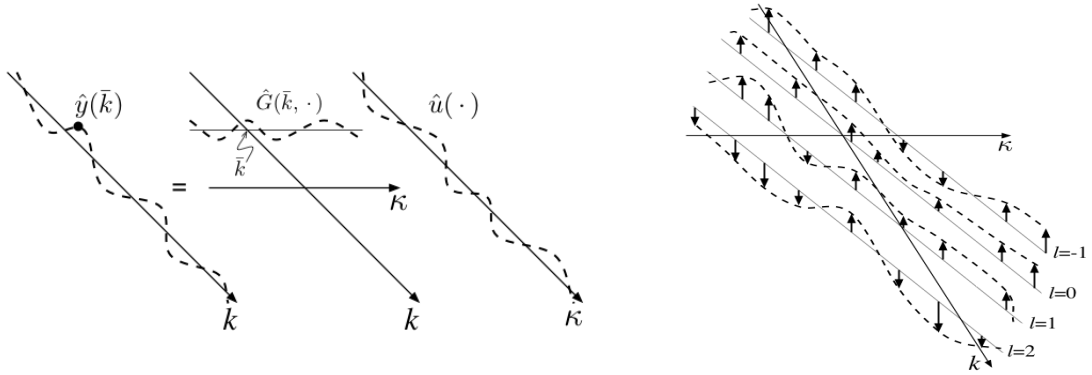


Figure 2.2: Left: The frequency kernel representation of a general spatial operator G for $d = 1$. Right: The frequency kernel representation of a spatially periodic operator G for $d = 1$.

G and \hat{G} (termed the *kernel functions* of the operator) may contain distributions in general, see Figure 2.2 (left).

It is a standard fact that if the operator G is spatially invariant (i.e. if it commutes with all spatial shifts), then its representation in the Fourier domain is a multiplication operator [21] [5], that is, there exists a function $\hat{g}(k)$ such that

$$\hat{y}(k) = \hat{g}(k) \hat{u}(k). \quad (2.7)$$

This means that the kernel $\hat{G}(k, \kappa)$ in (2.6) can be represented by

$$\hat{G}(k, \kappa) = \hat{g}(k) \delta(k - \kappa).$$

One way to think about this is that spatially invariant operators have Fourier kernel functions $\hat{G}(k, \kappa)$ that are ‘diagonal’, i.e. they are a function of only $k - \kappa$. This can be visualized as an ‘impulse sheet’ along the diagonal $k = \kappa$ whose strength is given by the function $\hat{g}(k)$.

We now investigate the structure of the kernel function for spatially periodic operators. Consider a spatially periodic multiplication operator with period $\mathbf{X} = 2\pi\Omega^{-*}$ of the form

$$y(x) = e^{j(\Omega)^*x} u(x),$$

with $l \in \mathbb{Z}^d$. From the standard shift property of the Fourier transform, we have

$$\hat{y}(k) = \hat{u}(k - \Omega l),$$

i.e. \hat{y} is a shifted version of \hat{u} . Such shifts are represented in (2.6) by kernel functions of the form

$$\hat{G}(k, \kappa) = \delta(k - \kappa - \Omega l).$$

This can be visualized as an impulse sheet of constant strength along the sub-diagonal $k - \kappa = \Omega l$.

Now consider multiplication by a general periodic function $f(x)$ of period $X = 2\pi\Omega^{-*}$. Let f_l be the Fourier series coefficients of $f(x)$, i.e.

$$f(x) = \sum_{l \in \mathbb{Z}^d} f_l e^{j(\Omega l)^* x}.$$

Using the above, the shift property of the Fourier transform repeatedly, and the linearity of multiplication operators, we conclude that

$$y(x) = f(x) u(x) \iff \hat{y}(k) = \sum_{l \in \mathbb{Z}^d} f_l \hat{u}(k - \Omega l),$$

i.e. \hat{y} is the sum of weighted shifts of \hat{u} . Thus, the kernel function of a periodic pure multiplication operator is of the form

$$\hat{G}(k, \kappa) = \sum_{l \in \mathbb{Z}^d} f_l \delta(k - \kappa - \Omega l), \quad (2.8)$$

which converges in the sense of distributions. This can be visualized as an array of diagonal impulse sheets at $k - \kappa = \Omega l$ with relative strength given by f_l , the l^{th} Fourier series coefficient of the function $f(x)$.

Now we investigate the structure of a general periodic operator. First, the cascade of a pure multiplication by $e^{j(\Omega l)^* x}$ followed by a spatially invariant operator with Fourier symbol $\hat{g}(k)$ has a kernel function given by

$$\hat{g}(k) \delta(k - \kappa - \Omega l).$$

It is easy to see that sums and cascades of such basic periodic operators produce an operator with a kernel function (in the space of distributions) of the form

$$\hat{G}(k, \kappa) = \sum_{l \in \mathbb{Z}^d} \hat{g}_l(k) \delta(k - \kappa - \Omega l), \quad (2.9)$$

where $\hat{g}_l(k)$, for each k , can in general be a matrix. Such a kernel function can be visualized in Figure 2.2 (right).

In this dissertation, we consider spatially periodic operators with kernel functions of the form (2.9). These operators are completely specified by the family of (matrix-valued) functions $\{\hat{g}_l(k)\}_{l \in \mathbb{Z}^d}$. It is interesting to observe certain special subclasses:

1. A *spatially invariant* operator has a kernel function of the form (2.9) in which $\hat{g}_l = 0$ for $l \neq 0$ (i.e. it is purely ‘diagonal’).

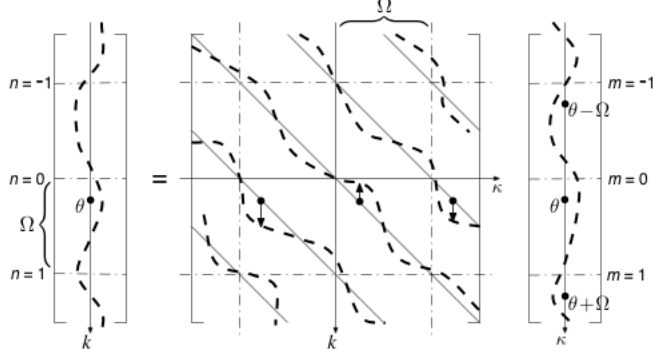


Figure 2.3: The action of the kernel function of a periodic operator for $d = 1$.

2. A *periodic pure multiplication* operator has a kernel function of the form (2.9) in which all the functions \hat{g}_l are constant in their arguments (i.e. it is a ‘Toeplitz’ operator).

Let us return to the general kernel representation (2.9). We next show how the special structure of (2.9) can be exploited to yield a new representation for \hat{G} . Consider the equation $\hat{y} = \hat{G}\hat{u}$. To find $\hat{y}(k)$ for a given k , one can imagine the action of \hat{G} on $\hat{u}(\cdot)$ as that depicted in Figure 2.3. Recall from Section 2.4 that $k \in \mathbb{R}^d$ can be written as $\theta + \Omega n$ for some $n \in \mathbb{Z}^d$ and $\theta \in \Theta$. From (2.6) and (2.9),

$$\begin{aligned}
\hat{y}(\theta + \Omega n) &= \int_{\mathbb{R}^d} \hat{G}(\theta + \Omega n, \kappa) \hat{u}(\kappa) d\kappa \\
&= \sum_{l \in \mathbb{Z}^d} \hat{g}_l(\theta + \Omega n) \hat{u}(\theta + \Omega n - \Omega l) = \sum_{m \in \mathbb{Z}^d} \hat{g}_{n-m}(\theta + \Omega n) \hat{u}(\theta + \Omega m).
\end{aligned} \tag{2.10}$$

Now if we form the infinite ‘lattices’ $y_\theta := \{\hat{y}(\theta + \Omega n)\}_{n \in \mathbb{Z}^d}$ and $u_\theta := \{\hat{u}(\theta + \Omega m)\}_{m \in \mathbb{Z}^d}$, then (2.10) can be written as

$$y_\theta = \mathcal{G}_\theta u_\theta, \tag{2.11}$$

where \mathcal{G}_θ is composed of the elements $\{\hat{g}_l(\theta + \Omega n)\}_{l, n \in \mathbb{Z}^d}$. As θ varies in Θ , \mathcal{G}_θ fully describes the kernel \hat{G} . In the sequel we freely interchange between the two representations \hat{G} and \mathcal{G}_θ . Let us make this more concrete by looking at a special case.

Let us examine the above relationships for the case of $d = 1$. Since $x \in \mathbb{R}$ the period X is a real scalar, $\Omega = \frac{2\pi}{X}$, $\mathbb{U} = [0, 1)$, and $\Theta = [0, \Omega)$. For *any* given $\theta \in [0, \Omega)$, the infinite lattices y_θ and u_θ can be written as bi-infinite vectors, \mathcal{G}_θ

as a bi-infinite matrix, and (2.10)–(2.11) as

$$\begin{bmatrix} \vdots \\ \hat{y}(\theta-\Omega) \\ \hat{y}(\theta) \\ \hat{y}(\theta+\Omega) \\ \vdots \end{bmatrix} = \begin{bmatrix} \ddots & \ddots & \ddots & \ddots & \ddots \\ \ddots & \hat{g}_0(\theta-\Omega) & \hat{g}_{-1}(\theta-\Omega) & \hat{g}_{-2}(\theta-\Omega) & \ddots \\ \ddots & \hat{g}_1(\theta) & \hat{g}_0(\theta) & \hat{g}_{-1}(\theta) & \ddots \\ \ddots & \hat{g}_2(\theta+\Omega) & \hat{g}_1(\theta+\Omega) & \hat{g}_0(\theta+\Omega) & \ddots \\ \ddots & \ddots & \ddots & \ddots & \ddots \end{bmatrix} \begin{bmatrix} \vdots \\ \hat{u}(\theta-\Omega) \\ \hat{u}(\theta) \\ \hat{u}(\theta+\Omega) \\ \vdots \end{bmatrix}. \quad (2.12)$$

In this setting, the discussed special subclasses of operators have particularly simple forms:

1. Spatially invariant operators have the *diagonal* representation

$$\mathcal{G}_\theta = \begin{bmatrix} \ddots & & & \\ & \hat{g}(\theta+\Omega n) & & \\ & & \ddots & \end{bmatrix}, \quad (2.13)$$

2. Periodic pure multiplication operators have the *Toeplitz* representation

$$\mathcal{G}_\theta = \begin{bmatrix} \ddots & \ddots & \ddots & \ddots & \ddots \\ \ddots & f_0 & f_{-1} & f_{-2} & \ddots \\ \ddots & f_1 & f_0 & f_{-1} & \ddots \\ \ddots & f_2 & f_1 & f_0 & \ddots \\ \ddots & \ddots & \ddots & \ddots & \ddots \end{bmatrix}. \quad (2.14)$$

We remind the reader again that as mentioned in the section on terminology, throughout this dissertation we choose to ignore the Euclidean dimension of $\hat{g}(\cdot)$ and f_i . Thus, precisely put, \mathcal{G}_θ is ‘*block*’ *diagonal* in (2.13) and ‘*block*’ *Toeplitz* in (2.14).

Example 1 If $A = \partial_x$, then the Fourier symbol of A is jk , and

$$\mathcal{A}_\theta = \begin{bmatrix} \ddots & & & \\ & j\theta + j\Omega n & & \\ & & \ddots & \end{bmatrix}.$$

Notice that since \mathcal{A}_θ is diagonal, its diagonal elements constitute its eigenvalues and thus \mathcal{A}_θ has pure point spectrum. Note also that since the eigenvalues $j\theta + jn\Omega$ of \mathcal{A}_θ grow unbounded as $|n|$ grows, \mathcal{A}_θ is an unbounded operator.

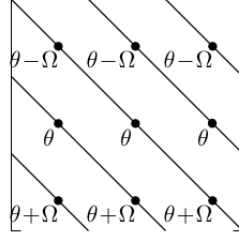


Figure 2.4: Graphical interpretation of \mathcal{G}_θ for $d = 1$ and $\theta \in [0, \Omega)$. Note that θ need only change in $[0, \Omega)$ to fully capture \hat{G} .

If $f(x) = \cos(\Omega x)$, then $f(x) = \frac{1}{2}(e^{j\Omega x} + e^{-j\Omega x})$, and

$$\mathcal{F} = \frac{1}{2} \begin{bmatrix} \ddots & \ddots & & & \\ \ddots & 0 & 1 & & \\ & 1 & 0 & \ddots & \\ & & & \ddots & \ddots \end{bmatrix},$$

where we have dropped the θ subscript in \mathcal{F} as it is independent of this variable.

■

Remark 1 Another way to interpret the new representation introduced above is to think of \mathcal{G}_θ , for every given θ , as a ‘sample’ of \hat{G} ; see Figure 2.4. As θ changes in Θ , this ‘sampling grid’ slides on the impulse sheets of \hat{G} . ■

Remark 2 As θ assumes values in Θ , one can also interpret u_θ as a lifted (in frequency) version of $\hat{u}(\cdot)$ [9, 10]. Let \mathcal{M}_θ denote the unitary lifting operator such that $u_\theta = \mathcal{M}_\theta \hat{u}$, $y_\theta = \mathcal{M}_\theta \hat{y}$, and $\mathcal{G}_\theta = \mathcal{M}_\theta \hat{G} \mathcal{M}_\theta^*$. We will henceforth refer to this representation of functions and operators as the lifted representation.

Suppose \hat{u} belongs to a dense subset \mathcal{D} of $L^2(\mathbb{R}^d)$ such that

$$\hat{u} \in \mathcal{D} \subset L^2(\mathbb{R}^d) \implies u_\theta \in \ell^2(\mathbb{Z}^d) \text{ for every } \theta \in \Theta.$$

Then since \mathcal{M}_θ is unitary and therefore preserves norms,

$$\|\hat{u}\|_{L^2}^2 = \int_{\mathbb{R}^d} \|\hat{u}(k)\|^2 dk = \sum_{m \in \mathbb{Z}^d} \int_{\Theta} \|\hat{u}(\theta + \Omega m)\|^2 d\theta = \int_{\Theta} \|u_\theta\|_{\ell^2}^2 d\theta,$$

where $\|\cdot\|$ is the standard Euclidean norm. We also have

$$\sum_{l \in \mathbb{Z}^d} \int_{\mathbb{R}^d} \text{trace}[\hat{g}_l(k) \hat{g}_l^*(k)] dk = \int_{\Theta} \text{trace}[\mathcal{G}_\theta \mathcal{G}_\theta^*] d\theta = \int_{\Theta} \|\mathcal{G}_\theta\|_{\text{HS}}^2 d\theta, \quad (2.15)$$

with $\|T\|_{\text{HS}}^2 := \text{trace}[TT^*]$ being the square of the Hilbert-Schmidt norm¹ of T . ■

Remark 3 It is well known that the trace of a finite-dimensional matrix is equal to the sum of the elements on its main diagonal. This easily extends to the case of operators on $\ell^2(\mathbb{Z})$, which can be thought of as infinite-dimensional matrices. But it may not be obvious what is meant by the trace of an operator on $\ell^2(\mathbb{Z}^d)$. Since we will often use the notion of the trace of such operators in this work, it is worth mentioning here that the trace has a more fundamental definition. If $\{e_i\}_{i \in \mathbb{Z}^d}$ denotes an orthonormal basis of $\ell^2(\mathbb{Z}^d)$, then for those operators T on $\ell^2(\mathbb{Z}^d)$ for which the following quantity is finite we have $\text{trace}[T] = \sum_{i \in \mathbb{Z}^d} e_i^* T e_i$ [20]. ■

Remark 4 From the unitary property of \mathcal{M}_θ it follows that G is a bounded operator if and only if \mathcal{G}_θ is a bounded operator for all $\theta \in \bar{\Theta}$. ■

For a different method of deriving the representations (2.13)–(2.14) we refer the reader to [22] [23].

2.5.2 Spectral-Correlation Density Operators

Let $u(x)$ be a wide-sense *stationary* random field. We define its Fourier transform as $\hat{u}(k) = \int_{\mathbb{R}^d} e^{-jk^*x} u(x) dx$.² Let $R^u = \mathcal{E}\{u(x) u^*(\chi)\}$. Then it follows that

$$\begin{aligned} \hat{S}^u(k, \kappa) &:= \mathcal{E}\{\hat{u}(k) \hat{u}^*(\kappa)\} \\ &= \int_{\mathbb{R}^d} \int_{\mathbb{R}^d} e^{-j(k^*x - \kappa^*\chi)} R^u(x, \chi) d\chi dx. \end{aligned} \quad (2.16)$$

\hat{S}^u is the Fourier transform of R^u and is called the *spectral-correlation density* of u . Notice that \hat{S}^u is a function of two variables, as opposed to the (power) spectral density function which is a function of only one frequency variable.

Since the random field u is wide-sense stationary, we have $R^u(x, \chi) = R^u(x - \chi)$. Therefore from (2.16) the spectral-correlation density of u assumes the form

$$\hat{S}^u(k, \kappa) = \hat{S}_0^u(k) \delta(k - \kappa),$$

where $\hat{S}_0^u(k)$ is the (power) spectral density of u . Heuristically, the above equation means that \hat{u} is an irregular function of frequency in a way that no two samples $\hat{u}(k)$ and $\hat{u}(\kappa)$, $k \neq \kappa$, of \hat{u} are correlated [12].

¹The Hilbert-Schmidt norm of an operator is a generalization of the Frobenius norm of finite-dimensional matrices $\|A\|_{\text{F}}^2 = \sum_{m,n} |a_{mn}|^2 = \text{trace}[AA^*]$.

²Technically, the sample paths of wide-sense stationary signals are persistent and not finite-energy functions [12] and hence their Fourier transforms fail to exist, i.e., $\int_{x \in \mathbb{R}^d} e^{-jk^*x} u(x) dx$ does not converge as a quadratic-mean integral. This problem can be circumvented by introducing the *integrated Fourier transform* [12] [24]. We will proceed formally and not pursue this direction here.

Next we consider a wide-sense *cyclostationary* random field $u(x)$ whose auto-correlation satisfies (2.5). The next theorem describes the structure of \hat{S}^u .

Theorem 1 *Let u be a wide-sense cyclostationary random field with autocorrelation $R^u(x, \chi) = R^u(x + Xm, \chi + Xm)$, $m \in \mathbb{Z}^d$. Then u has the spectral-correlation density*

$$\hat{S}^u(k, \kappa) = \sum_{l \in \mathbb{Z}^d} \hat{S}_l^u(k) \delta(k - \kappa - \Omega l) \quad (2.17)$$

for some family of functions \hat{S}_l^u , $l \in \mathbb{Z}^d$.

Proof: See Appendix. ■

Thus for a general cyclostationary signal the spectral-correlation density, as an operator in the Fourier domain, can be visualized as in Figure 2.2 (right). Equation (2.17) implies that $\hat{u}(k)$ has only nonzero correlation with the samples $\hat{u}(k - \Omega l)$, $l \in \mathbb{Z}^d$, with $\hat{S}_l^u(k)$ characterizing the amount of correlation. Hence in contrast to stationary signals, different frequency components of cyclostationary signals are correlated.

The following change of variables gives \hat{S}^u a more transparent interpretation [25]

$$\begin{cases} \mu := \frac{k - \kappa}{2} \\ \varkappa := \frac{k + \kappa}{2} \end{cases} \implies \begin{cases} k = \varkappa + \frac{\mu}{2} \\ \kappa = \varkappa - \frac{\mu}{2} \end{cases}$$

Essentially, μ characterizes the (continuum of) subdiagonals of \hat{S}^u and \varkappa determines the position on the μ^{th} subdiagonal, as demonstrated in Figure 2.5 (left). Let us define

$$\hat{Q}^u(\varkappa, \mu) := \mathcal{E}\left\{\hat{u}\left(\varkappa + \frac{\mu}{2}\right) \hat{u}^*\left(\varkappa - \frac{\mu}{2}\right)\right\}. \quad (2.18)$$

From (2.16), (2.17), and (2.18) it follows that

$$\hat{Q}^u(\varkappa, \mu) = \begin{cases} \hat{S}_l^u(k) & \mu = \Omega l, l \in \mathbb{Z}^d, \\ 0 & \text{otherwise.} \end{cases} \quad (2.19)$$

In words, $\hat{Q}^u(\varkappa, \mu)$ is zero unless μ is such that $\hat{Q}^u(\varkappa, \mu)$ lands on one of the impulse sheets $\hat{S}_l^u(\cdot)$. Let us see what this means in terms of \hat{u} . Notice from (2.18) and (2.19) that for a general cyclostationary signal u , $\hat{Q}^u(\varkappa, \mu)$ is only nonzero if the samples $\hat{u}\left(\varkappa + \frac{\mu}{2}\right)$ and $\hat{u}^*\left(\varkappa - \frac{\mu}{2}\right)$ of \hat{u} are a distance $\mu = \Omega l$ apart for some $l \in \mathbb{Z}^d$; see Figure 2.5 (right). Once such a μ is reached, $\hat{Q}^u(\varkappa, \mu)$ shows

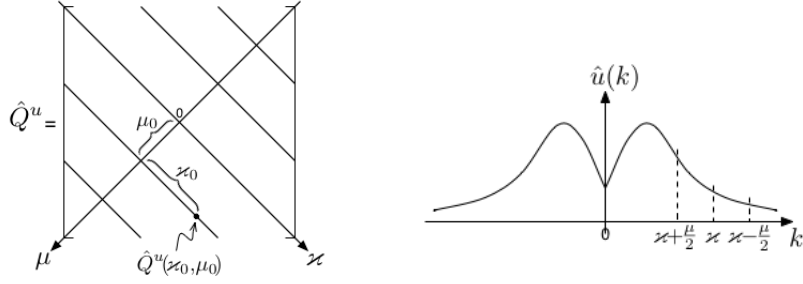


Figure 2.5: Graphical interpretation of $\hat{Q}^u(\varkappa, \mu)$ for $d = 1$.

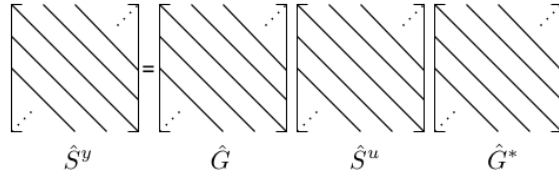


Figure 2.6: Composition of spatially periodic operators in the frequency domain for $d = 1$.

the amount of correlation between all such sample-pairs of \hat{u} as \varkappa varies.³

Finally, the spectral-correlation density of the output of a periodic operator with a cyclostationary input, $y = Gu$, is given by

$$\begin{aligned}
 \hat{S}^y(k, \kappa) &= \mathcal{E}\{\hat{y}(k) \hat{y}^*(\kappa)\} = \mathcal{E}\{(\hat{G}\hat{u})(k) (\hat{G}\hat{u})^*(\kappa)\} \\
 &= \mathcal{E}\left\{\int_{\mathbb{R}^d} \int_{\mathbb{R}^d} \hat{G}(k, \kappa_1) \hat{u}(\kappa_1) \hat{u}^*(\kappa_2) \hat{G}^*(\kappa_2, \kappa) d\kappa_1 d\kappa_2\right\} \\
 &= \int_{\mathbb{R}^d} \int_{\mathbb{R}^d} \hat{G}(k, \kappa_1) \hat{S}^u(\kappa_1, \kappa_2) \hat{G}^*(\kappa_2, \kappa) d\kappa_1 d\kappa_2 \\
 &= (\hat{G} \hat{S}^u \hat{G}^*)(k, \kappa), \tag{2.20}
 \end{aligned}$$

where $\hat{S}^u(\kappa_1, \kappa_2) := \mathcal{E}\{\hat{u}(\kappa_1) \hat{u}^*(\kappa_2)\}$, and $\hat{G} \hat{S}^u \hat{G}^*$ indicates the ‘composition’ of kernels. It is possible to show that periodic kernels (with a common period) are closed under addition and composition. Hence from (2.9), (2.17), and (2.20), it follows that \hat{S}^y too is a periodic kernel. It is helpful to visualize the composition $\hat{S}^y = \hat{G} \hat{S}^u \hat{G}^*$ as shown in Figure 2.6. Such a kernel composition in $d = 1$ can be thought of as an extended form of matrix multiplication where the matrix elements are characterized by the continuously-varying indices k, κ . Of course if u is a wide-sense stationary random field and/or G is a spatially invariant operator, then \hat{S}^u and/or \hat{G} will become a diagonal operator in Figure 2.6. Finally the composition

³Compare this with the case of wide-sense stationary signals where \hat{S}^u is diagonal and hence $\hat{Q}^u(\varkappa, \mu) = 0$ for all $\mu \neq 0$, i.e. $\hat{u}(\varkappa)$ is not correlated to any sample other than itself.

defined by (2.20) can also be represented in the lifted representation by

$$\mathcal{S}_\theta^y = \mathcal{G}_\theta \mathcal{S}_\theta^u \mathcal{G}_\theta^*. \quad (2.21)$$

2.6 Representations of Spatially Periodic Systems

Consider the spatially periodic system G described by

$$\begin{aligned} [\partial_t \psi](t, x) &= [A \psi](t, x) + [B u](t, x), \\ y(t, x) &= [C \psi](t, x) + [D u](t, x), \end{aligned} \quad (2.22)$$

where $x \in \mathbb{R}^d$, A , B , C and D are spatially periodic operators⁴ with a common period X . A is defined on a dense domain $\mathcal{D} \subset L^2(\mathbb{R}^d)$ and is closed, and B , C , and D are bounded operators. u , y and ψ are the spatio-temporal input, output and state of the system, respectively. Clearly, for any given time t , $\psi(t, \cdot)$ is a spatial function on $L^2(\mathbb{R}^d)$, and thus (2.22) is an infinite-dimensional linear system.

We refer to the operators A , B , C , D as the *system operators*. We specifically refer to A as the *infinitesimal generator* of the system. We assume that A generates a *strongly continuous semigroup* (also known as a C_0 -semigroup) denoted by e^{At} [3].

Example 2 Consider the spatially periodic heat equation on $x \in \mathbb{R}$

$$\begin{aligned} \partial_t \psi(t, x) &= (\partial_x^2 - \alpha \cos(\Omega x)) \psi(t, x) + u(t, x), \\ y(t, x) &= \psi(t, x), \end{aligned} \quad (2.23)$$

with real $\alpha \neq 0$ and $\Omega > 0$.⁵ Clearly $A = \partial_x^2 + \alpha \cos(\Omega x)$ with domain

$$\mathcal{D} = \left\{ \phi \in L^2(\mathbb{R}) \mid \phi, \frac{d\phi}{dx} \text{ absolutely continuous, } \frac{d^2\phi}{dx^2} \in L^2(\mathbb{R}) \right\},$$

$B = C = \delta(x)$ are the identity convolution operator on $L^2(\mathbb{R})$, and $D \equiv 0$. ■

⁴Any number of these operators can be spatially invariant, such operators constituting a subclass of spatially periodic operators.

⁵By $\partial_t \psi(t, x)$ and $\partial_x^2 \psi(t, x)$ we mean the spatio-temporal functions $\partial_t \psi$ and $\partial_x^2 \psi$ evaluated at the point (t, x) .

The system (2.22) can also be represented by a spatio-temporal kernel G ,

$$\begin{aligned} y(t, x) &= (Gu)(t, x) \\ &= \int_{\mathbb{R}^d} \int_0^\infty G(t, \tau; x, \chi) u(\tau, \chi) d\tau d\chi, \end{aligned}$$

where G satisfies

$$G(t, \tau; x, \chi) = G(t - \tau; x, \chi), \quad (2.24)$$

$$G(t, \tau; x + Xm, \chi + Xm) = G(t, \tau; x, \chi), \quad (2.25)$$

for all $t \geq \tau \geq 0$ and all $x, \chi \in \mathbb{R}^d$, with an abuse of notation in using G in (2.24) to represent both the kernel and the temporal impulse response of the system.

On the other hand, one could apply the spatial Fourier transform to both sides of (2.22) to get

$$\begin{aligned} [\partial_t \hat{\psi}](t, k) &= [\hat{A} \hat{\psi}](t, k) + [\hat{B} \hat{u}](t, k), \\ \hat{y}(t, k) &= [\hat{C} \hat{\psi}](t, k) + [\hat{D} \hat{u}](t, k), \end{aligned} \quad (2.26)$$

with $k \in \mathbb{R}^d$. This system corresponds to the kernel

$$\hat{G}(t, \tau; k, \kappa) = \hat{G}(t - \tau; k, \kappa), \quad (2.27)$$

$$\hat{G}(t, \tau; k, \kappa) = \sum_{l \in \mathbb{Z}^d} \hat{G}_l(t, \tau; k) \delta(k - \kappa - \Omega l), \quad (2.28)$$

for all $t \geq \tau \geq 0$ and $k, \kappa \in \mathbb{R}^d$. Notice that for any given t , $\hat{G}(t; \cdot, \cdot)$ is a Fourier kernel of the form illustrated in Figure 2.2. Applying the lifting transform to both sides of (2.26) we have

$$\begin{aligned} [\partial_t \psi_\theta](t) &= [\mathcal{A}_\theta \psi_\theta](t) + [\mathcal{B}_\theta u_\theta](t), \\ y_\theta(t) &= [\mathcal{C}_\theta \psi_\theta](t) + [\mathcal{D}_\theta u_\theta](t), \end{aligned} \quad (2.29)$$

with $\theta \in \Theta$. The impulse response of (2.29) has the form

$$\mathcal{G}_\theta(t) = \mathcal{C}_\theta e^{\mathcal{A}_\theta t} \mathcal{B}_\theta + \mathcal{D}_\theta. \quad (2.30)$$

Finally, the transfer functions of the systems (2.22), (2.26), (2.29), correspond respectively to

$$\begin{aligned} G(\omega) &:= C(j\omega I - A)^{-1}B + D, \\ \hat{G}(\omega) &:= \hat{C}(j\omega \hat{I} - \hat{A})^{-1}\hat{B} + \hat{D}, \\ G_\theta(\omega) &:= \mathcal{C}_\theta(j\omega \mathcal{I} - \mathcal{A}_\theta)^{-1}\mathcal{B}_\theta + \mathcal{D}_\theta. \end{aligned}$$

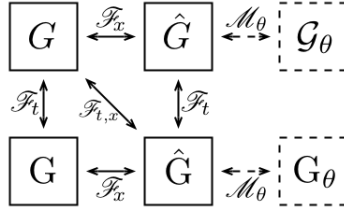


Figure 2.7: Relationship between different representations of the spatio-temporal system G . \mathcal{F}_x is the spatial Fourier transform, and \mathcal{F}_t the temporal Fourier transform. \mathcal{M}_θ is the frequency lifting operator.

Figure 2.7 summarizes the notational conventions used in this work.

Example 2 continued *Let us return to the example of the periodic heat equation on the real line described by (2.23). Rewriting the system in its lifted representation we have*

$$\begin{aligned}\partial_t \psi_\theta(t) &= \mathcal{A}_\theta \psi_\theta(t) + \mathcal{B}_\theta u_\theta(t), \\ y_\theta(t) &= \mathcal{C}_\theta \psi_\theta(t) + \mathcal{D}_\theta u_\theta(t),\end{aligned}\tag{2.31}$$

with $\theta \in [0, \Omega)$, where from Example 1 of Section 2.5

$$\mathcal{A}_\theta = \begin{bmatrix} \ddots & & & \\ & \ddots & & \\ & & -(\theta + \Omega n)^2 & \\ & & & \ddots \end{bmatrix} - \frac{\alpha}{2} \begin{bmatrix} \ddots & \ddots & & \\ & \ddots & 0 & 1 \\ & & 1 & 0 \\ & & & \ddots \\ & & & & \ddots & \ddots \end{bmatrix},\tag{2.32}$$

$$\mathcal{B}_\theta = \mathcal{C}_\theta = \begin{bmatrix} \ddots & & & \\ & \ddots & & \\ & & 1 & \\ & & & \ddots \end{bmatrix}, \quad \mathcal{D}_\theta \equiv 0,\tag{2.33}$$

$$\mathbf{G}_\theta(\omega) = \mathcal{C}_\theta (j\omega\mathbf{I} - \mathcal{A}_\theta)^{-1} \mathcal{B}_\theta + \mathcal{D}_\theta = \begin{bmatrix} \ddots & \ddots & & & \\ & \ddots & \ddots & & \\ & & \ddots & \alpha/2 & \\ \alpha/2 & j\omega + (\theta + \Omega n)^2 & \alpha/2 & & \\ & & \alpha/2 & \ddots & \ddots \\ & & & \ddots & \ddots \end{bmatrix}^{-1}.\tag{2.34}$$

Notice that (2.31)–(2.34) is now fully decoupled in the variable θ . In other words, (2.23) is equivalent to the family of state-space representations (2.31)–(2.33) pa-

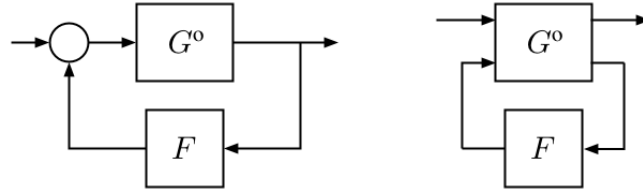


Figure 2.8: Left: A spatially periodic system, as the closed-loop interconnection of a spatially invariant system G^o and a spatially periodic operator F . Right: A spatially periodic system can be written as the LFT of a system G^o with spatially invariant dynamics and a spatially periodic operator F .

parameterized by $\theta \in [0, \Omega)$. ■

Remark 5 *An advantage of the lifted representation is that it allows for (2.31) to be treated like a multivariable system (under minor technical assumptions). It is then possible to extend many existing tools from linear systems theory to (2.31). For example Chapter 4 generalizes the Nyquist criterion to determine the stability of (2.31), Chapter 5 uses the algebraic Lyapunov equation to calculate the \mathcal{H}^2 -norm of G , and Chapter 6 employs Geršgorin-like arguments to locate the spectrum of \mathcal{A}_θ . Also [22] [26] use the lifted representation to investigate the occurrence of parametric resonance in spatially periodic systems.*

Remark 6 *It is interesting to note that (2.23) can be written as the feedback interconnection of the spatially invariant system G^o*

$$\begin{aligned}\partial_t \psi(t, x) &= \partial_x^2 \psi(t, x) + w(t, x), \\ y(t, x) &= \psi(t, x),\end{aligned}$$

and the (memoryless) spatially periodic multiplication operator $F(x) = -\alpha \cos(\Omega x)$,

$$w(t, x) = -\alpha \cos(\Omega x) y(t, x) + u(t, x),$$

as in Figure 5.1 (left).

More generally, a wide class of spatially periodic systems can be written as the LFT (linear fractional transformation [27]) of a spatially periodic system with spatially invariant dynamics, and a bounded spatially periodic pure multiplication operator. To be more concrete, the spatially periodic system

$$\begin{aligned}\partial_t \psi(t, x) &= A \psi(t, x) + B u(t, x), \\ y(t, x) &= C \psi(t, x) + D u(t, x),\end{aligned}$$

can be considered as

$$\begin{aligned}\partial_t \psi(t, x) &= (A^\circ + B^\circ F C^\circ) \psi(t, x) + B u(t, x), \\ y(t, x) &= C \psi(t, x) + D u(t, x),\end{aligned}\tag{2.35}$$

where the (possibly unbounded) operators $A^\circ, B^\circ, C^\circ$ are spatially invariant, the bounded operators B, C, D are spatially periodic, and F is a bounded spatially periodic pure multiplication operator. $A^\circ, B^\circ, C^\circ$ and $E := B^\circ F C^\circ$ are all defined on a dense domain $\mathcal{D} \subset L^2(\mathbb{R})$. Finally, (2.35) corresponds to the LFT of the system

$$G^\circ = \left[\begin{array}{c|cc} A^\circ & B & B^\circ \\ \hline C & D & 0 \\ C^\circ & 0 & 0 \end{array} \right]$$

and the operator F , as shown Figure 5.1 (right). ■

Finally, the spectral-correlation density of the output y of a linear spatially periodic system G with input u is given by

$$\begin{aligned}\hat{R}^y(t, \tau; k, \kappa) &= \mathcal{E}\{\hat{y}(t, k) \hat{y}^*(\tau, \kappa)\} = \mathcal{E}\{(\hat{G}\hat{u})(t, k) (\hat{G}\hat{u})^*(\tau, \kappa)\} \\ &= \mathcal{E}\left\{ \int \hat{G}(t, \tau_1; k, \kappa_1) \hat{u}(\tau_1, \kappa_1) \hat{u}^*(\tau_2, \kappa_2) \hat{G}^*(\tau_2, \tau; \kappa_2, \kappa) d\kappa_1 d\kappa_2 d\tau_1 d\tau_2 \right\} \\ &= \int \hat{G}(t, \tau_1; k, \kappa_1) \hat{R}^u(\tau_1, \tau_2; \kappa_1, \kappa_2) \hat{G}^*(\tau_2, \tau; \kappa_2, \kappa) d\kappa_1 d\kappa_2 d\tau_1 d\tau_2 \\ &= (\hat{G} \hat{R}^u \hat{G}^*)(t, \tau; k, \kappa),\end{aligned}\tag{2.36}$$

where $\hat{R}^u(\tau_1, \tau_2; \kappa_1, \kappa_2) := \mathcal{E}\{\hat{u}(\tau_1, \kappa_1) \hat{u}^*(\tau_2, \kappa_2)\}$. If u is taken to be wide-sense stationary in the temporal direction and wide-sense cyclostationary in the spatial direction, then

$$\hat{R}^u(t, \tau; k, \kappa) = \hat{R}^u(t - \tau; k, \kappa),\tag{2.37}$$

$$\hat{R}^u(t, \tau; k, \kappa) = \sum_{l \in \mathbb{Z}^d} \hat{R}_l^u(t, \tau; k) \delta(k - \kappa - \Omega l),\tag{2.38}$$

for all $t \geq \tau \geq 0$ and $k, \kappa \in \mathbb{R}^d$. Comparing (2.37)–(2.38) and (2.27)–(2.28), it is clear that in (2.36) the operators \hat{G} , \hat{R}^u and \hat{G}^* are all spatially periodic with a common period and have the same structure. Hence, by the closedness under compositions of such operators, \hat{R}^y will inherit the same structure and we have

$$\hat{R}^y(t, \tau; k, \kappa) = \hat{R}^y(t - \tau; k, \kappa),\tag{2.39}$$

$$\hat{R}^y(t, \tau; k, \kappa) = \sum_{l \in \mathbb{Z}^d} \hat{R}_l^y(t, \tau; k) \delta(k - \kappa - \Omega l).\tag{2.40}$$

2.7 Appendix to Chapter 2

Proof of Theorem 1

From $R^u(x, \chi) = R^u(x + Xm, \chi + Xm)$ and using $\xi := x - \chi$ we have

$$R^u(x, \chi) = R^u(\chi + \xi, \chi) = R^u(\chi + Xm + \xi, \chi + Xm),$$

which means that $R^u(\chi + \xi, \chi)$ is periodic in χ and hence admits a Fourier series expansion

$$R^u(\chi + \xi, \chi) = \sum_{l \in \mathbb{Z}^d} r_l(\xi) e^{j(\Omega l)^* \chi}.$$

Thus $R^u(x, \chi) = \sum_l r_l(x - \chi) e^{j(\Omega l)^* \chi}$. Substituting in (2.16) and using the change of variables $\sigma := k - \kappa$,

$$\begin{aligned} \hat{S}^u(k, \kappa) &= \int_{\mathbb{R}^d} \int_{\mathbb{R}^d} e^{-j(k^* x - \kappa^* \chi)} R^u(x, \chi) dx d\chi \\ &= \int_{\mathbb{R}^d} \int_{\mathbb{R}^d} e^{-j\sigma^* \chi} e^{-jk^*(x-\chi)} \sum_{l \in \mathbb{Z}^d} r_l(x - \chi) e^{j(\Omega l)^* \chi} dx d\chi \\ &= \sum_{l \in \mathbb{Z}^d} \int_{\mathbb{R}^d} e^{-j\sigma^* \chi + j(\Omega l)^* \chi} \int_{\mathbb{R}^d} e^{-jk^*(x-\chi)} r_l(x - \chi) dx d\chi \\ &= \sum_{l \in \mathbb{Z}^d} \int_{\mathbb{R}^d} e^{-j(\sigma - \Omega l)^* \chi} \hat{S}_l^u(k) d\chi = \sum_{l \in \mathbb{Z}^d} \hat{S}_l^u(k) \delta(k - \kappa - \Omega l), \end{aligned}$$

where $\hat{S}_l^u(\cdot)$ is the Fourier transform of $r_l(\cdot)$.

Chapter 3

Norms of Spatially Periodic Systems

Does anyone believe that the difference between the Lebesgue and Riemann integrals can have physical significance, and that whether say, an airplane would or would not fly could depend on this difference? If such were claimed, I should not care to fly in that plane.

R. W. Hamming

3.1 Introduction

In this chapter we introduce the notion of the \mathcal{H}^2 - and \mathcal{H}^∞ -norms for spatially periodic *systems*, and give both deterministic and stochastic interpretations of our definition for the \mathcal{H}^2 -norm. To motivate this, we first examine the definition of these norms for the case of spatially periodic *operators*, which we denote by $\mathcal{H}_{\text{sp}}^2$ and $\mathcal{H}_{\text{sp}}^\infty$. Again the bi-infinite matrix representation (i.e., the frequency lifted representation) plays a central role in allowing us to extend methods from standard linear systems theory to compute the norms of spatially periodic systems. This representation is also used to discuss truncations and the numerical calculation of norms. We finish the chapter with some examples. Throughout this chapter, it is always assumed that the spatially periodic system G is exponentially stable.

Notation: We shall denote by \underline{G} the system described by (2.22) but with $D \equiv 0$, i.e., $G = \underline{G} + D$. Clearly, all the statements and definitions made for G therein apply equally to \underline{G} , mutatis mutandis. We also define \underline{R}^y to be the output autocorrelation of the system \underline{G} given an input with autocorrelation R^u . ■

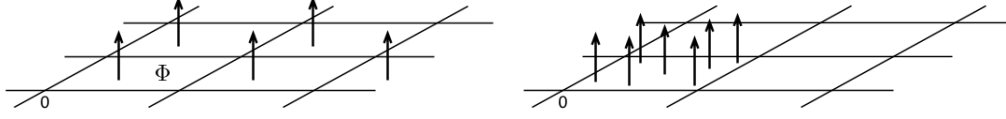


Figure 3.1: Left: All impulses occur at points that are distance Xm apart, $m \in \mathbb{Z}^2$. Right: Spatial impulses applied at different points inside of a primitive cell Φ in \mathbb{R}^2 .

3.2 Deterministic Interpretation of the \mathcal{H}^2 -Norm

3.2.1 Spatially Periodic Operators

In [28] the problem of defining the \mathcal{H}^2 -norm of a linear time-periodic system is addressed. Here we employ a similar approach to define the $\mathcal{H}_{\text{sp}}^2$ -norm of a spatially periodic operator.

Let us consider a scalar spatially periodic *operator* with kernel $G(x, \chi) = G(x + Xm, \chi + Xm)$, $m \in \mathbb{Z}^d$. First, notice that $G(\cdot, \chi)$ is the response¹ of G to a spatial impulse applied at the point χ , $v^\chi(x) := \delta(x - \chi)$. Since G is not spatially invariant, the response of the system to the input $v^{\chi_1}(x)$ could in general be different from its response to $v^{\chi_2}(x)$ if $\chi_2 \neq \chi_1$. This is unless χ_1 and χ_2 satisfy $\chi_2 = \chi_1 + Xm$, $m \in \mathbb{Z}^d$, in which case the response to the first input will merely be a shifted version of the response to the second input and vice versa (due to the spatial periodicity of G). For example in Figure 3.1 (left) the response to each delta is only a shifted version of the response to another. This means that to fully capture the effect of the periodic operator, one needs to ‘excite’ all its responses to impulse inputs given at every point inside one primitive cell Φ , and then take their average on the volume $V(\Phi)$ of the primitive cell; see Figure 3.1 (right). Thus we define the $\mathcal{H}_{\text{sp}}^2$ -norm of a spatially periodic operator as

$$\|G\|_{\mathcal{H}_{\text{sp}}^2}^2 := \frac{1}{V(\Phi)} \int_{\Phi} \left[\int_{\mathbb{R}^d} |(Gv^\chi)(x)|^2 dx \right] d\chi. \quad (3.1)$$

We next give a characterization of this norm in the frequency domain.

¹Here by ‘response’ we mean a purely spatial function; there are no temporal variations at this point.

Theorem 2 *If G is a scalar spatially periodic operator, we have*

$$\|G\|_{\mathcal{H}_{sp}^2}^2 := \frac{1}{V(\Phi)} \int_{\Phi} \int_{\mathbb{R}^d} |G(x, \chi)|^2 dx d\chi \quad (3.2)$$

$$= \frac{1}{2\pi} \sum_{l \in \mathbb{Z}^d} \int_{\mathbb{R}^d} |\hat{G}_l(k)|^2 dk \quad (3.3)$$

$$= \frac{1}{2\pi} \int_{\Theta} \text{trace}[\mathcal{G}_\theta \mathcal{G}_\theta^*] d\theta. \quad (3.4)$$

Proof: See Appendix. ■

Notice that (3.3) is nothing but the integral of the amplitudes of all the impulse sheets \hat{G}_l . Also, comparing (3.4) and (2.15) we have $\|G\|_{\mathcal{H}_{sp}^2}^2 = \frac{1}{2\pi} \int_{\Theta} \|\mathcal{G}_\theta\|_{\text{HS}}^2 d\theta$.

3.2.2 Linear Spatially Periodic Systems

Now consider a scalar linear spatially periodic *system* described by its kernel $G(t - \tau; x, \chi)$ which satisfies (2.24)–(2.25), and let us assume for now that $D \equiv 0$. Inspired by the discussions of the previous subsection we define

$$\|G\|_{\mathcal{H}^2}^2 := \frac{1}{V(\Phi)} \int_{\Phi} \int_{\mathbb{R}^d} \int_0^\infty |G(t; x, \chi)|^2 dt dx d\chi.$$

This definition can be interpreted as

$$\|G\|_{\mathcal{H}^2}^2 = \frac{1}{V(\Phi)} \int_{\Phi} \int_{\mathbb{R}^d} \int_0^\infty |(Gu^\chi)(t, x)|^2 dt dx d\chi,$$

where $u^\chi(t, x) := w(t)v^\chi(x) = \delta(t)\delta(x - \chi)$ [29].² Hence for an exponentially stable MIMO (multi-input multi-output) system G with $D \neq 0$, the appropriate definition of the \mathcal{H}^2 -norm is given by

$$\begin{aligned} \|G\|_{\mathcal{H}^2}^2 &:= \|\underline{G}\|_{\mathcal{H}^2}^2 + \|D\|_{\mathcal{H}_{sp}^2}^2 \\ &= \frac{1}{V(\Phi)} \int_{\Phi} \int_{\mathbb{R}^d} \int_0^\infty \text{trace}[\underline{G}(t; x, \chi) \underline{G}^*(t; \chi, x)] dt dx d\chi + \|D\|_{\mathcal{H}_{sp}^2}^2. \end{aligned} \quad (3.5)$$

Notice that if a spatially periodic system G has no temporal dynamics (i.e. it is a memoryless system), it becomes a purely spatial one $G = D$, where D is a spatially periodic operator. Thus $\|\underline{G}\|_{\mathcal{H}^2}^2 = 0$ and one employs the arguments of the previous subsection to find $\|G\|_{\mathcal{H}^2}^2 = \|D\|_{\mathcal{H}_{sp}^2}^2$. It is also interesting to view the \mathcal{H}^2 -norm in the spatial-frequency domain.

²We have used the fact that G is time-invariant and thus $\delta(t)$ is enough to capture its complete temporal response.

Theorem 3 Consider the exponentially stable spatially periodic system G with $\mathcal{G}_\theta(t) = \mathcal{C}_\theta e^{A_\theta t} \mathcal{B}_\theta + \mathcal{D}_\theta$. If $\|G\|_{\mathcal{H}^2}^2$ as defined in (3.5) exists and is finite, then

$$\begin{aligned} \|G\|_{\mathcal{H}^2}^2 &= \frac{1}{2\pi} \int_{\Theta} \int_0^\infty \text{trace}[\underline{\mathcal{G}}_\theta(t) \underline{\mathcal{G}}_\theta^*(t)] dt d\theta + \|D\|_{\mathcal{H}_{sp}^2}^2 \\ &= \frac{1}{4\pi^2} \int_{\Theta} \int_{-\infty}^\infty \text{trace}[\underline{\mathcal{G}}_\theta(\omega) \underline{\mathcal{G}}_\theta^*(\omega)] d\omega d\theta + \|D\|_{\mathcal{H}_{sp}^2}^2 \\ &= \frac{1}{4\pi^2} \int_{-\infty}^\infty \sum_{l \in \mathbb{Z}^d} \int_{\mathbb{R}^d} \text{trace}[\hat{\underline{\mathcal{G}}}_l(\omega; k) \hat{\underline{\mathcal{G}}}_l^*(\omega; k)] dk d\omega + \|D\|_{\mathcal{H}_{sp}^2}^2. \end{aligned}$$

In addition,

$$\|G\|_{\mathcal{H}^2}^2 = \frac{1}{2\pi} \int_{\Theta} \text{trace}[\mathcal{C}_\theta \mathcal{P}_\theta \mathcal{C}_\theta^*] d\theta + \|D\|_{\mathcal{H}_{sp}^2}^2 = \frac{1}{2\pi} \int_{\Theta} \text{trace}[\mathcal{B}_\theta^* \mathcal{Q}_\theta \mathcal{B}_\theta] d\theta + \|D\|_{\mathcal{H}_{sp}^2}^2,$$

where \mathcal{P}_θ and \mathcal{Q}_θ are the solutions of the (θ -parameterized) algebraic Lyapunov equations

$$\mathcal{A}_\theta \mathcal{P}_\theta + \mathcal{P}_\theta \mathcal{A}_\theta^* = -\mathcal{B}_\theta \mathcal{B}_\theta^*, \quad \mathcal{A}_\theta^* \mathcal{Q}_\theta + \mathcal{Q}_\theta \mathcal{A}_\theta = -\mathcal{C}_\theta^* \mathcal{C}_\theta. \quad (3.6)$$

Proof: See Appendix. ■

Remark 7 It is known that for spatially distributed systems in dimensions $d \geq 2$, exponential stability is not enough to guarantee finiteness of the \mathcal{H}^2 -norm [30]. We will see an example of such a system in Section 3.6. Theorem 9 in the Appendix gives a sufficient condition for the \mathcal{H}^2 -norm to be finite in any spatial dimension.

3.3 Stochastic Interpretation of the \mathcal{H}^2 -Norm

3.3.1 Spatially Periodic Operators

Consider a scalar spatially periodic operator with Fourier kernel

$$\hat{G}(k, \kappa) = \sum_{l \in \mathbb{Z}^R} \hat{G}_l(k) \delta(k - \kappa - \Omega l).$$

Assume that G is fed with a wide-sense stationary spatial random field $v(x)$ with autocorrelation $R^v(x - \chi)$ and spectral-correlation density $\hat{S}^v(k, \kappa) = \hat{S}_0^v(k) \delta(k - \kappa)$, where $\hat{S}_0^v(k)$ is the spectral density of v . Then as seen in Section 2.5.2 the output $y(x) = (Gv)(x)$ will have the spectral-correlation density

$$\hat{S}^y = \hat{G} \hat{S}^v \hat{G}^*,$$

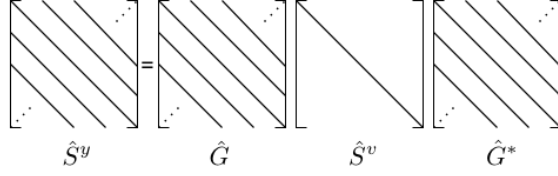


Figure 3.2: If a spatially periodic system G is given a stationary input u , the output y is cyclostationary.

which can be visualized as in Figure 3.2. Thus \hat{S}^y inherits the structure of \hat{G} and hence it becomes a *cyclostationary* random field. More specifically,

$$\begin{aligned}\hat{S}^y(k, \kappa) &= (\hat{G} \hat{S}^v \hat{G}^*)(k, \kappa) \\ &=: \sum_{l \in \mathbb{Z}^d} \hat{S}_l^y(k) \delta(k - \kappa - \Omega l),\end{aligned}\tag{3.7}$$

where

$$\hat{S}_0^y(k) = \sum_{l \in \mathbb{Z}^d} |\hat{G}_l(k)|^2 \hat{S}_0^v(k),\tag{3.8}$$

and all other $\hat{S}_l^y(k)$, $0 \neq l \in \mathbb{Z}^d$, can be found by forming the composition (3.7). Therefore the autocorrelation R^y satisfies

$$R^y(x + Xm, \chi + Xm) = R^y(x, \chi),$$

for all $m \in \mathbb{Z}^d$ and we have the following theorem.

Theorem 4 *Consider the scalar spatially periodic operator G . If $y = Gu$ and u is a white random field, then*

$$\begin{aligned}\|G\|_{\mathcal{H}_{sp}^2}^2 &= \frac{1}{V(\Phi)} \int_{\Phi} R^y(x, x) dx \\ &= \frac{1}{2\pi} \int_{\mathbb{R}^d} \hat{S}_0^y(k) dk.\end{aligned}$$

Proof: See Appendix. ■

To summarize, the \mathcal{H}_{sp}^2 -norm of a spatially periodic operator has the the following stochastic interpretation; it is the average over one period of the variance of the output random field when the input is a white random field.

3.3.2 Linear Spatially Periodic Systems

Now consider the scalar linear spatially periodic system described by $G(t - \tau; x, \chi)$ which satisfies (2.24)–(2.25), and let us assume for now that $D \equiv 0$. Suppose that

the system is given an input $u(t, x)$ which is a wide-sense stationary random field in both the temporal and the spatial directions, with autocorrelation function

$$\begin{aligned} R^u(t, \tau; x, \chi) &= R^u(t - \tau; x, \chi), \\ R^u(t, \tau; x, \chi) &= R^u(t, \tau; x - \chi), \end{aligned}$$

for all $t \geq \tau \geq 0$ and $x, \chi \in \mathbb{R}^d$. By what has been shown in the preceding subsection, we know that the output of the system $y(t, x) = (Gu)(t, x)$ is a random field with autocorrelation $R^y(t, \tau; x, \chi)$ that satisfies

$$\begin{aligned} R^y(t, \tau; x, \chi) &= R^y(t - \tau; x, \chi), \\ R^y(t, \tau; x + Xm, \chi + Xm) &= R^y(t, \tau; x, \chi), \end{aligned}$$

for all $t \geq \tau \geq 0$, $x, \chi \in \mathbb{R}^d$ and $m \in \mathbb{Z}^d$. Namely, the output random field remains wide-sense stationary in the temporal direction (due to the time-invariance of G), but inherits the spatial-periodicity of the system and as such becomes a cyclostationary random field in the spatial direction. The above identities are equivalent to those expressed in the spatial frequency domain in (2.39)–(2.40).

In particular, if the input u is a white random field in both the spatial and temporal directions, $\hat{S}^u(\omega, \nu; k, \kappa) = \delta(\omega - \nu) \delta(k - \kappa)$, then

$$\|G\|_{\mathcal{H}^2}^2 = \frac{1}{V(\Phi)} \int_{\Phi} R^y(0; x, x) dx.$$

Hence for an exponentially stable MIMO system G with $D \neq 0$, the stochastic interpretation of the \mathcal{H}^2 -norm would be

$$\begin{aligned} \|G\|_{\mathcal{H}^2}^2 &= \|\underline{G}\|_{\mathcal{H}^2}^2 + \|D\|_{\mathcal{H}_{\text{sp}}^2}^2 \\ &= \frac{1}{V(\Phi)} \int_{\Phi} \text{trace}[\underline{R}^y(0; x, x)] dx + \|D\|_{\mathcal{H}_{\text{sp}}^2}^2 \\ &= \frac{1}{4\pi^2} \int_{-\infty}^{\infty} \int_{\mathbb{R}^d} \text{trace}[\hat{\underline{S}}_0^y(\omega; k)] dk d\omega + \|D\|_{\mathcal{H}_{\text{sp}}^2}^2, \end{aligned}$$

where $\hat{\underline{S}}^y$ is the spatio-temporal Fourier transform of \underline{R}^y , and one can employ the stochastic methods of the previous subsection to find $\|D\|_{\mathcal{H}_{\text{sp}}^2}^2$.

Remark 8 *As mentioned previously, for certain spatial systems in dimensions $d \geq 2$ with white random input the value of the variance $R^y(0; x, x)$ may be infinite [30]. These are systems for which (3.14) is not finite. In such cases the output random field can still be given an interpretation in the sense of distributions [31]. Also, one can still compute the two-point correlations $R^y(\Delta t; x, x)$ and $R^y(0; x, x + \Delta x)$, which will be finite for $\Delta t \neq 0$ and $\Delta x \neq 0$. We give an example of this in Section 3.6. ■*

3.4 The \mathcal{H}^∞ -Norm

3.4.1 Spatially Periodic Operators

We define the $\mathcal{H}_{\text{sp}}^\infty$ -norm of a bounded spatial operator G as its L^2 -induced norm $\|G\|_{L^2/L^2}$.

Theorem 5 *If G is a bounded spatially periodic operator, then*

$$\|G\|_{\mathcal{H}_{\text{sp}}^\infty}^2 := \|G\|_{L^2/L^2}^2 = \|\hat{G}\|_{L^2/L^2}^2 = \sup_{\theta \in \Theta} \|\mathcal{G}_\theta\|_{\ell^2/\ell^2}^2 = \sup_{\theta \in \Theta} \sup_{\lambda \in \Sigma(\mathcal{G}_\theta^* \mathcal{G}_\theta)} |\lambda|.$$

Proof: See Appendix. ■

Example 3 *Let us compute the $\mathcal{H}_{\text{sp}}^\infty$ -norm of the bounded spatially periodic pure multiplication operator G described by the periodic function $F(x) = \cos(\Omega x)$. First notice that since G is already a multiplication (i.e. diagonal) operator in the spatial domain, a spatial Fourier transform will not lead to a simplification in this particular problem. In fact*

$$\|G\|_{L^2/L^2} = \sup_{x \in \mathbb{R}} |\cos(\Omega x)| = 1.$$

But for illustrative purposes, let us also calculate this norm in the spatial-frequency domain. $\mathcal{G}_\theta = \mathcal{F}$ has the form given in Example 1 of Section 2.5. One can write $\mathcal{F} = \frac{1}{2}\mathcal{R} + \frac{1}{2}\mathcal{L}$ where \mathcal{R} and \mathcal{L} are the right- and left-shift operators on ℓ^2 , respectively,

$$\mathcal{R} = \begin{bmatrix} \ddots & \ddots & & & \\ \ddots & 0 & 0 & & \\ & 1 & 0 & \ddots & \\ & & \ddots & \ddots & \end{bmatrix}, \quad \mathcal{L} = \begin{bmatrix} \ddots & \ddots & & & \\ \ddots & 0 & 1 & & \\ & 0 & 0 & \ddots & \\ & & \ddots & \ddots & \end{bmatrix}.$$

Clearly, $\|\mathcal{F}\|_{\ell^2/\ell^2} \leq \frac{1}{2}\|\mathcal{R}\|_{\ell^2/\ell^2} + \frac{1}{2}\|\mathcal{L}\|_{\ell^2/\ell^2}$. Since \mathcal{R} and \mathcal{L} are shift operators, they are unitary, and thus $\|\mathcal{R}\|_{\ell^2/\ell^2} = \|\mathcal{L}\|_{\ell^2/\ell^2} = 1$, which means that $\|\mathcal{F}\|_{\ell^2/\ell^2} \leq 1$. It is not hard to show that this upper bound is actually achieved, and hence $\|\hat{G}\|_{L^2/L^2} = \sup_{\theta \in \Theta} \|\mathcal{G}_\theta\|_{\ell^2/\ell^2} = 1$.

Finally we demonstrate that this norm can also be found from the spectrum of $\mathcal{G}_\theta^ \mathcal{G}_\theta$. It is not hard to show that $\Sigma(\mathcal{G}_\theta^* \mathcal{G}_\theta) = \Sigma(\mathcal{F}^* \mathcal{F}) = [0, 1]$, and as a result $\sup_{\theta \in \Theta} \sup_{\lambda \in \Sigma(\mathcal{G}_\theta^* \mathcal{G}_\theta)} |\lambda| = 1$. ■*

3.4.2 Linear Spatially Periodic Systems

We define the \mathcal{H}^∞ -norm of a spatially periodic system G as its spatio-temporal L^2 -induced norm. In the following, by the spatio-temporal function $u \in L^2_{L^2(\mathbb{R}^d)}$ we mean that at any given time t , $u(t, \cdot)$ is a spatial function in $L^2(\mathbb{R}^d)$ such that $\int_0^\infty \|u(t, \cdot)\|_{L^2(\mathbb{R}^d)}^2 dt < \infty$. Let \mathbf{u} denote the temporal Fourier transform of u , and $\mathbf{G}\mathbf{u}$ the temporal Fourier transform of $G u$. We have

$$\|G\|_{\mathcal{H}^\infty}^2 := \sup_{u \in L^2_{L^2}} \frac{\|G u\|_{L^2_{L^2}}^2}{\|u\|_{L^2_{L^2}}^2} = \sup_{\mathbf{u} \in L^2_{L^2}} \frac{\|\mathbf{G}\mathbf{u}\|_{L^2_{L^2}}^2}{\|\mathbf{u}\|_{L^2_{L^2}}^2} = \sup_{\omega \in \mathbb{R}} \|G(\omega)\|_{L^2/L^2}^2.$$

Notice here that for every given ω , $G(\omega)$ is a spatially periodic operator on $L^2(\mathbb{R}^d)$. Now for a spatial function $v \in L^2(\mathbb{R}^d)$ let \hat{v} denote the spatial Fourier transform of v , and $\hat{G}(\omega)\hat{v}$ the spatial Fourier transform of $G(\omega)v$. Then

$$\begin{aligned} \sup_{\omega \in \mathbb{R}} \|G(\omega)\|_{L^2/L^2}^2 &= \sup_{\omega \in \mathbb{R}} \sup_{v \in L^2} \frac{\|G(\omega)v\|_{L^2}^2}{\|v\|_{L^2}^2} = \sup_{\omega \in \mathbb{R}} \sup_{\hat{v} \in L^2} \frac{\|\hat{G}(\omega)\hat{v}\|_{L^2}^2}{\|\hat{v}\|_{L^2}^2} \\ &= \sup_{\omega \in \mathbb{R}} \sup_{\theta \in \Theta} \sup_{v_\theta \in \ell^2} \frac{\|G_\theta(\omega)v_\theta\|_{\ell^2}^2}{\|v_\theta\|_{\ell^2}^2} = \sup_{\omega \in \mathbb{R}} \sup_{\theta \in \Theta} \|G_\theta(\omega)\|_{\ell^2/\ell^2}^2, \end{aligned}$$

where again we have used the property that the Fourier and lifting transforms preserve norms. Finally, using Theorem 5,

$$\sup_{\omega \in \mathbb{R}} \sup_{\theta \in \Theta} \|G_\theta(\omega)\|_{\ell^2/\ell^2}^2 = \sup_{\omega \in \mathbb{R}} \sup_{\theta \in \Theta} \sup_{\lambda \in \Sigma(G_\theta^*(\omega)G_\theta(\omega))} |\lambda|.$$

We have thus proved the following theorem.

Theorem 6 *For the exponentially stable spatially periodic system G ,*

$$\begin{aligned} \|G\|_{\mathcal{H}^\infty}^2 &= \sup_{\omega \in \mathbb{R}} \|G(\omega)\|_{L^2/L^2}^2 = \sup_{\omega \in \mathbb{R}} \sup_{\theta \in \Theta} \|G_\theta(\omega)\|_{\ell^2/\ell^2}^2 \\ &= \sup_{\omega \in \mathbb{R}} \sup_{\theta \in \Theta} \sup_{\lambda \in \Sigma(G_\theta^*(\omega)G_\theta(\omega))} |\lambda|. \end{aligned}$$

■

3.5 Numerical Implementation and Finite Dimensional Truncations

In order to numerically calculate the \mathcal{H}^2 - or \mathcal{H}^∞ -norm of a spatially periodic system, one has to perform a finite-dimensional truncation of the infinite-dimensional operators that describe the system. For example, to calculate the \mathcal{H}^2 -norm via

the Lyapunov equations in Theorem 3, a truncation of the operators \mathcal{A}_θ , \mathcal{B}_θ and \mathcal{C}_θ has to be performed. The same applies to the operator $G_\theta(\omega)$ if it is desired to calculate the \mathcal{H}^∞ -norm as in Theorem 6. And clearly one needs to verify whether the \mathcal{H}^2 - and \mathcal{H}^∞ -norms of the original system can be arbitrarily-well approximated via these finite-dimensional approximations as the truncation size increases.

Throughout this section we assume for simplicity that $d = 1$, i.e., the spatial coordinate has dimension one. We also assume that the spatially periodic system G can be written in the configuration described by (2.35) and depicted in Figure 5.1 (right), i.e. G is the system resulting from the LFT of a spatially periodic system G° and a (memoryless and bounded) spatially periodic multiplication operator F . We assume B° and C° are bounded operators, $D \equiv 0$, and that both G and G° are exponentially stable and have finite \mathcal{H}^2 - and \mathcal{H}^∞ -norms. The final assumption implies, in particular, that $\rho(A)$ and $\rho(A^\circ)$ both contain \mathbb{C}^+ .

Notation: We use $\Pi T \Pi$ to denote the $(2N+1) \times (2N+1)$ truncation of the bi-infinite matrix representation of an operator T on ℓ^2 , where Π is the projection defined by

$$\text{diag} \left\{ \dots, 0, \underbrace{I, \dots, I}_{\substack{\text{center} \\ \downarrow \\ 2N+1 \text{ times}}}, \dots, I, 0, \dots \right\}.$$

Of the properties of Π is that it commutes with all (block) diagonal operators, $T \Pi = \Pi T = \Pi T \Pi$ for diagonal T , and also $\Pi \Pi = \Pi$. The following notational conventions may seem rather tedious but the main idea is in fact very simple. The truncated operator $\mathfrak{B}_\theta := \Pi \mathcal{B}_\theta \Pi$ denotes the *bi-infinite* matrix made from \mathcal{B}_θ by replacing all entries outside the center $(2N+1) \times (2N+1)$ block with zeros. The operator $\mathbb{B}_\theta := \Pi \mathcal{B}_\theta \Pi \big|_{\Pi \ell^2}$ (the restriction of \mathcal{B}_θ to the subspace $\Pi \ell^2$) denotes the $(2N+1) \times (2N+1)$ *finite* matrix equal to the center $(2N+1) \times (2N+1)$ block of \mathfrak{B}_θ (or that of \mathcal{B}_θ). Thus

$$\mathcal{B}_\theta = \begin{bmatrix} \ddots & \vdots & \ddots \\ \cdots & \mathbb{B}_\theta & \cdots \\ \ddots & \vdots & \ddots \end{bmatrix}, \quad \mathfrak{B}_\theta = \begin{bmatrix} 0 & 0 & 0 \\ 0 & \mathbb{B}_\theta & 0 \\ 0 & 0 & 0 \end{bmatrix},$$

where \mathcal{B}_θ and \mathfrak{B}_θ are *infinite*-dimensional matrices acting on ℓ^2 and \mathbb{B}_θ a *finite*-dimensional matrix. The same notational conventions apply to \mathfrak{C}_θ , $\mathfrak{A}_\theta^\circ$, $\mathfrak{B}_\theta^\circ$, $\mathfrak{C}_\theta^\circ$, \mathfrak{F} , and \mathcal{C}_θ , \mathcal{A}_θ° , \mathcal{B}_θ° , \mathcal{C}_θ° , \mathcal{F} . In addition, recall that $\mathcal{A}_\theta := \mathcal{A}_\theta^\circ + \mathcal{B}_\theta^\circ \mathcal{F} \mathcal{C}_\theta^\circ$, $G_\theta^\circ(\omega) := \mathcal{C}_\theta(j\omega \mathcal{I} - \mathcal{A}_\theta^\circ)^{-1} \mathcal{B}_\theta$, and $G_\theta(\omega) := \mathcal{C}_\theta(j\omega \mathcal{I} - \mathcal{A}_\theta)^{-1} \mathcal{B}_\theta$. \blacksquare

3.5.1 \mathcal{H}^∞ -norm

It is known that a compact operator $T \in \mathcal{B}_0(\ell^2)$ can be approximated arbitrarily-well by finite-dimensional matrices [32]. In fact it follows from the definition of a compact operator that the entries $\{t_{nm}\}_{n,m \in \mathbb{Z}}$ of the matrix representation of T decay in all directions such that $\|T - \Pi T\|_{\ell^2/\ell^2}$, $\|T - T\Pi\|_{\ell^2/\ell^2}$, and $\|T - \Pi T\Pi\|_{\ell^2/\ell^2}$ all approach zero as N grows large.

The main assumption here is that

$$\sup_{\omega \in \mathbb{R}} \|(j\omega I - \hat{A}^\circ(k))^{-1}\| \rightarrow 0 \quad \text{as} \quad |k| \rightarrow \infty. \quad (3.9)$$

This implies the compactness of the diagonal operator $(j\omega\mathcal{I} - \mathcal{A}_\theta^\circ)^{-1}$ for all $\omega \in \mathbb{R}$ and $\theta \in [0, \Omega)$. The fact that compact operators form a two-sided ideal in the algebra of bounded operators $\mathcal{B}(\ell^2)$ and arguments similar to those in the proof of Theorem 9 can now be used to show that $(j\omega\mathcal{I} - \mathcal{A}_\theta)^{-1}$ and $\mathbf{G}_\theta(\omega)$ belong to $\mathcal{B}_0(\ell^2)$ for all $\omega \in \mathbb{R}$ and $\theta \in [0, \Omega)$. This is the result we were looking for, namely, $\mathbf{G}_\theta(\omega)$ is a compact operator on ℓ^2 and as such can be approximated to any degree of accuracy by $\Pi \mathbf{G}_\theta(\omega) \Pi$.

But we are still not done. The desired scenario is to only have to compute

$$\mathbf{G}_\theta(\omega) := \mathbf{C}_\theta (j\omega\mathbf{I} - [\mathbf{A}_\theta^\circ + \mathbf{B}_\theta^\circ \mathbf{F} \mathbf{C}_\theta^\circ])^{-1} \mathbf{B}_\theta,$$

because only in this case do we have the amenity of dealing with the finite-dimensional matrices $\mathbf{A}_\theta := \mathbf{A}_\theta^\circ + \mathbf{B}_\theta^\circ \mathbf{F} \mathbf{C}_\theta^\circ$, \mathbf{B}_θ , and \mathbf{C}_θ . Therefore it is important to find the relationship between $\Pi \mathbf{G}_\theta(\omega) \Pi$ and $\mathbf{G}_\theta(\omega)$. Notice that we can not directly compare $\mathbf{C}_\theta (j\omega\mathcal{I} - [\mathcal{A}_\theta^\circ + \mathcal{B}_\theta^\circ \mathcal{F} \mathcal{C}_\theta^\circ])^{-1} \mathbf{B}_\theta$ and $\mathbf{C}_\theta (j\omega\mathbf{I} - \mathbf{A}_\theta^\circ + \mathbf{B}_\theta^\circ \mathbf{F} \mathbf{C}_\theta^\circ)^{-1} \mathbf{B}_\theta$ because they live on different operator spaces. Establishing a connection between $\mathbf{G}_\theta(\omega)$ and $\mathbf{G}_\theta(\omega)$ will be the objective of the next theorem and it is done through the use of the truncated operators \mathfrak{B}_θ , \mathfrak{C}_θ , ... , and the transfer function

$$\mathfrak{G}_\theta(\omega) := \mathfrak{C}_\theta (j\omega\mathcal{I} - [\mathcal{A}_\theta^\circ + \mathfrak{B}_\theta^\circ \mathfrak{F} \mathfrak{C}_\theta^\circ])^{-1} \mathfrak{B}_\theta.$$

It is important to notice in $\mathfrak{G}_\theta(\omega)$ that the diagonal operator \mathcal{A}_θ° has *not* been truncated. Also, $j\omega\mathcal{I} - [\mathcal{A}_\theta^\circ + \mathfrak{B}_\theta^\circ \mathfrak{F} \mathfrak{C}_\theta^\circ]$ is invertible if and only if $j\omega\mathcal{I} - \mathcal{A}_\theta^\circ$ and $j\omega\mathbf{I} - [\mathbf{A}_\theta^\circ + \mathbf{B}_\theta^\circ \mathbf{F} \mathbf{C}_\theta^\circ]$ are invertible.

Remark 9 *The difficulty in relating $\Pi \mathbf{G}_\theta(\omega) \Pi$ to $\mathfrak{G}_\theta(\omega)$ and $\mathbf{G}_\theta(\omega)$ is due to \mathbf{B}_θ , \mathbf{C}_θ , \mathcal{F} being non-diagonal and Π not commuting with non-diagonal operators. This is precisely the reason why $\Pi \mathbf{G}_\theta(\omega) \Pi \neq \mathfrak{G}_\theta(\omega)$. $\Pi \mathbf{G}_\theta(\omega) \Pi$ is found by composing $\mathbf{G}_\theta(\omega)$ first and then applying Π , whereas $\mathfrak{G}_\theta(\omega)$ is found by applying Π to \mathbf{B}_θ , \mathbf{C}_θ , \mathcal{F} first and then carrying out the composition. These two are in general not equal unless all operators present in the system are diagonal. Indeed, if \mathbf{B}_θ , \mathbf{C}_θ , \mathcal{F} were all diagonal, then $\mathbf{G}_\theta(\omega)$ would be diagonal, we would have $\Pi \mathbf{G}_\theta(\omega) \Pi = \mathfrak{G}_\theta(\omega)$,*

and $\mathbf{G}_\theta(\omega)$ would be nothing but a diagonal matrix made up of the center $2N+1$ diagonal elements of $\mathfrak{G}_\theta(\omega)$ (or $\mathbf{G}_\theta(\omega)$). \blacksquare

Theorem 7 Consider an exponentially stable spatially periodic system described by (2.35) with finite \mathcal{H}^∞ -norm, and suppose that $\sup_{\omega \in \mathbb{R}} \|(j\omega I - \hat{A}^\circ(k))^{-1}\| \rightarrow 0$ as $|k| \rightarrow \infty$. Then

$$\sup_{\omega \in \mathbb{R}} \sup_{\theta \in [0, \Omega]} \|\mathbf{G}_\theta(\omega) - \mathfrak{G}_\theta(\omega)\| \rightarrow 0 \quad \text{as} \quad N \rightarrow \infty.$$

In particular, if $\mathbf{G}_\theta(\omega)$ exists for all $\omega \in \mathbb{R}$ and $\theta \in [0, \Omega)$, then

$$\sup_{\omega \in \mathbb{R}} \sup_{\theta \in [0, \Omega)} \|\mathbf{G}_\theta(\omega)\| = \sup_{\omega \in \mathbb{R}} \sup_{\theta \in [0, \Omega)} \|\mathfrak{G}_\theta(\omega)\| \rightarrow \sup_{\omega \in \mathbb{R}} \sup_{\theta \in [0, \Omega)} \|\mathbf{G}_\theta(\omega)\|$$

as $N \rightarrow \infty$.

Proof: See Appendix. \blacksquare

The significance of the above theorem is that the \mathcal{H}^∞ -norm of G in Theorem 6 can now be computed from

$$\|G\|_{\mathcal{H}^\infty}^2 \approx \sup_{\omega \in \mathbb{R}} \sup_{\theta \in [0, \Omega)} \|\mathbf{G}_\theta(\omega)\|,$$

and one need only deal with the finite-dimensional matrices \mathbf{A}_θ , \mathbf{B}_θ and \mathbf{C}_θ .

3.5.2 \mathcal{H}^2 -norm

For a Hilbert-Schmidt operator $T \in \mathcal{B}_2(\ell^2)$ with matrix representation $\{t_{mn}\}_{m,n \in \mathbb{Z}}$ we have $\sum_{m,n=-\infty}^{\infty} |t_{mn}|^2 < \infty$ [33]. In particular this means that $\|T - \Pi T\|_{\text{HS}}$, $\|T - T\Pi\|_{\text{HS}}$, and $\|T - \Pi T \Pi\|_{\text{HS}}$ all approach zero as N grows large, where $\|T\|_{\text{HS}}^2 := \text{trace}[T T^*]$. As opposed to the previous paragraph and the proof of Theorem 7 where the submultiplicative property of the induced ℓ^2 norm plays a central role, in this paragraph and in the proof of the proceeding Theorem 8 we make use of the fact that Hilbert-Schmidt operators form a two-sided ideal in the algebra of bounded operators on ℓ^2 [20]. Namely if $T_0, T_1 \in \mathcal{B}(\ell^2)$ and $T_2 \in \mathcal{B}_2(\ell^2)$, then $T_0 T_2 T_1 \in \mathcal{B}_2(\ell^2)$ and $\|T_0 T_2 T_1\|_{\text{HS}} \leq \|T_0\|_{\ell^2/\ell^2} \|T_2\|_{\text{HS}} \|T_1\|_{\ell^2/\ell^2}$.

The main assumption here is that

$$\int_{-\infty}^{\infty} \int_{\mathbb{R}} \|(j\omega I - \hat{A}^\circ(k))^{-1}\|_{\text{F}}^2 dk d\omega < \infty,$$

and that $A^\circ(\cdot)$ satisfies the regularity conditions given in Theorem 9. Arguments similar to those in the proof of Theorem 9 can now be used to show that the operators $(j\omega\mathcal{I} - \mathcal{A}_\theta^\circ)^{-1}$, $(j\omega\mathcal{I} - \mathcal{A}_\theta)^{-1}$ and $G_\theta(\omega)$ belong to $\mathcal{B}_2(\ell^2)$ for all $\omega \in \mathbb{R}$ and $\theta \in [0, \Omega)$. Therefore $G_\theta(\omega)$ is a Hilbert-Schmidt operator and as such can be approximated to any degree of accuracy (in the sense of the Hilbert-Schmidt norm) by $\Pi G_\theta(\omega) \Pi$.

But as in the previous section on the \mathcal{H}^∞ -norm, our desired scenario is to only have to deal with the finite-dimensional systems

$$\mathbf{G}_\theta(\omega) = \mathbf{C}_\theta (j\omega\mathbf{I} - [\mathbf{A}_\theta^\circ + \mathbf{B}_\theta^\circ \mathbf{F} \mathbf{C}_\theta^\circ])^{-1} \mathbf{B}_\theta.$$

In particular, we would like to compute the \mathcal{H}^2 -norm by solving Lyapunov equations involving only the finite-dimensional matrices \mathbf{A}_θ , \mathbf{B}_θ , and \mathbf{C}_θ . The following theorem uses of the truncated systems

$$\mathfrak{G}_\theta(\omega) = \mathfrak{C}_\theta (j\omega\mathcal{I} - [\mathcal{A}_\theta^\circ + \mathfrak{B}_\theta^\circ \mathfrak{F} \mathfrak{C}_\theta^\circ])^{-1} \mathfrak{B}_\theta.$$

to establish the connection between $G_\theta(\omega)$ and $\mathbf{G}_\theta(\omega)$.

Theorem 8 *Consider an exponentially stable spatially periodic system described by (2.35) with finite \mathcal{H}^2 -norm, and suppose that $\int_{\mathbb{R}} \int_{-\infty}^{\infty} \|(j\omega\mathbf{I} - \hat{A}^\circ(k))^{-1}\|_{\mathbb{F}}^2 dk d\omega < \infty$. Then*

$$\int_0^\Omega \int_{-\infty}^{\infty} \|G_\theta(\omega) - \mathbf{G}_\theta(\omega)\|_{\text{HS}}^2 d\omega d\theta \rightarrow 0 \quad \text{as } N \rightarrow \infty.$$

In particular, if $G_\theta(\omega)$ exists for all $\omega \in \mathbb{R}$ and $\theta \in [0, \Omega)$, then

$$\int_0^\Omega \int_{-\infty}^{\infty} \|G_\theta(\omega)\|_{\mathbb{F}}^2 d\omega d\theta = \int_0^\Omega \int_{-\infty}^{\infty} \|\mathfrak{G}_\theta(\omega)\|_{\text{HS}}^2 d\omega d\theta \rightarrow \int_0^\Omega \int_{-\infty}^{\infty} \|G_\theta(\omega)\|_{\text{HS}}^2 d\omega d\theta$$

as $N \rightarrow \infty$.

Proof: *See Appendix.* ■

The significance of the above theorem is that the \mathcal{H}^2 -norm of G can now be computed from

$$\|G\|_{\mathcal{H}^2}^2 \approx \frac{1}{2\pi} \int_0^\Omega \text{trace}[\mathbf{C}_\theta \mathbf{P}_\theta \mathbf{C}_\theta^*] d\theta = \frac{1}{2\pi} \int_0^\Omega \text{trace}[\mathbf{B}_\theta^* \mathbf{Q}_\theta \mathbf{B}_\theta] d\theta$$

where \mathbf{P}_θ and \mathbf{Q}_θ are the solutions of the finite-dimensional Lyapunov equations

$$\mathbf{A}_\theta \mathbf{P}_\theta + \mathbf{P}_\theta \mathbf{A}_\theta^* = -\mathbf{B}_\theta \mathbf{B}_\theta^*, \quad \mathbf{A}_\theta^* \mathbf{Q}_\theta + \mathbf{Q}_\theta \mathbf{A}_\theta = -\mathbf{C}_\theta^* \mathbf{C}_\theta.$$

Obviously this is much simpler than solving the infinite-dimensional Lyapunov equations (3.6) of Theorem 3.

3.6 Examples

In this section we illustrate how system norms of PDEs can be changed by the introduction of spatially periodic coefficients. We also present an example of a stable system in two spatial dimensions for which the \mathcal{H}^2 -norm is not finite. For more examples, we refer the reader to [22] [26] [34] where spectral analysis is employed to show that depending on the amplitude and frequency of the periodic coefficients, both the stability and the input-output gains of the original PDE can be modified. This phenomenon is referred to as “parametric resonance” and is encountered in many problems of physical significance.

First Example

In this example we show that the system norms and stability of a PDE with periodic coefficients can be altered by changing the amplitude and frequency of the periodic term. Let us consider the periodic PDE

$$\begin{aligned}\partial_t \psi &= -(\partial_x^2 + 1)^2 \psi - c\psi + \alpha \cos(\Omega x) \partial_x \psi + u \\ y &= \psi.\end{aligned}\tag{3.10}$$

Clearly, for $\alpha = 0$ the system becomes spatially invariant.

Figure 3.3 illustrates the dependence of the \mathcal{H}^2 -norm of this system on the amplitude α and frequency Ω of the spatially periodic term for $c = 0.1$. The calculations were done by taking a large enough truncation of the \mathcal{A}_θ , \mathcal{B}_θ and \mathcal{C}_θ matrices, and then using the Lyapunov method of Theorem 3.³

The system is exponentially stable for $\alpha = 0$. As α is increased from zero, the \mathcal{H}^2 -norm increases or decreases depending on the value of Ω . For $0 < \Omega \lesssim 1.2$ the \mathcal{H}^2 -norm will decrease as the amplitude α of the periodic term is increased. This decrease is most significant at $\Omega \approx 0.5$. On the other hand, for $\Omega \gtrsim 1.2$ the \mathcal{H}^2 -norm increases as α grows, this increase being most significant at $\Omega \approx 2$. As a matter of fact, for many pairs (Ω, α) the \mathcal{H}^2 -norm is infinite (these correspond to the points left blank in the plots of Figure 3.3). This means that for such pairs the periodic term has *destabilized* the system.

Next we take $c = -0.1$, see Figure 3.4. Notice that the system is *unstable* for $\alpha = 0$, and as such, has infinite \mathcal{H}^2 -norm. As α is increased from zero, the

³To determine an appropriate truncation size N , we increase N from small values until the difference between the \mathcal{H}_2 -norms of the two systems obtained from truncation sizes N and $2N$ becomes small enough compared to the \mathcal{H}_2 -norm of either of these systems.

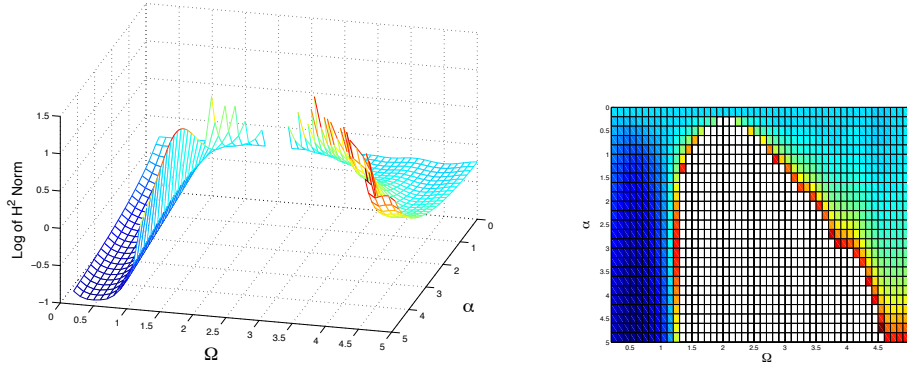


Figure 3.3: The \mathcal{H}^2 -norm of the system (3.10) as a function of amplitude and frequency of the spatially periodic term for $c = 0.1$.

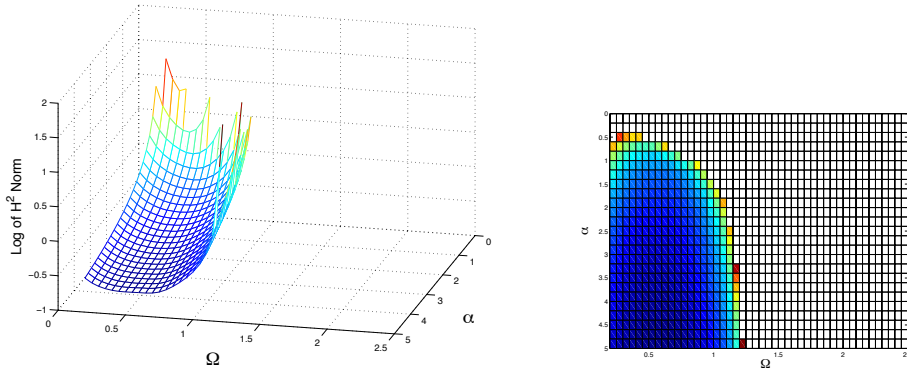


Figure 3.4: The \mathcal{H}^2 -norm of the system (3.10) as a function of amplitude and frequency of the spatially periodic term for $c = -0.1$.

\mathcal{H}^2 -norm remains infinite for $\Omega \gtrsim 1.2$. On the other hand, for $0 < \Omega \lesssim 1.2$ the \mathcal{H}^2 -norm first becomes finite, and then decreases, as α grows in amplitude. Hence the periodic term effectively *stabilizes* the system. The best choice for Ω to most reduce the \mathcal{H}^2 -norm is seen to be $\Omega \approx 0.5$.

We remark here that the above analysis can not be performed using conventional tools, e.g. Floquet analysis of periodic PDEs, as this type of analysis does not easily lend itself to the computation of system norms.

Finally, notice that the spatially periodic system (3.10) can also be considered as the feedback interconnection of a spatially invariant system and a spatially periodic operator. Using the notation introduced in Remark 6 and comparing (3.10) and (2.35) we have

$$A^\circ = -(\partial_x^2 + 1)^2 + c, \quad B^\circ = 1, \quad C^\circ = \partial_x, \quad B = 1, \quad C = 1, \quad F(x) = \alpha \cos(\Omega x).$$

Second Example

In this example we show that the \mathcal{H}^2 -norm of exponentially stable systems on spatial domains with dimension $d \geq 2$ may actually be infinite, and that in such cases a statistical analysis still yields valuable information about the system. Consider

$$\begin{aligned}\partial_t \psi &= \partial_x^2 \psi + \partial_y^2 \psi - \psi + u \\ y &= \psi,\end{aligned}$$

or, in the spatial frequency domain,

$$\begin{aligned}\partial_t \hat{\psi} &= -(k_x^2 + k_y^2 + 1) \hat{\psi} + \hat{u} \\ \hat{y} &= \hat{\psi}.\end{aligned}\tag{3.11}$$

The system is spatially invariant, $\hat{A}(k) = \hat{A}^\circ(k) = -k_x^2 - k_y^2 - 1$, $k = \begin{bmatrix} k_x \\ k_y \end{bmatrix} \in \mathbb{R}^2$, and [see Chapter 4 for details on how to find the spectrum of A]

$$\Sigma(A) = \Sigma(\hat{A}) = \overline{\bigcup_{k_x, k_y \in \mathbb{R}} (-k_x^2 - k_y^2 - 1)} = (-\infty, -1].$$

It is not hard to show that this system satisfies the spectrum-determined growth condition (because it is normal), is exponentially stable, and has \mathcal{H}^∞ -norm equal to one. Let us now calculate its \mathcal{H}^2 -norm. The system is spatially invariant and thus $\hat{G}_l(\omega, k) = 0$, $l \neq 0$, and $\hat{G}_0(\omega, k) = \frac{1}{j\omega + k_x^2 + k_y^2 + 1}$. From Theorem 3 we have

$$\begin{aligned}\|G\|_{\mathcal{H}^2}^2 &= \frac{1}{4\pi^2} \int_{-\infty}^{\infty} \int_{\mathbb{R}^2} \frac{1}{\omega^2 + (k_x^2 + k_y^2 + 1)^2} dk_x dk_y d\omega \\ &= \frac{1}{4\pi} \int_{\mathbb{R}^2} \frac{1}{k_x^2 + k_y^2 + 1} dk_x dk_y = \frac{1}{4} \int_{\mathbb{R}} \frac{1}{\sqrt{k_y^2 + 1}} dk_y,\end{aligned}$$

which is not finite. In other words, the response of the system to a spatio-temporal impulse is not square integrable (i.e. it has infinite energy), see Remark 8.

Turning to statistical interpretations, let us now consider the two-point correlations of the output, with the assumption that the system is fed with a white random field. For example, we choose the (temporal) two-point correlations $R^y(\Delta t; x, x) = R^y(\Delta t; 0)$, $\Delta t > 0$. Using (3.11) it is simple to show that

$$\begin{aligned}R^y(\Delta t; 0) &= \frac{1}{2\pi} \int_0^\infty \int_{\mathbb{R}^2} e^{-(k_x^2 + k_y^2 + 1)t} e^{-(k_x^2 + k_y^2 + 1)(t + \Delta t)} dk_x dk_y dt \\ &= \frac{1}{2\pi} \int_0^\infty \frac{e^{-(2t + \Delta t)}}{2t + \Delta t} dt = \frac{1}{4\pi} \int_{\Delta t}^\infty \frac{e^{-t}}{t} dt,\end{aligned}\tag{3.12}$$

which is finite for every $\Delta t > 0$ ⁴. Similar computations can be done for the (spatial) two-point correlations $R^y(0; x, x + \Delta x) = R^y(0; \Delta x)$, which are also finite for $\Delta x \neq 0$.

Let us look more closely at the function $r(t) := \int_t^\infty \frac{e^{-\tau}}{\tau} d\tau$ of (3.12). For small values of $t > 0$, $r(t)$ behaves like the log function, which has a *nonsummable* singularity [35] at $t = 0$. Such functions can be *regularized* using the theory of distributions [35]. Hence $r(t)$ (and thus $R^y(\Delta t; 0)$) can be given a meaning in the sense of distributions. This is not surprising since the autocorrelation of the input random field, $R^u(t; x) = \delta(t) \delta(x)$, is itself a distribution.

3.7 Appendix to Chapter 3

Theorem 9: Finiteness of \mathcal{H}^2 -Norm

Let us denote by $\mathcal{W}(\mathbb{R}^d)$ the Sobolev space

$$\mathcal{W}(\mathbb{R}^d) := \left\{ \phi \in L^2(\mathbb{R}^d) \mid \phi \text{ absolutely continuous, } \frac{d\phi}{dk} \in L^2(\mathbb{R}^d) \right\}, \quad (3.13)$$

and we can state the following theorem.

Theorem 9 *Let G be an exponentially stable spatially periodic system with representation (2.35), let B^o and C^o be bounded operators, and let $\rho(A^o)$ contain \mathbb{C}^+ . Suppose $\hat{A}^o(\cdot)$ denotes the Fourier symbol of A^o and that the matrix-valued function $\phi(k) = (sI - \hat{A}^o(k))^{-1}$ belongs to $\mathcal{W}(\mathbb{R}^d)$ for some $s \in \rho(A^o)$ in the sense that*

$$\begin{aligned} \int_{\mathbb{R}^d} \| (sI - \hat{A}^o(k))^{-1} \|_{\mathbb{F}}^2 dk < \infty, & \quad (sI - \hat{A}^o(k))^{-1} \text{ abs. cont. in } k, \\ \text{and} \quad \int_{\mathbb{R}^d} \left\| \frac{d}{dk} (sI - \hat{A}^o(k))^{-1} \right\|_{\mathbb{F}}^2 dk < \infty, \end{aligned}$$

with $\| \cdot \|_{\mathbb{F}}$ denoting the Frobenius norm. Then $\|G\|_{\mathcal{H}^2}^2$ is finite if

$$\int_{-\infty}^{\infty} \int_{\mathbb{R}^d} \| (j\omega I - \hat{A}^o(k))^{-1} \|_{\mathbb{F}}^2 dk d\omega < \infty. \quad (3.14)$$

Proof: Without loss of generality we assume $D \equiv 0$. Since G is exponentially stable, Theorem 5.1.5 and Lemma A.6.17 of [3] imply that

$$\sup_{\operatorname{Re}(s) \geq 0} \| (sI - A)^{-1} \|_{L^2/L^2} = \sup_{\omega \in \mathbb{R}} \| (j\omega I - A)^{-1} \|_{L^2/L^2} < \infty.$$

⁴Notice that $\|G\|_{\mathcal{H}^2}^2 = R^y(0; 0) = \infty$.

Therefore

$$\sup_{\omega \in \mathbb{R}} \| I + B^\circ F C^\circ (j\omega I - A)^{-1} \|_{L^2/L^2}^2 < \infty. \quad (3.15)$$

On the other hand, from the theory of Sobolev spaces it can be shown that if $\hat{A}^\circ(\cdot)$ satisfies

$$(sI - \hat{A}^\circ(\cdot))^{-1} \in \mathcal{W}(\mathbb{R}^d) \quad \text{for some } s \in \rho(A^\circ),$$

then the (matrix-valued) sequence $\{(sI - \hat{A}^\circ(\theta + \Omega n))^{-1}\}_{n \in \mathbb{Z}^d}$ is such that $\sum_{n \in \mathbb{Z}^d} \| (sI - \hat{A}^\circ(\theta + \Omega n))^{-1} \|_{\mathbb{F}}^2 < \infty$ for every $\theta \in \Theta$, or equivalently

$$(s\mathcal{I} - \mathcal{A}_\theta^\circ)^{-1} \in \mathcal{B}_2(\ell^2).$$

Additionally, for any other point $\zeta \in \rho(A^\circ)$ the relation

$$(\zeta\mathcal{I} - \mathcal{A}_\theta^\circ)^{-1} = (s\mathcal{I} - \mathcal{A}_\theta^\circ)^{-1} (\mathcal{I} - (\zeta - s)(\zeta\mathcal{I} - \mathcal{A}_\theta^\circ)^{-1})$$

and the fact that Hilbert-Schmidt operators form a two-sided ideal in the algebra of bounded operators $\mathcal{B}(\ell^2)$ yields that $(\zeta\mathcal{I} - \mathcal{A}_\theta^\circ)^{-1} \in \mathcal{B}_2(\ell^2)$ [20]. Thus $(s\mathcal{I} - \mathcal{A}_\theta^\circ)^{-1} \in \mathcal{B}_2(\ell^2)$ for all $s \in \rho(A^\circ)$ and $\theta \in \Theta$. Similarly, the identity

$$(s\mathcal{I} - \mathcal{A}_\theta)^{-1} = (s\mathcal{I} - \mathcal{A}_\theta^\circ)^{-1} (\mathcal{I} + \mathcal{B}_\theta^\circ \mathcal{F} \mathcal{C}_\theta^\circ (s\mathcal{I} - \mathcal{A}_\theta)^{-1})$$

together with $(s\mathcal{I} - \mathcal{A}_\theta^\circ)^{-1} \in \mathcal{B}_2(\ell^2)$ gives $(s\mathcal{I} - \mathcal{A}_\theta)^{-1} \in \mathcal{B}_2(\ell^2)$ for all s that belong to both $\rho(A)$ and $\rho(A^\circ)$ and all $\theta \in \Theta$. Consequently $\|G_\theta(s)\|_{\text{HS}} = \|\mathcal{C}_\theta (s\mathcal{I} - \mathcal{A}_\theta)^{-1} \mathcal{B}_\theta\|_{\text{HS}}$ exists and

$$\begin{aligned} \|G_\theta(s)\|_{\text{HS}}^2 &\leq \|\mathcal{B}_\theta\|_{\ell^2/\ell^2}^2 \|\mathcal{C}_\theta\|_{\ell^2/\ell^2}^2 \|(\mathcal{I} + \mathcal{B}_\theta^\circ \mathcal{F} \mathcal{C}_\theta^\circ (s\mathcal{I} - \mathcal{A}_\theta)^{-1})\|_{\ell^2/\ell^2}^2 \\ &\quad \|(s\mathcal{I} - \mathcal{A}_\theta^\circ)^{-1}\|_{\text{HS}}^2. \end{aligned}$$

Now, by assumption the imaginary axis belongs to both $\rho(A)$ and $\rho(A^\circ)$. Hence from (3.15), the boundedness of B and C , and Theorems 5 and 6,

$$\begin{aligned} &\sup_{\Theta} \|\mathcal{B}_\theta\|_{\ell^2/\ell^2}^2 \sup_{\Theta} \|\mathcal{C}_\theta\|_{\ell^2/\ell^2}^2 \sup_{\omega \in \mathbb{R}} \sup_{\Theta} \|(\mathcal{I} + \mathcal{B}_\theta^\circ \mathcal{F} \mathcal{C}_\theta^\circ (j\omega\mathcal{I} - \mathcal{A}_\theta)^{-1})\|_{\ell^2/\ell^2}^2 \\ &= \|B\|_{L^2/L^2}^2 \|C\|_{L^2/L^2}^2 \sup_{\omega \in \mathbb{R}} \|I + B^\circ F C^\circ (j\omega I - A)^{-1}\|_{L^2/L^2}^2 \\ &=: M. \end{aligned}$$

⁵The requirement on the boundedness of B° and C° in the theorem statement is too strong and can be relaxed if $B^\circ F C^\circ$ is relatively bounded w.r.t. A in the sense that $\sup_{\omega \in \mathbb{R}} \|B^\circ F C^\circ (j\omega I - A)^{-1}\|_{L^2/L^2}^2 < \infty$.

Therefore from Theorem 3

$$\begin{aligned}
\|G\|_{\mathcal{H}^2}^2 &= \frac{1}{4\pi^2} \int_{\Theta} \int_{-\infty}^{\infty} \|G_{\theta}(\omega)\|_{\text{HS}}^2 d\omega d\theta \\
&\leq \frac{M}{4\pi^2} \int_{-\infty}^{\infty} \int_{\Theta} \|(j\omega\mathcal{I} - \mathcal{A}_{\theta}^{\circ})^{-1}\|_{\text{HS}}^2 d\omega d\theta \\
&= \frac{M}{4\pi^2} \int_{-\infty}^{\infty} \int_{\mathbb{R}^d} \|(j\omega I - \hat{A}^{\circ}(k))^{-1}\|_{\text{F}}^2 dk d\omega,
\end{aligned}$$

Thus $\|G\|_{\mathcal{H}^2}^2$ is finite if $\int_{-\infty}^{\infty} \int_{\mathbb{R}^d} \|(j\omega I - \hat{A}^{\circ}(k))^{-1}\|_{\text{F}}^2 dk d\omega$ is finite. ■

Proof of Theorem 2

Using the Plancharel theorem we have

$$\begin{aligned}
\|G\|_{\mathcal{H}_{\text{sp}}^2}^2 &= \frac{1}{\text{V}(\Phi)} \int_{\Phi} \int_{\mathbb{R}^d} (Gv^{\chi})^*(x) (Gv^{\chi})(x) dx d\chi \\
&= \frac{1}{2\pi\text{V}(\Phi)} \int_{\Phi} \int_{\mathbb{R}^d} (\hat{G}\hat{v}^{\chi})^*(k) (\hat{G}\hat{v}^{\chi})(k) dk d\chi \\
&= \frac{1}{2\pi\text{V}(\Phi)} \int_{\Phi} \int \int \int_{\mathbb{R}^d} (\hat{v}^{\chi})^*(\kappa_1) \hat{G}^*(\kappa_1, k) \hat{G}(k, \kappa_2) \hat{v}^{\chi}(\kappa_2) d\kappa_1 d\kappa_2 dk d\chi.
\end{aligned}$$

Define \hat{K} to be the composition $\hat{G}^*\hat{G}$, i.e. $\hat{K}(\kappa_1, \kappa_2) = \int_{\mathbb{R}^d} \hat{G}^*(\kappa_1, k) \hat{G}(k, \kappa_2) dk$. The exact expression for \hat{K} is not required here; what is important is that \hat{K} has the same structure as \hat{G} and \hat{G}^* , namely

$$\hat{K}(\kappa_1, \kappa_2) = (\hat{G}^*\hat{G})(\kappa_1, \kappa_2) = \sum_{l \in \mathbb{Z}^d} \hat{K}_l(\kappa_1) \delta(\kappa_1 - \kappa_2 - \Omega l).$$

Using $\hat{v}^{\chi}(\kappa) = e^{-j\kappa^*\chi}$, this means that

$$\begin{aligned}
\|G\|_{\mathcal{H}_{\text{sp}}^2}^2 &= \frac{1}{2\pi\text{V}(\Phi)} \int_{\Phi} \int_{\mathbb{R}^d} \int_{-\infty}^{\infty} e^{j\kappa_1^*\chi} \hat{K}(\kappa_1, \kappa_2) e^{-j\kappa_2^*\chi} d\kappa_1 d\kappa_2 d\chi \\
&= \frac{1}{2\pi\text{V}(\Phi)} \int_{\Phi} \int_{\mathbb{R}^d} \sum_{l \in \mathbb{Z}^d} e^{j\kappa_1^*\chi} \hat{K}_l(\kappa_1) e^{-j(\kappa_1 - \Omega l)^*\chi} d\kappa_1 d\chi \\
&= \frac{1}{2\pi} \int_{\mathbb{R}^d} \int_{\Phi} \left[\frac{1}{\text{V}(\Phi)} \sum_{l \in \mathbb{Z}^d} e^{-j(\Omega l)^*\chi} d\chi \right] \hat{K}_l(\kappa) d\kappa = \frac{1}{2\pi} \int_{\mathbb{R}^d} \hat{K}_0(\kappa) d\kappa,
\end{aligned}$$

where we have used that $\frac{1}{V(\Phi)} \int_{\Phi} e^{j(\Omega l)^* x} dx = 1$ only for $l = 0$ and equal to zero for $l \neq 0$. It is not difficult to show that $\hat{K}_0(\kappa) = \sum_{l \in \mathbb{Z}^d} |\hat{G}_l(\kappa)|^2$, and thus

$$\|G\|_{\mathcal{H}_{\text{sp}}^2}^2 = \frac{1}{2\pi} \sum_{l \in \mathbb{Z}^d} \int_{\mathbb{R}^d} |\hat{G}_l(\kappa)|^2 d\kappa = \frac{1}{2\pi} \int_{\Theta} \text{trace}[\mathcal{G}_\theta \mathcal{G}_\theta^*] d\theta.$$

Proof of Theorem 3

We prove the theorem for $D \equiv 0$. Defining $u^\chi(t, x) := w(t) v^\chi(x) = \delta(t) \delta(x - \chi)$ and proceeding formally, (3.5) can be rewritten as

$$\begin{aligned} \|G\|_{\mathcal{H}^2}^2 &= \frac{1}{V(\Phi)} \int_{\Phi} \int_{\mathbb{R}^d} \int_0^\infty \text{trace}[(G u^\chi)(G u^\chi)^*] dt dx d\chi \\ &= \frac{1}{2\pi V(\Phi)} \int_{\Phi} \int_{\Theta} \int_0^\infty \text{trace}[(\mathcal{G}_\theta(t) v_\theta^\chi)(\mathcal{G}_\theta(t) v_\theta^\chi)^*] dt d\theta d\chi, \end{aligned}$$

where $\mathcal{G}_\theta(t) = \mathcal{C}_\theta e^{\mathcal{A}_\theta t} \mathcal{B}_\theta$. Using $\frac{1}{2\pi V(\Phi)} \int_{\Phi} (v_\theta^\chi)(v_\theta^\chi)^* d\chi = \mathcal{I}$, it then follows that

$$\begin{aligned} \|G\|_{\mathcal{H}^2}^2 &= \frac{1}{2\pi} \int_{\Theta} \int_0^\infty \text{trace}[\mathcal{G}_\theta(t) \mathcal{G}_\theta^*(t)] dt d\theta \\ &= \frac{1}{4\pi^2} \int_{\Theta} \int_{-\infty}^\infty \text{trace}[\mathcal{G}_\theta(\omega) \mathcal{G}_\theta^*(\omega)] d\omega d\theta \\ &= \frac{1}{4\pi^2} \int_{-\infty}^\infty \sum_{l \in \mathbb{Z}^d} \int_{\mathbb{R}^d} \text{trace}[\hat{\mathcal{G}}_l(\omega; k) \hat{\mathcal{G}}_l^*(\omega; k)] dk d\omega. \end{aligned}$$

Finally, it is a standard result of linear systems theory [27] that

$$\int_0^\infty \text{trace}[\mathcal{C}_\theta e^{\mathcal{A}_\theta t} \mathcal{B}_\theta \mathcal{B}_\theta^* e^{\mathcal{A}_\theta^* t} \mathcal{C}_\theta^*] dt = \text{trace}[\mathcal{C}_\theta \mathcal{P}_\theta \mathcal{C}_\theta^*],$$

where \mathcal{P}_θ is the solution of the (θ -parameterized) algebraic Lyapunov equation

$$\mathcal{A}_\theta \mathcal{P}_\theta + \mathcal{P}_\theta \mathcal{A}_\theta^* = -\mathcal{B}_\theta \mathcal{B}_\theta^*.$$

Hence we also have

$$\|G\|_{\mathcal{H}^2}^2 = \frac{1}{2\pi} \int_{\Theta} \text{trace}[\mathcal{C}_\theta \mathcal{P}_\theta \mathcal{C}_\theta^*] d\theta.$$

Proof of Theorem 4

Treating $R^y(\cdot, \cdot)$ as a kernel, $R^y(x, x)$ can be found by applying the function $v^x(\chi) = \delta(\chi - x)$ to R^y from both sides,

$$\begin{aligned}
R^y(x, x) &= \int_{\mathbb{R}^d} \int_{\mathbb{R}^d} (v^x)^*(\chi_1) R^y(\chi_1, \chi_2) v^x(\chi_2) d\chi_1 d\chi_2 \\
&= \frac{1}{2\pi} \int_{\mathbb{R}^d} \int_{\mathbb{R}^d} e^{j\kappa_1^* x} \hat{S}^y(\kappa_1, \kappa_2) e^{-j\kappa_2^* x} d\kappa_1 d\kappa_2 \\
&= \frac{1}{2\pi} \sum_{l \in \mathbb{Z}^d} \int_{\mathbb{R}^d} \int_{\mathbb{R}^d} e^{j(\kappa_1 - \kappa_2)^* x} \hat{S}_l^y(\kappa_1) \delta(\kappa_1 - \kappa_2 - \Omega l) d\kappa_1 d\kappa_2 \\
&= \frac{1}{2\pi} \sum_{l \in \mathbb{R}^d} \int_{\mathbb{R}^d} e^{j(\Omega l)^* x} \hat{S}_l^y(k) dk,
\end{aligned}$$

where establishing the third equality we have used (3.7). Let us now consider

$$\begin{aligned}
\frac{1}{V(\Phi)} \int_{\Phi} R^y(x, x) dx &= \frac{1}{V(\Phi)} \int_{\Phi} \left[\frac{1}{2\pi} \sum_{l \in \mathbb{Z}^d} \int_{\mathbb{R}^d} e^{j(\Omega l)^* x} \hat{S}_l^y(k) dk \right] dx \\
&= \frac{1}{2\pi} \int_{\mathbb{R}^d} \sum_{l \in \mathbb{Z}^d} \left[\frac{1}{V(\Phi)} \int_{\Phi} e^{j(\Omega l)^* x} dx \right] \hat{S}_l^y(k) dk \\
&= \frac{1}{2\pi} \int_{\mathbb{R}^d} \hat{S}_0^y(k) dk = \frac{1}{2\pi} \int_{\mathbb{R}^d} \sum_{l \in \mathbb{Z}^d} |\hat{G}_l(k)|^2 \hat{S}_0^v(k) dk,
\end{aligned}$$

the last equality following from (3.8). Finally, if v is a white random field, then $\hat{S}_0^v(k) = 1$ for all k , and we have

$$\frac{1}{V(\Phi)} \int_{\Phi} R^y(x, x) dx = \frac{1}{2\pi} \int_{\mathbb{R}^d} \sum_{l \in \mathbb{Z}^d} |\hat{G}_l(k)|^2 dk = \frac{1}{V(\Phi)} \int_{\Phi} \int_{\mathbb{R}^d} |G(x, \chi)|^2 dx d\chi,$$

and comparison with (3.2) gives $\|G\|_{\mathcal{H}_{\text{sp}}^2}^2 = \frac{1}{V(\Phi)} \int_{\Phi} R^y(x, x) dx$.

Proof of Theorem 5

We have ⁶

$$\|G\|_{\mathcal{H}_{\text{sp}}^\infty}^2 = \|G\|_{L^2/L^2}^2 = \|\hat{G}\|_{L^2/L^2}^2 = \sup_{\theta \in \Theta} \|\mathcal{G}_\theta\|_{\ell^2/\ell^2}^2,$$

where the second equality follows from the unitary property of the Fourier transform and the last equality follows from the fact that \mathcal{G}_θ is a multiplication operator

⁶Unless specified otherwise, by L^2 we mean $L^2(\mathbb{R}^d)$ and by ℓ^2 we mean $\ell^2(\mathbb{Z}^d)$.

on the space $L^2(\Theta)$ [32]. To prove the final equality of the theorem statement,

$$\|\mathcal{G}_\theta\|_{\ell^2/\ell^2}^2 = \|\mathcal{G}_\theta^* \mathcal{G}_\theta\|_{\ell^2/\ell^2} = \sup_{\lambda \in \Sigma(\mathcal{G}_\theta^* \mathcal{G}_\theta)} |\lambda|$$

where the first and second equalities follow from Theorem VI.3 and Theorem VI.6 of [36], respectively.

Proof of Theorem 7

For any $\omega \in \mathbb{R}$ the following identities hold

$$\begin{aligned} \mathcal{C}_\theta (j\omega \mathcal{I} - [\mathcal{A}_\theta^\circ + \mathcal{B}_\theta^\circ \mathcal{F} \mathcal{C}_\theta^\circ])^{-1} \mathcal{B}_\theta &= \mathcal{C}_\theta (j\omega \mathcal{I} - \mathcal{A}_\theta^\circ)^{-1} \\ &\quad (\mathcal{I} - \mathcal{B}_\theta^\circ \mathcal{F} \mathcal{C}_\theta^\circ (j\omega \mathcal{I} - \mathcal{A}_\theta^\circ)^{-1})^{-1} \mathcal{B}_\theta, \end{aligned} \quad (3.16)$$

$$\begin{aligned} \mathfrak{C}_\theta (j\omega \mathcal{I} - [\mathcal{A}_\theta^\circ + \mathfrak{B}_\theta^\circ \mathfrak{F} \mathfrak{C}_\theta^\circ])^{-1} \mathfrak{B}_\theta &= \mathfrak{C}_\theta (j\omega \mathcal{I} - \mathcal{A}_\theta^\circ)^{-1} \\ &\quad (\mathcal{I} - \mathfrak{B}_\theta^\circ \mathfrak{F} \mathfrak{C}_\theta^\circ (j\omega \mathcal{I} - \mathcal{A}_\theta^\circ)^{-1})^{-1} \mathfrak{B}_\theta \end{aligned} \quad (3.17)$$

and the proof proceeds as follows. Using (3.16) and (3.17) we show that

$$\sup_{\omega \in \mathbb{R}} \sup_{\theta \in [0, \Omega]} \|\mathcal{C}_\theta (j\omega \mathcal{I} - [\mathcal{A}_\theta^\circ + \mathcal{B}_\theta^\circ \mathcal{F} \mathcal{C}_\theta^\circ])^{-1} \mathcal{B}_\theta - \mathfrak{C}_\theta (j\omega \mathcal{I} - [\mathcal{A}_\theta^\circ + \mathfrak{B}_\theta^\circ \mathfrak{F} \mathfrak{C}_\theta^\circ])^{-1} \mathfrak{B}_\theta\| \rightarrow 0 \quad (3.18)$$

as $N \rightarrow \infty$. From (3.18) it follows that

$$\sup_{\omega \in \mathbb{R}} \sup_{\theta \in [0, \Omega]} \|\mathfrak{G}_\theta(\omega)\| \rightarrow \sup_{\omega \in \mathbb{R}} \sup_{\theta \in [0, \Omega]} \|\mathcal{G}_\theta(\omega)\| \quad \text{as } N \rightarrow \infty.$$

But since $j\omega \mathcal{I}$ and \mathcal{A}_θ° are both diagonal, it is readily seen that the operator

$$\mathfrak{C}_\theta (j\omega \mathcal{I} - [\mathcal{A}_\theta^\circ + \mathfrak{B}_\theta^\circ \mathfrak{F} \mathfrak{C}_\theta^\circ])^{-1} \mathfrak{B}_\theta = \mathfrak{C}_\theta \Pi (j\omega \mathcal{I} - [\mathcal{A}_\theta^\circ + \mathfrak{B}_\theta^\circ \mathfrak{F} \mathfrak{C}_\theta^\circ])^{-1} \Pi \mathfrak{B}_\theta$$

when restricted to the subspace $\Pi \ell^2$ is nothing but the finite-dimensional matrix

$$\mathcal{C}_\theta (j\omega \mathcal{I} - [\mathcal{A}_\theta^\circ + \mathcal{B}_\theta^\circ \mathcal{F} \mathcal{C}_\theta^\circ])^{-1} \mathcal{B}_\theta,$$

and in particular $\sup_{\omega, \theta} \|\mathcal{G}_\theta(\omega)\| = \sup_{\omega, \theta} \|\mathfrak{G}_\theta(\omega)\|$. This means that

$$\sup_{\omega \in \mathbb{R}} \sup_{\theta \in [0, \Omega]} \|\mathcal{G}_\theta(\omega)\| \rightarrow \sup_{\omega \in \mathbb{R}} \sup_{\theta \in [0, \Omega]} \|\mathfrak{G}_\theta(\omega)\| \quad \text{as } N \rightarrow \infty.$$

Let us now return to showing (3.18). To avoid clutter we use $\mathcal{E}_\theta = \mathcal{B}_\theta^\circ \mathcal{F} \mathcal{C}_\theta^\circ$,

$\mathfrak{E}_\theta := \mathfrak{B}_\theta^\circ \mathfrak{F} \mathfrak{C}_\theta^\circ$, and $\mathcal{R}_\theta^\circ := (j\omega I - \mathcal{A}_\theta^\circ)^{-1}$. From (3.16) and (3.17) we have

$$\begin{aligned} & \mathcal{C}_\theta (j\omega I - [\mathcal{A}_\theta^\circ + \mathcal{E}_\theta])^{-1} \mathcal{B}_\theta - \mathfrak{C}_\theta (j\omega I - [\mathcal{A}_\theta^\circ + \mathfrak{E}_\theta])^{-1} \mathfrak{B}_\theta \\ &= \mathcal{C}_\theta \mathcal{R}_\theta^\circ (\mathcal{I} - \mathcal{E}_\theta \mathcal{R}_\theta^\circ)^{-1} \mathcal{B}_\theta - \mathfrak{C}_\theta \mathcal{R}_\theta^\circ (\mathcal{I} - \mathfrak{E}_\theta \mathcal{R}_\theta^\circ)^{-1} \mathfrak{B}_\theta \\ &= \mathcal{C}_\theta \mathcal{R}_\theta^\circ (\mathcal{I} - \mathcal{E}_\theta \mathcal{R}_\theta^\circ)^{-1} \mathcal{B}_\theta \pm \mathfrak{C}_\theta \mathcal{R}_\theta^\circ (\mathcal{I} - \mathcal{E}_\theta \mathcal{R}_\theta^\circ)^{-1} \mathcal{B}_\theta \\ &\quad \pm \mathfrak{C}_\theta \mathcal{R}_\theta^\circ (\mathcal{I} - \mathfrak{E}_\theta \mathcal{R}_\theta^\circ)^{-1} \mathcal{B}_\theta - \mathfrak{C}_\theta \mathcal{R}_\theta^\circ (\mathcal{I} - \mathfrak{E}_\theta \mathcal{R}_\theta^\circ)^{-1} \mathfrak{B}_\theta. \end{aligned}$$

Grouping the terms, taking the norm of both sides and simplifying, we arrive at

$$\begin{aligned} & \|\mathcal{C}_\theta (sI - [\mathcal{A}_\theta^\circ + \mathcal{E}_\theta])^{-1} \mathcal{B}_\theta - \mathfrak{C}_\theta (sI - [\mathcal{A}_\theta^\circ + \mathfrak{E}_\theta])^{-1} \mathfrak{B}_\theta\| \tag{3.19} \\ &\leq \|\mathcal{C}_\theta \mathcal{R}_\theta^\circ - \mathfrak{C}_\theta \mathcal{R}_\theta^\circ\| \|(\mathcal{I} - \mathcal{E}_\theta \mathcal{R}_\theta^\circ)^{-1} \mathcal{B}_\theta\| \\ &\quad + \|\mathfrak{C}_\theta (\mathcal{I} - \mathcal{R}_\theta^\circ \mathfrak{E}_\theta)^{-1}\| \|\mathcal{R}_\theta^\circ \mathcal{B}_\theta - \mathcal{R}_\theta^\circ \mathfrak{B}_\theta\| \\ &\quad + \|\mathfrak{C}_\theta \mathcal{R}_\theta^\circ\| \|(\mathcal{I} - \mathcal{E}_\theta \mathcal{R}_\theta^\circ)^{-1}\| \|\mathcal{E}_\theta \mathcal{R}_\theta^\circ - \mathfrak{E}_\theta \mathcal{R}_\theta^\circ\| \\ &\quad \quad \quad \|(\mathcal{I} - \mathfrak{E}_\theta \mathcal{R}_\theta^\circ)^{-1}\| \|\mathcal{B}_\theta\|. \end{aligned}$$

We give an argument corresponding to the first term on the right side of the above inequality. Similar arguments apply to the second and third terms. We wish to show

$$\sup_{\omega \in \mathbb{R}} \sup_{\theta \in [0, \Omega)} \|\mathcal{C}_\theta \mathcal{R}_\theta^\circ - \mathfrak{C}_\theta \mathcal{R}_\theta^\circ\| \|(\mathcal{I} - \mathcal{E}_\theta \mathcal{R}_\theta^\circ)^{-1} \mathcal{B}_\theta\| \rightarrow 0 \quad \text{as } N \rightarrow \infty. \tag{3.20}$$

Since G is stable, $\sup_{\omega, \theta} \|(\mathcal{I} - \mathcal{E}_\theta \mathcal{R}_\theta^\circ)^{-1} \mathcal{B}_\theta\| = M$ for some $M > 0$. On the other hand

$$\begin{aligned} \|\mathcal{C}_\theta \mathcal{R}_\theta^\circ - \mathfrak{C}_\theta \mathcal{R}_\theta^\circ\| &= \|\mathcal{C}_\theta \mathcal{R}_\theta^\circ \pm \mathcal{C}_\theta \Pi \mathcal{R}_\theta^\circ - \Pi \mathcal{C}_\theta \Pi \mathcal{R}_\theta^\circ\| \tag{3.21} \\ &\leq \|\mathcal{C}_\theta\| \|\mathcal{R}_\theta^\circ - \Pi \mathcal{R}_\theta^\circ\| + \|\mathcal{C}_\theta \Pi - \Pi \mathcal{C}_\theta \Pi\| \|\Pi \mathcal{R}_\theta^\circ\|. \end{aligned}$$

From (3.20) and (3.21) we have

$$\begin{aligned} & \sup_{\omega \in \mathbb{R}} \sup_{\theta \in [0, \Omega)} \|(\mathcal{I} - \mathcal{E}_\theta \mathcal{R}_\theta^\circ)^{-1} \mathcal{B}_\theta\| \|\mathcal{C}_\theta \mathcal{R}_\theta^\circ - \mathfrak{C}_\theta \mathcal{R}_\theta^\circ\| \\ &\leq M \sup_{\omega \in \mathbb{R}} \sup_{\theta \in [0, \Omega)} \|\mathcal{C}_\theta \mathcal{R}_\theta^\circ - \mathfrak{C}_\theta \mathcal{R}_\theta^\circ\| \\ &\leq M \sup_{\omega \in \mathbb{R}} \sup_{\theta \in [0, \Omega)} (\|\mathcal{C}_\theta\| \|\mathcal{R}_\theta^\circ - \Pi \mathcal{R}_\theta^\circ\| + \|\mathcal{C}_\theta \Pi - \Pi \mathcal{C}_\theta \Pi\| \|\Pi \mathcal{R}_\theta^\circ\|) \\ &\leq M \|C\| \sup_{\omega \in \mathbb{R}} \sup_{\theta \in [0, \Omega)} \|\mathcal{R}_\theta^\circ - \Pi \mathcal{R}_\theta^\circ\| + M \varepsilon \sup_{\omega \in \mathbb{R}} \sup_{\theta \in [0, \Omega)} \|\Pi \mathcal{R}_\theta^\circ\| \\ &\leq M \|C\| \sup_{\omega \in \mathbb{R}} \sup_{|k| \geq K} \|(j\omega I - \hat{A}^\circ(k))^{-1}\| \\ &\quad + M \varepsilon \sup_{\omega \in \mathbb{R}} \sup_{|k| \leq K'} \|(j\omega I - \hat{A}^\circ(k))^{-1}\| \tag{3.22} \end{aligned}$$

where K, K' are positive constants that grow as the truncation size N is increased and $\varepsilon = \sup_{\theta} \|\mathcal{C}_{\theta} \Pi - \Pi \mathcal{C}_{\theta} \Pi\|$. Since by assumption $\sup_{\omega} \|(j\omega I - \hat{A}^{\circ}(k))^{-1}\| \rightarrow 0$ as $|k| \rightarrow \infty$, the first term in (3.22) goes to zero as $N \rightarrow \infty$. Also, the boundedness of C implies that ε goes to zero as $N \rightarrow \infty$. Thus (3.20) is proved. Similarly each term on the right of (3.19) goes to zero as N grows, and (3.18) is satisfied.

Proof of Theorem 8

We use $\mathcal{E}_{\theta} = \mathcal{B}_{\theta}^{\circ} \mathcal{F} \mathcal{C}_{\theta}^{\circ}$, $\mathfrak{E}_{\theta} = \mathfrak{B}_{\theta}^{\circ} \mathfrak{F} \mathfrak{C}_{\theta}^{\circ}$, and $\mathcal{R}_{\theta}^{\circ} = (j\omega \mathcal{I} - \mathcal{A}_{\theta}^{\circ})^{-1}$ to simplify notation. We would like to show that

$$\int_0^{\Omega} \int_{-\infty}^{\infty} \|\mathcal{C}_{\theta} (j\omega \mathcal{I} - [\mathcal{A}_{\theta}^{\circ} + \mathcal{E}_{\theta}])^{-1} \mathcal{B}_{\theta} - \mathfrak{C}_{\theta} (j\omega \mathcal{I} - [\mathcal{A}_{\theta}^{\circ} + \mathfrak{E}_{\theta}])^{-1} \mathfrak{B}_{\theta}\|_{\text{HS}}^2 d\omega d\theta \rightarrow 0 \quad (3.23)$$

as $N \rightarrow \infty$. From (3.16)–(3.17) we have

$$\begin{aligned} & \|\mathcal{C}_{\theta} (j\omega \mathcal{I} - [\mathcal{A}_{\theta}^{\circ} + \mathcal{E}_{\theta}])^{-1} \mathcal{B}_{\theta} - \mathfrak{C}_{\theta} (j\omega \mathcal{I} - [\mathcal{A}_{\theta}^{\circ} + \mathfrak{E}_{\theta}])^{-1} \mathfrak{B}_{\theta}\|_{\text{HS}} \\ & \leq \|\mathcal{C}_{\theta} \mathcal{R}_{\theta}^{\circ} - \mathfrak{C}_{\theta} \mathcal{R}_{\theta}^{\circ}\|_{\text{HS}} \|(\mathcal{I} - \mathcal{E}_{\theta} \mathcal{R}_{\theta}^{\circ})^{-1} \mathcal{B}_{\theta}\| \\ & \quad + \|\mathfrak{C}_{\theta} (\mathcal{I} - \mathcal{R}_{\theta}^{\circ} \mathfrak{E}_{\theta})^{-1}\| \|\mathcal{R}_{\theta}^{\circ} \mathcal{B}_{\theta} - \mathcal{R}_{\theta}^{\circ} \mathfrak{B}_{\theta}\|_{\text{HS}} \\ & \quad + \|\mathfrak{C}_{\theta} \mathcal{R}_{\theta}^{\circ}\| \|(\mathcal{I} - \mathcal{E}_{\theta} \mathcal{R}_{\theta}^{\circ})^{-1}\| \\ & \quad \quad \|\mathcal{E}_{\theta} \mathcal{R}_{\theta}^{\circ} - \mathfrak{E}_{\theta} \mathcal{R}_{\theta}^{\circ}\|_{\text{HS}} \|(\mathcal{I} - \mathfrak{E}_{\theta} \mathcal{R}_{\theta}^{\circ})^{-1}\| \|\mathcal{B}_{\theta}\|, \end{aligned}$$

where we have used that $\|UTV\|_{\text{HS}} \leq \|U\| \|T\|_{\text{HS}} \|V\|$ for $U, V \in \mathcal{B}(\ell^2)$ and $T \in \mathcal{B}_2(\ell^2)$ [20]. Squaring both sides of the above inequality,

$$\begin{aligned} & \|\mathcal{C}_{\theta} (j\omega \mathcal{I} - [\mathcal{A}_{\theta}^{\circ} + \mathcal{E}_{\theta}])^{-1} \mathcal{B}_{\theta} - \mathfrak{C}_{\theta} (j\omega \mathcal{I} - [\mathcal{A}_{\theta}^{\circ} + \mathfrak{E}_{\theta}])^{-1} \mathfrak{B}_{\theta}\|_{\text{HS}}^2 \quad (3.24) \\ & \leq \|\mathcal{C}_{\theta} \mathcal{R}_{\theta}^{\circ} - \mathfrak{C}_{\theta} \mathcal{R}_{\theta}^{\circ}\|_{\text{HS}}^2 \|(\mathcal{I} - \mathcal{E}_{\theta} \mathcal{R}_{\theta}^{\circ})^{-1} \mathcal{B}_{\theta}\|^2 \\ & \quad + \text{square of other terms...} \\ & \quad + 2\|\mathcal{C}_{\theta} \mathcal{R}_{\theta}^{\circ} - \mathfrak{C}_{\theta} \mathcal{R}_{\theta}^{\circ}\|_{\text{HS}} \|(\mathcal{I} - \mathcal{E}_{\theta} \mathcal{R}_{\theta}^{\circ})^{-1} \mathcal{B}_{\theta}\| \\ & \quad \quad \|\mathfrak{C}_{\theta} (\mathcal{I} - \mathcal{R}_{\theta}^{\circ} \mathfrak{E}_{\theta})^{-1}\| \|\mathcal{R}_{\theta}^{\circ} \mathcal{B}_{\theta} - \mathcal{R}_{\theta}^{\circ} \mathfrak{B}_{\theta}\|_{\text{HS}} \\ & \quad + \text{pairwise product of other terms...} \end{aligned}$$

We present an argument regarding the first term on the right of (3.24), with similar reasoning applying to the second and third terms. We prove that

$$\int_0^{\Omega} \int_{-\infty}^{\infty} \|(\mathcal{I} - \mathcal{E}_{\theta} \mathcal{R}_{\theta}^{\circ})^{-1} \mathcal{B}_{\theta}\|^2 \|\mathcal{C}_{\theta} \mathcal{R}_{\theta}^{\circ} - \mathfrak{C}_{\theta} \mathcal{R}_{\theta}^{\circ}\|_{\text{HS}}^2 d\omega d\theta \rightarrow 0 \quad \text{as } N \rightarrow \infty. \quad (3.25)$$

Since G is stable, $\sup_{\omega, \theta} \|(\mathcal{I} - \mathcal{E}_\theta \mathcal{R}_\theta^\circ)^{-1} \mathcal{B}_\theta\| = M$ for some $M > 0$. On the other hand

$$\begin{aligned}
\|\mathcal{C}_\theta \mathcal{R}_\theta^\circ - \mathfrak{C}_\theta \mathcal{R}_\theta^\circ\|_{\text{HS}}^2 &= \|\mathcal{C}_\theta \mathcal{R}_\theta^\circ \pm \mathcal{C}_\theta \Pi \mathcal{R}_\theta^\circ - \Pi \mathcal{C}_\theta \Pi \mathcal{R}_\theta^\circ\|_{\text{HS}}^2 \\
&\leq (\|\mathcal{C}_\theta\| \|\mathcal{R}_\theta^\circ - \Pi \mathcal{R}_\theta^\circ\|_{\text{HS}} + \|\mathcal{C}_\theta \Pi - \Pi \mathcal{C}_\theta \Pi\| \|\Pi \mathcal{R}_\theta^\circ\|_{\text{HS}})^2 \\
&= \|\mathcal{C}_\theta\|^2 \|\mathcal{R}_\theta^\circ - \Pi \mathcal{R}_\theta^\circ\|_{\text{HS}}^2 + \|\mathcal{C}_\theta \Pi - \Pi \mathcal{C}_\theta \Pi\|^2 \|\Pi \mathcal{R}_\theta^\circ\|_{\text{HS}}^2 \\
&\quad + 2 \|\mathcal{C}_\theta\| \|\mathcal{R}_\theta^\circ - \Pi \mathcal{R}_\theta^\circ\|_{\text{HS}} \|\mathcal{C}_\theta \Pi - \Pi \mathcal{C}_\theta \Pi\| \|\Pi \mathcal{R}_\theta^\circ\|_{\text{HS}}.
\end{aligned} \tag{3.26}$$

From (3.25) and (3.26) we have

$$\begin{aligned}
&\int_0^\Omega \int_{-\infty}^\infty \|(\mathcal{I} - \mathcal{E}_\theta \mathcal{R}_\theta^\circ)^{-1} \mathcal{B}_\theta\|^2 \|\mathcal{C}_\theta \mathcal{R}_\theta^\circ - \mathfrak{C}_\theta \mathcal{R}_\theta^\circ\|_{\text{HS}}^2 d\omega d\theta \\
&\leq M^2 \int_0^\Omega \int_{-\infty}^\infty \|\mathcal{C}_\theta \mathcal{R}_\theta^\circ - \mathfrak{C}_\theta \mathcal{R}_\theta^\circ\|_{\text{HS}}^2 d\omega d\theta \\
&\leq M^2 \int_0^\Omega \int_{-\infty}^\infty (\|\mathcal{C}_\theta\|^2 \|\mathcal{R}_\theta^\circ - \Pi \mathcal{R}_\theta^\circ\|_{\text{HS}}^2 + \|\mathcal{C}_\theta \Pi - \Pi \mathcal{C}_\theta \Pi\|^2 \|\Pi \mathcal{R}_\theta^\circ\|_{\text{HS}}^2 \\
&\quad + 2 \|\mathcal{C}_\theta\| \|\mathcal{R}_\theta^\circ - \Pi \mathcal{R}_\theta^\circ\|_{\text{HS}} \|\mathcal{C}_\theta \Pi - \Pi \mathcal{C}_\theta \Pi\| \|\Pi \mathcal{R}_\theta^\circ\|_{\text{HS}}) d\omega d\theta \\
&\leq M^2 \|C\|^2 \int_0^\Omega \int_{-\infty}^\infty \|\mathcal{R}_\theta^\circ - \Pi \mathcal{R}_\theta^\circ\|_{\text{HS}}^2 d\omega d\theta + M^2 \varepsilon^2 \int_0^\Omega \int_{-\infty}^\infty \|\Pi \mathcal{R}_\theta^\circ\|_{\text{HS}}^2 d\omega d\theta \\
&\quad + 2 M^2 \|C\|^2 \varepsilon^2 \int_0^\Omega \int_{-\infty}^\infty \|\mathcal{R}_\theta^\circ - \Pi \mathcal{R}_\theta^\circ\|_{\text{HS}} \|\Pi \mathcal{R}_\theta^\circ\|_{\text{HS}} d\omega d\theta \\
&\leq M^2 \|C\|^2 \int_{|k| \geq K} \int_{-\infty}^\infty \|(j\omega I - \hat{A}^\circ(k))^{-1}\|_{\text{F}}^2 d\omega dk \\
&\quad + M^2 \varepsilon^2 \int_{|k| \leq K'} \int_{-\infty}^\infty \|(j\omega I - \hat{A}^\circ(k))^{-1}\|_{\text{F}}^2 d\omega dk
\end{aligned} \tag{3.27}$$

where K, K' are positive constants that grow as the truncation size N is increased and $\varepsilon = \sup_\theta \|\mathcal{C}_\theta \Pi - \Pi \mathcal{C}_\theta \Pi\|$. Since by assumption $\int_{\mathbb{R}} \int_{-\infty}^\infty \|(j\omega I - \hat{A}^\circ(k))^{-1}\|_{\text{F}}^2 d\omega dk$ is finite, the first integral in (3.27) goes to zero as $N \rightarrow \infty$. Also, the boundedness of C implies that ε goes to zero as $N \rightarrow \infty$. Thus (3.25) is proved. The same procedure can be applied to the integral of every term on the right of (3.24) and therefore

$$\int_0^\Omega \int_{-\infty}^\infty \|\mathcal{C}_\theta (j\omega \mathcal{I} - [\mathcal{A}_\theta^\circ + \mathcal{E}_\theta])^{-1} \mathcal{B}_\theta - \mathfrak{C}_\theta (j\omega \mathcal{I} - [\mathcal{A}_\theta^\circ + \mathfrak{E}_\theta])^{-1} \mathfrak{B}_\theta\|_{\text{HS}}^2 d\omega d\theta \rightarrow 0$$

as $N \rightarrow \infty$, and (3.23) is shown. In particular

$$\int_0^\Omega \int_{-\infty}^\infty \|\mathfrak{G}_\theta(\omega)\|_{\text{HS}}^2 d\omega d\theta \rightarrow \int_0^\Omega \int_{-\infty}^\infty \|G_\theta(\omega)\|_{\text{HS}}^2 d\omega d\theta,$$

which together with $\mathbf{G}_\theta(\omega) = \Pi \mathfrak{G}_\theta(\omega) \Pi|_{\Pi\ell^2}$ gives

$$\int_0^\Omega \int_{-\infty}^\infty \|\mathbf{G}_\theta(\omega)\|_{\mathbb{F}}^2 d\omega d\theta \rightarrow \int_0^\Omega \int_{-\infty}^\infty \|\mathbf{G}_\theta(\omega)\|_{\text{HS}}^2 d\omega d\theta.$$

Chapter 4

Stability of Spatially Periodic Systems and the Nyquist Criterion

The shortest path between two truths in the real domain passes through the complex domain.

J. Hadamard

4.1 Introduction

In this chapter we begin by briefly reviewing some basic facts regarding the spectrum of spatially periodic infinitesimal generators and the exponential stability of spatially periodic systems in Section 4.2. We formulate the Nyquist stability problem for such systems in Section 4.3. We develop an analog of the conventional Nyquist stability criterion for spatially periodic systems in Section 4.4. Finally we tackle numerical issues in Section 4.5.

4.2 Stability Conditions and Spectrum of the Infinitesimal Generator

Since the Fourier and lifting transformations are both unitary and the spectral properties of operators remain preserved under unitary transformations, we have

$$\Sigma(A) = \Sigma(\hat{A}) = \overline{\bigcup_{\theta \in \Theta} \Sigma(\mathcal{A}_\theta)} = \bigcup_{\theta \in \bar{\Theta}} \Sigma(\mathcal{A}_\theta), \quad (4.1)$$

with the last equality being valid under the assumption of continuous dependence of \mathcal{A}_θ on θ . In the case where A is spatially invariant and thus $\mathcal{A}_\theta =$

$\text{diag}\{\dots, \hat{A}_0(\theta + \Omega n), \dots\}$, we have $\Sigma(\mathcal{A}_\theta) = \overline{\bigcup_{n \in \mathbb{Z}^d} \Sigma_p(\hat{A}_0(\theta + \Omega n))}$, and (4.1) further simplifies to

$$\Sigma(A) = \overline{\bigcup_{k \in \mathbb{R}^d} \Sigma_p(\hat{A}_0(k))}.$$

A strongly continuous semigroup (also known as a C_0 -semigroup) on a Hilbert space is called exponentially stable if there exist positive constants M and β such that [3]

$$\|e^{At}\| \leq M e^{-\beta t} \quad \text{for } t \geq 0.$$

The temporal growth properties of spatially distributed systems are preserved under Fourier transformation in the spatial variable, and thus the exponential stability of (2.22) is equivalent to that of (2.26). Similarly, since (2.26) and (2.29) are related through a unitary transformation (namely lifting in spatial frequency), the exponential stability of one implies that of the other.

It is known that for spatially distributed systems, the condition that $\Sigma(A) \subset \mathbb{C}^-$ is not enough to guarantee exponential stability. There exist examples of strongly continuous semigroups where $\Sigma(A)$ lies entirely inside \mathbb{C}^- , but where $\|e^{At}\|$ actually grows exponentially; see [14] and more recently [15]. Still there are subclasses of strongly continuous semigroups for which $\Sigma(A) \subset \mathbb{C}^-$ *does* yield exponential stability. Such semigroups are said to satisfy the so-called *spectrum-determined growth condition* [16]. These semigroups include (but are not limited to) those for which the infinitesimal generator A is *sectorial*¹ [19] or is a *Riesz-spectral operator* [3].

In this chapter we focus on systems which *do* satisfy the spectrum-determined growth condition. Thus to establish exponential stability of the system it is sufficient to show that

- (a) A satisfies the spectrum-determined growth condition,
- (b) $\Sigma(\mathcal{A}_\theta) \subset \mathbb{C}^-$ for all $\theta \in \bar{\Theta}$.

From (4.1), (b) would mean that $\Sigma(A) \subset \mathbb{C}^-$, which together with (a) yields exponential stability.

Remark 10 *There are many advantages to checking the spectrum of \mathcal{A}_θ rather than that of A . This is because, in general, \mathcal{A}_θ has discrete spectrum. In the next section we exploit this property to extend the Nyquist stability criteria to a class of spatially periodic systems, and in Chapter 6 we use this to apply Geršgorin-like arguments to find $\Sigma_p(\mathcal{A}_\theta)$. ■*

¹Such operators are also known as the generators of *holomorphic* or *analytic* semigroups [17, 18].

4.3 Nyquist Stability Problem Formulation

Consider the spatially invariant system \mathbf{S}°

$$\begin{aligned} [\partial_t \psi](t, x) &= [A \psi](t, x) + [B u](t, x), \\ y(t, x) &= [C \psi](t, x), \end{aligned} \quad (4.2)$$

where $t \in [0, \infty)$ and $x \in \mathbb{R}$ with the following assumptions. A , B , and C are spatially invariant. The (possibly unbounded) operator A is defined on a dense domain $\mathcal{D} \subset L^2(\mathbb{R})$ and is closed. B and C are bounded operators.

Next we place the spatially invariant system \mathbf{S}° in feedback with a spatially periodic multiplication operator $\gamma F(x)$, $\|F(x)\| = 1$, $\gamma \in \mathbb{C}$, with spatial period $X = 2\pi/\Omega$ and Fourier series

$$F(x) = \sum_{l \in \mathbb{Z}} f_l e^{jl\Omega x}.$$

This forms the closed-loop system shown in Figure 4.1 (left) with infinitesimal generator $A^{\text{cl}} := A - B \gamma F C$. We separate the function F from the gain γ as in Figure 4.1 (right) to form the closed-loop system \mathbf{S}^{cl} , and it is our aim here to determine the stability of \mathbf{S}^{cl} as the feedback gain γ varies in \mathbb{C} .

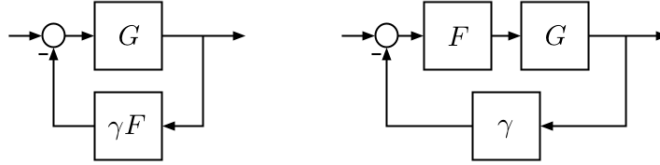


Figure 4.1: Left: The spatially periodic closed-loop system as the feedback interconnection of a spatially invariant system G and a spatially periodic multiplication operator F . Right: The closed-loop system \mathbf{S}^{cl} in the standard form for Nyquist stability analysis.

For simplicity, in this chapter we assume that all operators A , B , C and F are scalar (i.e., the Euclidean dimension of the state ψ is one). We also make the following assumptions on the infinitesimal generator A and its Fourier symbol $\hat{A}(\cdot)$.

Assumption ():* A is such that $|\hat{A}(k)| \geq a |k|^{1+\eta}$, $|k| > K$, for some $a > 0$, $\eta > 0$, $K > 0$,

*Assumption (**):* $\rho(A)$ contains a right sector of the complex plane $|\arg(z - \alpha)| \leq \frac{\pi}{2} + \varphi$, $\varphi > 0$, $\alpha \in \mathbb{R}$.

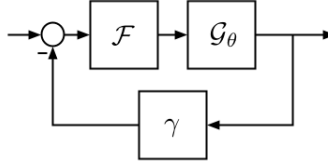


Figure 4.2: The closed-loop system $\mathbf{S}_\theta^{\text{cl}}$.

Remark 11 *Note that Assumption (**) does not prevent A from having spectrum inside \mathbb{C}^+ ; for example $\hat{A}(k)$ can reside in \mathbb{C}^+ for all k in some real interval $[k_1, k_2]$.² However, together with Assumption (*) it does constrain $\hat{A}(k)$ to stay inside \mathbb{C}^- as $|k| \rightarrow \infty$ and also become distant from the imaginary axis as $|k| \rightarrow \infty$. Indeed this is a natural assumption for many physical systems. ■*

Using lifting in the frequency domain, we showed in Chapter 2 how (4.2) can also be represented as

$$\begin{aligned} [\partial_t \psi_\theta](t) &= [\mathcal{A}_\theta \psi_\theta](t) + [\mathcal{B}_\theta u_\theta](t), \\ y_\theta(t) &= [\mathcal{C}_\theta \psi_\theta](t), \end{aligned} \quad (4.3)$$

with $\theta \in [0, \Omega)$ and $\mathcal{A}_\theta, \mathcal{B}_\theta, \mathcal{C}_\theta$ diagonal bi-infinite matrices. (4.3) describes the open-loop system $\mathbf{S}_\theta^{\text{o}}$ with temporal impulse response $\mathcal{G}_\theta(t) := \mathcal{C}_\theta e^{\mathcal{A}_\theta t} \mathcal{B}_\theta$, and transfer function

$$\begin{aligned} \mathcal{G}_\theta(s) &:= \mathcal{C}_\theta (s\mathcal{I} - \mathcal{A}_\theta)^{-1} \mathcal{B}_\theta \\ &= \text{diag} \left\{ \dots, \frac{\hat{C}(\theta + \Omega n) \hat{B}(\theta + \Omega n)}{s - \hat{A}(\theta + \Omega n)}, \dots \right\}. \end{aligned} \quad (4.4)$$

Finally, using the same bi-infinite matrix representation for the periodic operator $\gamma F(x)$ to get $\gamma \mathcal{F}$ and placing it in feedback with $\mathbf{S}_\theta^{\text{o}}$, we obtain the close-loop system $\mathbf{S}_\theta^{\text{cl}}$ in Figure 4.2 with infinitesimal generator $\mathcal{A}_\theta^{\text{cl}} := \mathcal{A}_\theta - \mathcal{B}_\theta \gamma \mathcal{F} \mathcal{C}_\theta$.

As mentioned in the beginning of this chapter, for a general spatially periodic operator A we have

$$\Sigma(A) = \bigcup_{\theta \in [0, \Omega]} \Sigma(\mathcal{A}_\theta)$$

where we have assumed continuous dependence of \mathcal{A}_θ on θ . Thus to prove $\Sigma(A^{\text{cl}}) \subset \mathbb{C}^-$, as needed to guarantee the exponential stability of \mathbf{S}^{cl} , it is necessary and sufficient to show that $\mathcal{A}_\theta^{\text{cl}} = \mathcal{A}_\theta - \mathcal{B}_\theta \gamma \mathcal{F} \mathcal{C}_\theta$ has spectrum inside \mathbb{C}^- for all $\theta \in$

²We remind the reader that for a scalar spatially invariant operator A , the spectrum $\Sigma(A)$ can be found from the Fourier symbol $\hat{A}(\cdot)$ using $\Sigma(A) = \overline{\bigcup_{k \in \mathbb{R}} \hat{A}(k)}$ with the bar denoting the closure of a set.

$[0, \Omega]$. In the next section we aim to develop a graphical method of checking whether or not $\Sigma(\mathcal{A}_\theta^{\text{cl}}) \subset \mathbb{C}^-$.

4.4 The Nyquist Stability Criterion for Spatially Periodic Systems

4.4.1 The Determinant Method

To motivate the development in this section, let us first consider a finite-dimensional (multi-input multi-output) LTI system $G(s)$ placed in feedback with a constant gain γI . In analyzing the closed-loop stability of such a system, we are concerned with the eigenvalues in \mathbb{C}^+ of the closed-loop A -matrix A^{cl} . If s is an eigenvalue of A^{cl} , then it satisfies $\det[sI - A^{\text{cl}}] = 0$. Now to check whether the equation $\det[sI - A^{\text{cl}}] = 0$ has solutions inside \mathbb{C}^+ , one can apply the argument principle to $\det[I + \gamma G(s)]$ as s traverses some curve \mathfrak{D} enclosing \mathbb{C}^+ . More precisely, let us assume that we are given a state-space realization of the open-loop system. Then using

$$\det[I + \gamma G(s)] = \frac{\det[sI - A^{\text{cl}}]}{\det[sI - A]}, \quad (4.5)$$

if one knows the number of unstable open-loop poles one can determine the number of unstable closed-loop poles by looking at the plot of $\det[I + \gamma G(s)]|_{s \in \mathfrak{D}}$.

But in the case of spatially distributed systems the open-loop and closed-loop infinitesimal generators \mathcal{A}_θ and $\mathcal{A}_\theta^{\text{cl}}$ are infinite-dimensional operators and, in general, can be *unbounded*. Hence it is not clear how to define the characteristic functions $\det[s\mathcal{I} - \mathcal{A}_\theta]$ and $\det[s\mathcal{I} - \mathcal{A}_\theta^{\text{cl}}]$, and one has to resort to operator theoretic arguments to relate the plot of $\det[\mathcal{I} + \gamma \mathcal{F}\mathcal{G}_\theta(s)]|_{s \in \mathfrak{D}^\theta}$ to the unstable modes of the open-loop and closed-loop systems.^{3,4} But first it has to be clarified what is meant by $\det[\mathcal{I} + \gamma \mathcal{F}\mathcal{G}_\theta(s)]$ for the infinite-dimensional operator $\mathcal{I} + \gamma \mathcal{F}\mathcal{G}_\theta(s)$. We need the following lemma.

Lemma 10 $\mathcal{F}\mathcal{G}_\theta(s) \in \mathcal{B}_1(\ell^2)$ for all $s \in \rho(\mathcal{A}_\theta)$.

Proof: See Appendix. ■

Since $\mathcal{F}\mathcal{G}_\theta(s) \in \mathcal{B}_1(\ell^2)$, one can now define [37] [20]

$$\det[\mathcal{I} + \gamma \mathcal{F}\mathcal{G}_\theta(s)] := \prod_{n \in \mathbb{Z}} (1 + \gamma \lambda_n^\theta(s)),$$

³ \mathfrak{D}^θ is a Nyquist path of the form shown in Figure 4.3 that does not pass through any eigenvalues of \mathcal{A}_θ .

⁴By Assumption (*) the multiplicity of each of the eigenvalues of \mathcal{A}_θ is finite and thus it can be shown that $\det[\mathcal{I} + \gamma \mathcal{F}\mathcal{G}_\theta(s)]$ is still a meromorphic function of s on \mathbb{C} . But it is not obvious what the analog of (4.5) is when \mathcal{A}_θ and $\mathcal{A}_\theta^{\text{cl}}$ are unbounded.

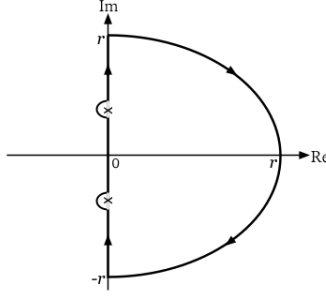


Figure 4.3: The closed contour \mathfrak{D}^θ traversed in the clockwise direction taken as the Nyquist path as $r \rightarrow \infty$. The indentations are arbitrarily made to avoid the eigenvalues of \mathcal{A}_θ (i.e., open-loop modes) on the imaginary axis.

where $\{\lambda_n^\theta(s)\}_{n \in \mathbb{Z}}$ are the eigenvalues of $\mathcal{G}_\theta(s)$. We are now ready to state a generalized form of the argument principle that is the analog of (4.5) applicable to systems with unbounded infinitesimal generators.

Theorem 11 *If $\det[\mathcal{I} + \gamma \mathcal{F} \mathcal{G}_\theta(s)] \neq 0$ for all $s \in \mathfrak{D}^\theta$,*

$$\begin{aligned} & C\left(0; \det[\mathcal{I} + \gamma \mathcal{F} \mathcal{G}_\theta(s)] \Big|_{s \in \mathfrak{D}^\theta}\right) \\ &= \operatorname{tr} \left[\frac{1}{2\pi j} \int_{\mathfrak{D}^\theta} (s\mathcal{I} - \mathcal{A}_\theta^{\text{cl}})^{-1} ds \right] - \operatorname{tr} \left[\frac{1}{2\pi j} \int_{\mathfrak{D}^\theta} (s\mathcal{I} - \mathcal{A}_\theta)^{-1} ds \right] \\ &= -(\text{number of eigenvalues of } \mathcal{A}_\theta^{\text{cl}} \text{ in } \mathbb{C}^+) \\ & \quad + (\text{number of eigenvalues of } \mathcal{A}_\theta \text{ in } \mathbb{C}^+), \end{aligned}$$

where \mathfrak{D}^θ is the Nyquist path shown in Figure 4.3 that does not pass through any eigenvalues of \mathcal{A}_θ , and encloses a finite number of them.

Proof: See Appendix. Also, a more general version of the this theorem is proved in [38] using the notion of the perturbation determinant. \blacksquare

Remark 12 $\mathcal{P}_\theta = -\frac{1}{2\pi j} \int_{\mathfrak{D}^\theta} (s\mathcal{I} - \mathcal{A}_\theta)^{-1} ds$ is the group-projection [39] [20] corresponding to the eigenvalues of \mathcal{A}_θ inside \mathfrak{D}^θ , and $\operatorname{tr}[\mathcal{P}_\theta]$ gives the total number of such eigenvalues [17]. Similarly $\operatorname{tr}[-\frac{1}{2\pi j} \int_{\mathfrak{D}^\theta} (s\mathcal{I} - \mathcal{A}_\theta^{\text{cl}})^{-1} ds]$ gives the total number of eigenvalues of $\mathcal{A}_\theta^{\text{cl}}$ in \mathfrak{D}^θ . Thus Theorem 11 allows us to determine the number of \mathbb{C}^+ eigenvalues of $\mathcal{A}_\theta^{\text{cl}}$ from knowledge of the number of \mathbb{C}^+ eigenvalues of \mathcal{A}_θ and the number of encirclements of the origin by the plot of $\det[\mathcal{I} + \gamma \mathcal{F} \mathcal{G}_\theta(s)]$ as s traverses \mathfrak{D}^θ . Recall that since $\mathcal{A}_\theta = \operatorname{diag}\{\dots, \hat{A}(\theta + \Omega n), \dots\}$, the eigenvalues of \mathcal{A}_θ are known, $\Sigma_p(\mathcal{A}_\theta) = \{\hat{A}(\theta + \Omega n)\}_{n \in \mathbb{Z}}$. \blacksquare

Remark 13 It now becomes clear why we use the \mathcal{A}_θ representation of the operator A . The proof of Theorem 11 relies on the fact that under Assumption (*) both

$(s\mathcal{I} - \mathcal{A}_\theta)^{-1}$ and $(s\mathcal{I} - \mathcal{A}_\theta^{\text{cl}})^{-1}$ are compact operators, which means the infinitesimal generators \mathcal{A}_θ and $\mathcal{A}_\theta^{\text{cl}}$ have discrete (pure point) spectrum for every value of θ . This allows for the introduction of the group projections seen in Theorem 11 and described in Remark 12. Such group projections can not be introduced for A and A^{cl} since they have continuous spectrum in general. ■

Remark 14 Since \mathcal{A}_θ has discrete spectrum, it has no finite accumulation points in the complex plane [17]. In particular, the eigenvalues of \mathcal{A}_θ can not converge to any finite point $j\omega_0$ of the imaginary axis. Yet by itself this does not rule out the possibility of the eigenvalues accumulating at $\pm j\infty$. But Assumption (**) guards against this by requiring that $\hat{A}(k)$ be bounded away from the imaginary axis as $|k| \rightarrow \infty$; see Remark 11. Thus the Nyquist path can be taken to run to infinity along the imaginary axis without any technical difficulties. ■

As a direct consequence of Theorem 11 we have the following.

Theorem 12 Assume p_+^θ denotes the number of eigenvalues of \mathcal{A}_θ inside \mathbb{C}^+ . For \mathfrak{D}^θ taken as above, $\Sigma_p(\mathcal{A}_\theta^{\text{cl}}) \subset \mathbb{C}^-$ iff

$$(a) \det[\mathcal{I} + \gamma\mathcal{F}\mathcal{G}_\theta(s)] \neq 0, \quad \forall s \in \mathfrak{D}^\theta,$$

and

$$(b) C\left(0; \det[\mathcal{I} + \gamma\mathcal{F}\mathcal{G}_\theta(s)]\Big|_{s \in \mathfrak{D}^\theta}\right) = p_+^\theta.$$

Finally, the closed-loop system G^{cl} is exponentially stable iff $\Sigma_p(\mathcal{A}_\theta^{\text{cl}}) \subset \mathbb{C}^-$ for all $\theta \in [0, \Omega]$. ■

4.4.2 The Eigenloci Method

The setback with the method described in the previous paragraph is that to show $\Sigma_p(\mathcal{A}_\theta^{\text{cl}}) \subset \mathbb{C}^-$, $\mathcal{A}_\theta^{\text{cl}} = \mathcal{A}_\theta - \mathcal{B}_\theta\gamma\mathcal{F}\mathcal{C}_\theta$, for different values of γ , one has to plot $\det[\mathcal{I} + \gamma\mathcal{F}\mathcal{G}_\theta(s)]\Big|_{s \in \mathfrak{D}^\theta}$ for each γ . Note that this includes having to calculate the determinant of an infinite dimensional matrix. This motivates the following eigenloci approach to Nyquist stability analysis, which is very similar to that performed in [8] for the case of time-periodic systems.

Let $\{\lambda_n^\theta(s)\}_{n \in \mathbb{Z}}$ constitute the eigenvalues of $\mathcal{F}\mathcal{G}_\theta(s)$. Then

$$\angle \det[\mathcal{I} + \gamma\mathcal{F}\mathcal{G}_\theta(s)] = \angle \prod_{n \in \mathbb{Z}} (1 + \gamma\lambda_n^\theta(s)). \quad (4.6)$$

But recall from Lemma 10 that $\mathcal{F}\mathcal{G}_\theta(s) \in \mathcal{B}_1(\ell^2)$ for every $s \in \rho(\mathcal{A}_\theta)$. This, in particular, means that $\mathcal{F}\mathcal{G}_\theta(s)$ is a compact operator and thus its eigenvalues $\lambda_n^\theta(s)$ accumulate at the origin as $|n| \rightarrow \infty$ [32]. As a matter of fact one can make a much stronger statement.

Lemma 13 *The eigenvalues $\lambda_n^\theta(s)$, $s \in \mathfrak{D}^\theta$, converge to the origin uniformly on \mathfrak{D}^θ .*

Proof: *See Appendix.* ■

Take the positive integer N_ϵ to be such that $|\lambda_n^\theta(s)| < \epsilon$, $s \in \mathfrak{D}^\theta$, for all $|n| > N_\epsilon$. Let us rewrite (4.6) as

$$\begin{aligned} \angle \det[\mathcal{I} + \gamma \mathcal{F}\mathcal{G}_\theta(s)] &= \angle \prod_{|n| \leq N_\epsilon} (1 + \gamma \lambda_n^\theta(s)) + \angle \prod_{|n| > N_\epsilon} (1 + \gamma \lambda_n^\theta(s)) \\ &= \sum_{|n| \leq N_\epsilon} \angle (1 + \gamma \lambda_n^\theta(s)) + \sum_{|n| > N_\epsilon} \angle (1 + \gamma \lambda_n^\theta(s)). \end{aligned} \quad (4.7)$$

It is clear that if $|\gamma| < \frac{1}{\epsilon}$ then for $|n| > N_\epsilon$ we have $|\gamma \lambda_n^\theta(s)| < 1$, and $1 + \gamma \lambda_n^\theta(s)$ can never circle the origin as s travels around \mathfrak{D}^θ . Thus for $|\gamma| < \frac{1}{\epsilon}$ the final sum in (4.7) will not contribute to the encirclements of the origin, and hence we lose nothing by considering only the first N_ϵ eigenvalues. There still remain some minor technicalities.

First, let D_ϵ denote the disk $|s| < \epsilon$ in the complex plane. Then said truncation may result in some eigenloci (parts of which reside inside D_ϵ) not forming closed loops. But notice that these can be arbitrarily closed inside D_ϵ , as this does not affect the encirclements [8].

The second issue is that for some values of $s \in \mathfrak{D}^\theta$, $\mathcal{F}\mathcal{G}_\theta(s)$ may have multiple eigenvalues, and hence there is ambiguity in how the eigenloci of the Nyquist diagram should be indexed. But this poses no problem as far as counting the encirclements is concerned, and it is always possible to find such an indexing; for a detailed treatment see [40].

Let us denote by $\{\lambda_n^\theta\}_{n \in \mathbb{Z}}$ the indexed eigenloci that make up the generalized Nyquist diagram. [To avoid confusion we stress the notation: $\lambda_n^\theta(s)$ is the n^{th} eigenvalue of $\mathcal{F}\mathcal{G}_\theta(s)$ for a given point $s \in \mathfrak{D}^\theta$, whereas λ_n^θ is the n^{th} eigenlocus traced out by $\lambda_n^\theta(s)$ as s travels once around \mathfrak{D}^θ .] From (4.7) and the above discussion it follows that

$$C\left(0; \det[\mathcal{I} + \gamma \mathcal{F}\mathcal{G}_\theta(s)]|_{s \in \mathfrak{D}^\theta}\right) = \sum_{|n| \leq N_\epsilon} C\left(-\frac{1}{\gamma}; \lambda_n^\theta\right)$$

which together with Theorem 12 gives the following.

Theorem 14 *Assume p_+^θ denotes the number of eigenvalues of \mathcal{A}_θ inside \mathbb{C}^+ . For \mathfrak{D}^θ and N_ϵ as defined previously, $\Sigma_p(\mathcal{A}_\theta^{cl}) \subset \mathbb{C}^-$ for $|\gamma| < \frac{1}{\epsilon}$ iff*

$$(a) \quad -\frac{1}{\gamma} \notin \{\lambda_n^\theta\}_{|n| \leq N_\epsilon},$$

and

$$(b) \sum_{|n| \leq N_\epsilon} C\left(-\frac{1}{\gamma}; \lambda_n^\theta(s)\right) = p_+^\theta.$$

Finally, the closed-loop system G^{cl} is exponentially stable iff $\Sigma_p(\mathcal{A}_\theta^{cl}) \subset \mathbb{C}^-$ for all $\theta \in [0, \Omega]$. ■

4.5 Numerical Implementation

4.5.1 Finite Truncations of System Operators

In the above development we showed that for a given $\epsilon > 0$, the eigenloci that fall within the disk $D_\epsilon = \{s \text{ s.t. } |s| < \epsilon\}$ play no role in the Nyquist stability analysis and can be ignored as long as $|\frac{1}{\gamma}| > \epsilon$.

This suggests that one could *truncate* \mathcal{A}_θ , \mathcal{B}_θ , \mathcal{C}_θ , \mathcal{F} first and then form a truncated version of $\mathcal{F}\mathcal{G}_\theta(s)$ and compute its eigenloci, thus effectively treating the stability problem as one for a family of (finite-dimensional) multivariable systems described by (4.3) parameterized by the variable θ .

The complication here is that although a truncation removes the infinite number of eigenloci that shrink to zero, it also affects *all other* eigenloci no matter how large the truncation is taken to be. Nevertheless, it can be shown that by increasing the size of the truncation the eigenloci of $\mathcal{F}\mathcal{G}_\theta(s)$ can be recovered to any accuracy.

As in Section 3.5 let Π be the projection on the first $2N + 1$ standard basis elements of ℓ^2 , $\{e_{-N}, \dots, e_0, \dots, e_N\}$, with the representation

$$\Pi = \text{diag}\left\{\dots, 0, \underbrace{1, \dots, 1}_{\substack{\text{center} \\ \downarrow \\ 2N+1 \text{ times}}}, \dots, 1, 0, \dots\right\}.$$

Thus $\Pi\mathcal{F}\Pi$ is the $(2N+1) \times (2N+1)$ truncation of \mathcal{F} , $\Pi\mathcal{G}_\theta(s)\Pi = \Pi\mathcal{G}_\theta(s) = \mathcal{G}_\theta(s)\Pi$ the $(2N+1) \times (2N+1)$ truncation of \mathcal{G}_θ ,⁵ and $\Pi\Pi = \Pi$. We have

Theorem 15 *If $\zeta \in \rho(\Pi\mathcal{F}\Pi\mathcal{G}_\theta(s))$, $s \in \mathfrak{D}^\theta$, and*

$$\|\mathcal{F}\mathcal{G}_\theta(s) - \Pi\mathcal{F}\Pi\mathcal{G}_\theta(s)\| \|(\zeta - \Pi\mathcal{F}\Pi\mathcal{G}_\theta(s))^{-1}\| < 1, \quad (4.8)$$

then $\zeta \in \rho(\mathcal{F}\mathcal{G}_\theta(s))$.

Proof: See Appendix. ■

⁵Recall that Π commutes with $\mathcal{G}_\theta(s)$ because the latter operator is diagonal.

Theorem 15 says that if a point ζ is not an eigenvalue of $\Pi\mathcal{F}\Pi\mathcal{G}_\theta(s)$ then it will not be an eigenvalue of $\mathcal{F}\mathcal{G}_\theta(s)$ if (4.8) holds. But we need a stronger result that addresses the location of the *eigenloci* rather than the eigenvalues. Namely that if ζ does not belong to the eigenloci of the truncated system then it will not belong to the eigenloci of the original system either. This is done in the next theorem.

Theorem 16 *If ζ does not belong to the eigenloci of $\Pi\mathcal{F}\Pi\mathcal{G}_\theta(s)$, $s \in \mathfrak{D}^\theta$, and*

$$\max_{s \in \mathfrak{D}^\theta} \|\mathcal{F}\mathcal{G}_\theta(s) - \Pi\mathcal{F}\Pi\mathcal{G}_\theta(s)\| \max_{s \in \mathfrak{D}^\theta} \|(\zeta - \Pi\mathcal{F}\Pi\mathcal{G}_\theta(s))^{-1}\| < 1, \quad (4.9)$$

then ζ does not belong to the eigenloci of $\mathcal{F}\mathcal{G}_\theta(s)$, $s \in \mathfrak{D}^\theta$.

Proof: *The proof is simple and is omitted.* ■

4.5.2 Regularity in the θ Parameter

In applying Theorems 12 and 14 one would hope for some kind of ‘regularity’ with respect to the variable θ . More concretely, in practice one would like to plot the eigenloci and check the Nyquist stability criterion for a *finite number* of $\theta_l \in [0, \Omega)$, say $\theta_1, \dots, \theta_L$, and be able to conclude stability for all $\theta \in [0, \Omega)$ if the θ_l are chosen close enough to each other.

Indeed, it is possible to show that if $\det[\mathcal{I} + \gamma\mathcal{F}\mathcal{G}_\theta(s)] \neq 0$ for all $s \in \mathfrak{D}^\theta$ then $\det[\mathcal{I} + \gamma\mathcal{F}\mathcal{G}_\theta(s)]$ is a continuous function of θ for all $s \in \mathfrak{D}^\theta$. In other words all points of the plot $\det[\mathcal{I} + \gamma\mathcal{F}\mathcal{G}_\theta(s)]|_{s \in \mathfrak{D}^\theta}$ change continuously with θ . This result is easy to prove using techniques presented in [20] and we omit the details. Moreover, one can show that the following much stronger assertion.

Theorem 17 *Let $\hat{A}(\kappa)$, $\hat{B}(\kappa)$, $\hat{C}(\kappa)$ be analytic functions of κ on some strip*

$$\mathfrak{R} = \{\zeta \text{ s.t. } -\varepsilon \leq \text{Im}(\zeta) \leq \varepsilon, \varepsilon > 0\}$$

of the complex plane. Then the eigenloci $\{\lambda_n^\theta\}_{n \in \mathbb{Z}}$ of $\mathcal{F}\mathcal{G}_\theta(s)$ change continuously with θ .

Proof: *See Appendix.* ■

4.6 An Illustrative Example

In this section we consider the example of a system governed by the spatially periodic PDE

$$\partial_t \psi(t, x) = \partial_x^2 \psi(t, x) - \gamma \cos(x) \psi(t, x) + \psi(t, x), \quad (4.10)$$

with $\gamma \in \mathbb{C}$. Let us rewrite this system in the form of an open-loop spatially invariant PDE described by

$$\begin{aligned}\partial_t \psi(t, x) &= \partial_x^2 \psi(t, x) + \psi(t, x) + u(t, x), \\ y(t, x) &= \psi(t, x),\end{aligned}$$

placed in feedback with the spatially periodic function

$$\gamma F(x) = \gamma \cos(x).$$

Now the problem is in the general from discussed in Section 4.3 with $A = \partial_x^2 + 1$, B and C being the identity operator, and $F(x) = \cos(x)$ [thus $\Omega = 1$]. Since $\hat{A}(k) = -k^2 + 1$, $k \in \mathbb{R}$, Assumptions (*) is satisfied. Also, since $\Sigma(A) = (-\infty, 1]$ then Assumption (***) is satisfied. Finally, from $\hat{A}(\kappa) = -\kappa^2 + 1$ and $\hat{B}(\kappa) = \hat{C}(\kappa) = 1$ it is clear that these symbols are analytic on the entire complex plane and thus the conditions of Theorem 17 are satisfied.

The representation of the system in the frequency domain is $\partial_t \psi_\theta(t) = (\mathcal{A}_\theta - \gamma \mathcal{F}) \psi_\theta(t)$, where $\mathcal{A}_\theta = \text{diag}\{\dots, -(\theta+n)^2+1, \dots\}$ for every $\theta \in [0, 1)$ and \mathcal{F} has the form shown in Example 1 of Section 2.5. Notice that the open-loop system is unstable; for example at $\theta = 0$, \mathcal{A}_θ has an eigenvalue at $\lambda = 1$. Next we demonstrate that by plotting the eigenloci one can read off from this plot the stability of the closed-loop system for any value of $\gamma \in \mathbb{C}$.

Recall that to test the stability of the closed-loop system, one has to apply the Nyquist criterion for every $\theta \in [0, 1)$. But since the conditions of Theorem 17 are satisfied we need only carry out the Nyquist analysis for a finite number of θ . We take Nyquist paths \mathfrak{D}^θ of the form shown in Figure 4.4(a) with $r = 20$. For every θ the indentation in \mathfrak{D}^θ is chosen appropriately so as to avoid the eigenvalues of \mathcal{A}_θ at the origin. Let us take a look at the Nyquist plots for two particular values of θ :

$\theta = 0$: $\lambda = 0, 0, 1$ are the eigenvalues of \mathcal{A}_0 inside \mathfrak{D}^0 , hence $p_+^0 = 3$, and we need three counter-clockwise encirclements of $-1/\gamma$ to achieve closed-loop stability. As can be seen in Figure 4.4(b) and its blown-up version (c), one possible choice would be to take $-1/\gamma$ to be purely imaginary and $-0.2j \leq -1/\gamma \leq 0.2j$. Clearly such $-1/\gamma$ is encircled three times by the eigenloci.

$\theta = 0.5$: $\lambda = 0.75, 0.75$ are the eigenvalues of $\mathcal{A}_{0.5}$ inside $\mathfrak{D}^{0.5}$, hence $p_+^{0.5} = 2$, and we need two counter-clockwise encirclements of $-1/\gamma$ to achieve closed-loop stability. Again, from Figure 4.4(d), if $-1/\gamma$ is taken to be purely imaginary and $-0.2j \leq -1/\gamma \leq 0.2j$, then $-1/\gamma$ is encircled twice by the eigenloci.

We do not draw the Nyquist plots for other values of θ but it can be shown that $-0.2j \leq -1/\gamma \leq 0.2j$ stabilizes the closed-loop system for all values of $\theta \in [0, 1)$ and thus stabilizes the original PDE (4.10).

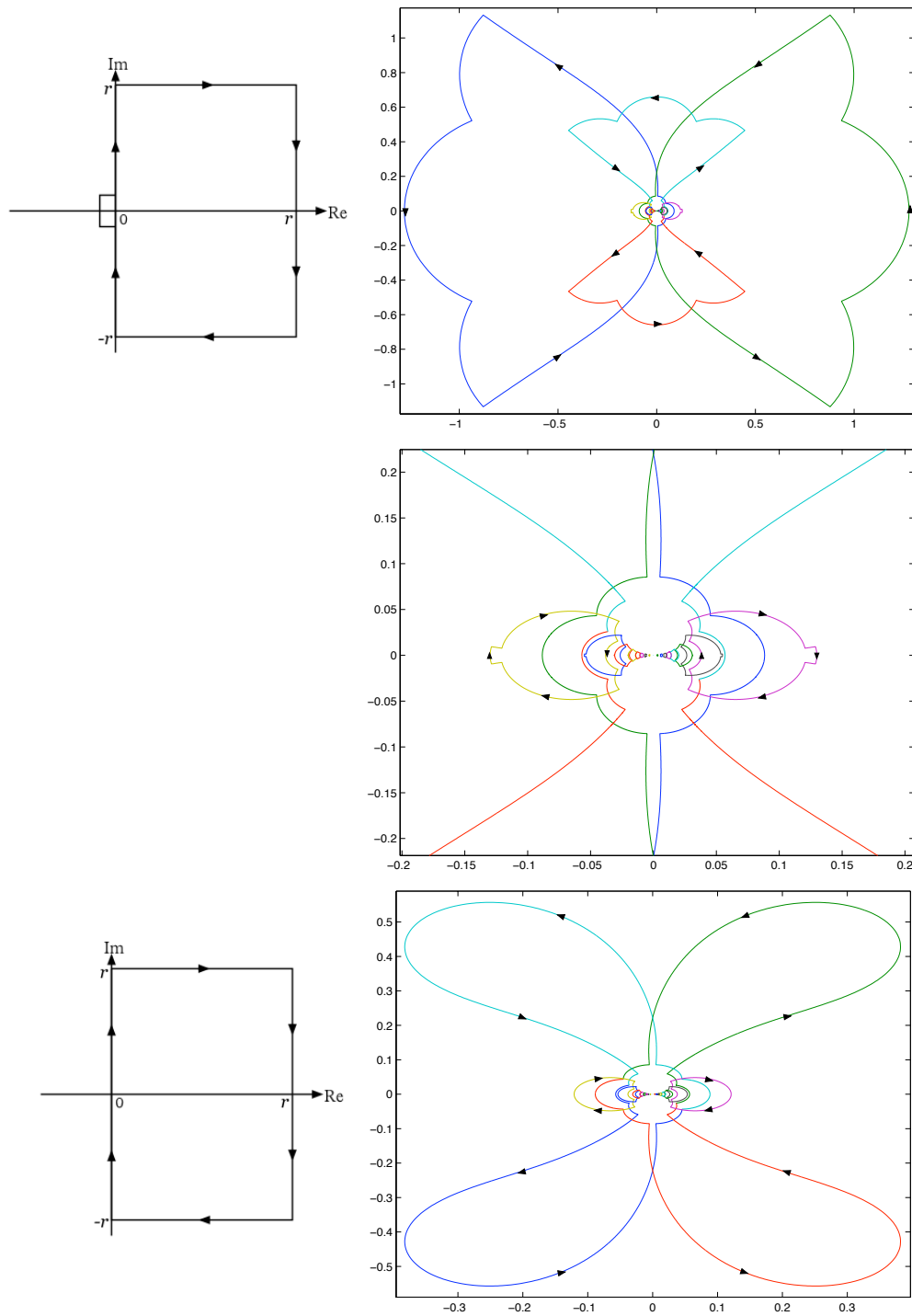


Figure 4.4: Top: The Nyquist path \mathcal{D}^0 ; The Nyquist plot for $\theta = 0$. Center: Blown-up version of the center part of the Nyquist plot for $\theta = 0$. Bottom: The Nyquist path $\mathcal{D}^{0.5}$; The Nyquist plot for $\theta = 0.5$.

4.7 Appendix to Chapter 4

Proof of Lemma 10

Since $s \in \rho(\mathcal{A}_\theta)$, then $s \neq \hat{A}(\theta + \Omega n)$ for any $n \in \mathbb{Z}$, which means that all elements of the diagonal operator $(s\mathcal{I} - \mathcal{A}_\theta)^{-1}$ are finite. Let $\varrho_n((s\mathcal{I} - \mathcal{A}_\theta)^{-1})$, $n = 1, 2, \dots$, be a reordering of these diagonal elements such that $|\varrho_1((s\mathcal{I} - \mathcal{A}_\theta)^{-1})| \geq |\varrho_2((s\mathcal{I} - \mathcal{A}_\theta)^{-1})| \geq \dots \geq 0$. Then $\sigma_n((s\mathcal{I} - \mathcal{A}_\theta)^{-1}) = |\varrho_n((s\mathcal{I} - \mathcal{A}_\theta)^{-1})|$, where σ_n denotes the n^{th} singular value. But from Assumption (*) it follows that $\sum_{n=1}^{\infty} \sigma_n((s\mathcal{I} - \mathcal{A}_\theta)^{-1}) < \infty$. Hence $(s\mathcal{I} - \mathcal{A}_\theta)^{-1} \in \mathcal{B}_1(\ell^2)$. But since B , C , and F are bounded operators, so are \mathcal{B}_θ , \mathcal{C}_θ , and \mathcal{F} . Thus $\mathcal{G}_\theta(s) \in \mathcal{B}_1(\ell^2)$ and $\mathcal{F}\mathcal{G}_\theta(s) \in \mathcal{B}_1(\ell^2)$ [20].

Proof of Theorem 11

To prove Theorem 11 we need the following lemma.

Lemma 18 *For $s \in \rho(\mathcal{A}_\theta)$, $\det[\mathcal{I} + \gamma\mathcal{F}\mathcal{G}_\theta(s)]$ is analytic in both γ and s .*

Proof: For $s \in \rho(\mathcal{A}_\theta)$, $\gamma\mathcal{F}\mathcal{G}_\theta(s) \in \mathcal{B}_1(\ell^2)$ by Lemma 10. Also $\gamma\mathcal{F}\mathcal{G}_\theta(s) = \gamma\mathcal{F}\mathcal{C}_\theta(s\mathcal{I} - \mathcal{A}_\theta)^{-1}\mathcal{B}_\theta$ is clearly analytic in both γ and s for $s \in \rho(\mathcal{A}_\theta)$. Then it follows from [20, p163] that $\det[\mathcal{I} + \gamma\mathcal{F}\mathcal{G}_\theta(s)]$ too is analytic in both γ and s for $s \in \rho(\mathcal{A}_\theta)$. ■

Proof of Theorem 11: Consider any point s in \mathfrak{D}^θ . Since \mathfrak{D}^θ does not pass through any eigenvalues of \mathcal{A}_θ , $s \in \rho(\mathcal{A}_\theta)$ and thus $\gamma\mathcal{F}\mathcal{C}_\theta(s\mathcal{I} - \mathcal{A}_\theta)^{-1}\mathcal{B}_\theta \in \mathcal{B}_1(\ell^2)$ from Lemma 10. Then from [37], $(\mathcal{I} + \gamma\mathcal{F}\mathcal{C}_\theta(s\mathcal{I} - \mathcal{A}_\theta)^{-1}\mathcal{B}_\theta)^{-1}$ exists and belongs to $\mathcal{B}(\ell^2)$ iff $\det[\mathcal{I} + \gamma\mathcal{F}\mathcal{C}_\theta(s\mathcal{I} - \mathcal{A}_\theta)^{-1}\mathcal{B}_\theta] \neq 0$, which is satisfied by assumption. Applying the matrix inversion lemma to $(\mathcal{I} + \gamma\mathcal{F}\mathcal{C}_\theta(s\mathcal{I} - \mathcal{A}_\theta)^{-1}\mathcal{B}_\theta)^{-1}$, we conclude that $s \in \rho(\mathcal{A}_\theta^{\text{cl}})$ and $(s\mathcal{I} - \mathcal{A}_\theta^{\text{cl}})^{-1} = (s\mathcal{I} - \mathcal{A}_\theta + \mathcal{B}_\theta\gamma\mathcal{F}\mathcal{C}_\theta)^{-1} \in \mathcal{B}(\ell^2)$.

Now since $(s\mathcal{I} - \mathcal{A}_\theta^{\text{cl}})^{-1}$, \mathcal{B}_θ , \mathcal{C}_θ , and \mathcal{F} all belong to $\mathcal{B}(\ell^2)$, and $(s\mathcal{I} - \mathcal{A}_\theta)^{-1} \in \mathcal{B}_1(\ell^2)$, we have $(s\mathcal{I} - \mathcal{A}_\theta^{\text{cl}})^{-1}\mathcal{B}_\theta\gamma\mathcal{F}\mathcal{C}_\theta(s\mathcal{I} - \mathcal{A}_\theta)^{-1} \in \mathcal{B}_1(\ell^2)$ [20]. Thus, from the identity

$$(s\mathcal{I} - \mathcal{A}_\theta^{\text{cl}})^{-1} - (s\mathcal{I} - \mathcal{A}_\theta)^{-1} = - (s\mathcal{I} - \mathcal{A}_\theta^{\text{cl}})^{-1}\mathcal{B}_\theta\gamma\mathcal{F}\mathcal{C}_\theta(s\mathcal{I} - \mathcal{A}_\theta)^{-1},$$

it follows that $(s\mathcal{I} - \mathcal{A}_\theta^{\text{cl}})^{-1} \in \mathcal{B}_1(\ell^2)$. In particular $(s\mathcal{I} - \mathcal{A}_\theta)^{-1}$ and $(s\mathcal{I} - \mathcal{A}_\theta^{\text{cl}})^{-1}$ are both in $\mathcal{B}_\infty(\ell^2)$, which means that \mathcal{A}_θ and $\mathcal{A}_\theta^{\text{cl}}$ both have discrete spectrum [17] and in

$$\begin{aligned} & \frac{1}{2\pi j} \int_{\mathfrak{D}^\theta} (s\mathcal{I} - \mathcal{A}_\theta^{\text{cl}})^{-1} ds - \frac{1}{2\pi j} \int_{\mathfrak{D}^\theta} (s\mathcal{I} - \mathcal{A}_\theta)^{-1} ds \\ &= - \frac{1}{2\pi j} \int_{\mathfrak{D}^\theta} (s\mathcal{I} - \mathcal{A}_\theta^{\text{cl}})^{-1} \mathcal{B}_\theta \gamma \mathcal{F} \mathcal{C}_\theta (s\mathcal{I} - \mathcal{A}_\theta)^{-1} ds \end{aligned}$$

each term on the left side is a finite-dimensional projection [20, p11, p15]. Taking the trace of both sides and changing the order of integration and trace on the right ⁶ we have

$$\begin{aligned} \operatorname{tr}\left[\frac{1}{2\pi j}\int_{\mathfrak{D}^\theta}(s\mathcal{I}-\mathcal{A}_\theta^{\text{cl}})^{-1}ds\right] &- \operatorname{tr}\left[\frac{1}{2\pi j}\int_{\mathfrak{D}^\theta}(s\mathcal{I}-\mathcal{A}_\theta)^{-1}ds\right] \\ &= -\frac{1}{2\pi j}\int_{\mathfrak{D}^\theta}\operatorname{tr}[(s\mathcal{I}-\mathcal{A}_\theta^{\text{cl}})^{-1}\mathcal{B}_\theta\gamma\mathcal{F}\mathcal{C}_\theta(s\mathcal{I}-\mathcal{A}_\theta)^{-1}]ds. \end{aligned} \quad (4.11)$$

From [17], the left side of (4.11) is equal to the number of eigenvalues of \mathcal{A}_θ in \mathbb{C}^+ minus the number of eigenvalues of $\mathcal{A}_\theta^{\text{cl}}$ in \mathbb{C}^+ .

On the other hand, let the path \mathfrak{C}^θ be that traversed by $\det[\mathcal{I} + \gamma\mathcal{F}\mathcal{G}_\theta(s)]$ as s travels once around \mathfrak{D}^θ . By Lemma 18, $\det[\mathcal{I} + \gamma\mathcal{F}\mathcal{G}_\theta(s)]$ is analytic in s , and if $\det[\mathcal{I} + \gamma\mathcal{F}\mathcal{G}_\theta(s)] \neq 0$ on \mathfrak{D}^θ we have

$$\begin{aligned} C\left(0; \det[\mathcal{I} + \gamma\mathcal{F}\mathcal{G}_\theta(s)]\Big|_{s \in \mathfrak{D}^\theta}\right) &= \frac{1}{2\pi j} \int_{\mathfrak{C}^\theta} \frac{dz}{z} \\ &= \frac{1}{2\pi j} \int_{\mathfrak{D}^\theta} \frac{\frac{d}{ds} \det[\mathcal{I} + \gamma\mathcal{F}\mathcal{G}_\theta(s)]}{\det[\mathcal{I} + \gamma\mathcal{F}\mathcal{G}_\theta(s)]} ds. \end{aligned} \quad (4.12)$$

Using [20, p163] and the assumption $\det[\mathcal{I} + \gamma\mathcal{F}\mathcal{G}_\theta(s)] \neq 0$, $s \in \mathfrak{D}^\theta$, we arrive at

$$\begin{aligned} \frac{\frac{d}{ds} \det[\mathcal{I} + \gamma\mathcal{F}\mathcal{G}_\theta(s)]}{\det[\mathcal{I} + \gamma\mathcal{F}\mathcal{G}_\theta(s)]} &= \operatorname{tr}\left[(\mathcal{I} + \gamma\mathcal{F}\mathcal{G}_\theta(s))^{-1} \frac{d}{ds} \gamma\mathcal{F}\mathcal{G}_\theta(s)\right] \\ &= -\operatorname{tr}[(s\mathcal{I} - \mathcal{A}_\theta^{\text{cl}})^{-1} \mathcal{B}_\theta \gamma \mathcal{F} \mathcal{C}_\theta (s\mathcal{I} - \mathcal{A}_\theta)^{-1}]. \end{aligned}$$

This, together with (4.12) and (4.11) gives the required result.

Proof of Lemma 13

For $s \in \mathfrak{D}^\theta \subset \rho(\mathcal{A}_\theta)$, $\det[\mathcal{I} + \gamma\mathcal{F}\mathcal{G}_\theta(s)]$ is analytic in both γ and s by Lemma 18. The proof now proceeds exactly as in [8, p140] and is omitted.

Proof of Theorem 15

This is a direct consequence of Theorem 3.17, Chap IV of [17]. Using the notation of [17], for $s \in \mathfrak{D}^\theta$ take $T := \Pi\mathcal{F}\Pi\mathcal{G}_\theta(s)$, $A := \mathcal{F}\mathcal{G}_\theta(s) - \Pi\mathcal{F}\Pi\mathcal{G}_\theta(s)$, and $S := T + A = \mathcal{F}\mathcal{G}_\theta(s)$. Since T and A are bounded operators then $b = 0$ and $a = \|\mathcal{F}\mathcal{G}_\theta(s) - \Pi\mathcal{F}\Pi\mathcal{G}_\theta(s)\|$, again using the notation of [17]. The theorem statement now follows from (4.8) and [17, p214].

⁶Since $(s\mathcal{I} - \mathcal{A}_\theta^{\text{cl}})^{-1}\mathcal{B}_\theta\gamma\mathcal{F}\mathcal{C}_\theta(s\mathcal{I} - \mathcal{A}_\theta)^{-1} \in \mathcal{B}_1(\ell^2)$, its trace is well-defined and finite.

Proof of Theorem 17

It is simple to show that if $\hat{A}(\kappa)$ is an analytic function of κ on \mathfrak{R} , then it is an *analytic family in the sense of Kato* on \mathfrak{R} ; see [41, p14]. We now form the operator $\mathcal{A}_\vartheta = \text{diag}\{\dots, \hat{A}(\vartheta + \Omega n), \dots\}$ where ϑ is a variable on an open strip Θ that contains the real interval $[0, \Omega)$. It is immediate that \mathcal{A}_ϑ too is an analytic family in the sense of Kato on Θ . [The existence of Θ is guaranteed by the existence of \mathfrak{R} .] Let $\Upsilon := \{(\vartheta, z) \mid \vartheta \in \Theta, z \in \rho(\mathcal{A}_\vartheta)\}$. Then from [41, Thm XII.7] it follows that $(z - \mathcal{A}_\vartheta)^{-1}$ is an analytic (operator-valued) function of the the two variables ϑ and z on Υ . In particular, if $\hat{B}(\kappa)$ and $\hat{C}(\kappa)$ are analytic functions of κ on \mathfrak{R} then $\mathcal{F}\mathcal{G}_\vartheta(z) = \mathcal{F}\mathcal{B}_\vartheta(z - \mathcal{A}_\vartheta)^{-1}\mathcal{C}_\vartheta$ is an analytic (operator-valued) function of the the two variables ϑ and z on Υ . Let $\lambda^\theta(s)$ be an eigenvalue of multiplicity i of the bounded operator $\mathcal{F}\mathcal{G}_\theta(s)$, $\theta \in [0, \Omega)$ and $s \in \mathfrak{D}^\theta$. Then for (ϑ, z) near (θ, s) there are exactly i eigenvalues of $\mathcal{F}\mathcal{G}_\vartheta(z)$ near $\lambda^\theta(s)$ [17, p107]. We now restrict ϑ and z to vary only on $[0, \Omega)$ and \mathfrak{D}^θ , respectively, and we have that the eigenvalues of $\mathcal{F}\mathcal{G}_\theta(s)$ are continuous in both θ and s in the sense just described. Since \mathfrak{D}^θ is a closed set then it follows that the eigenloci $\{\lambda_n^\theta\}_{n \in \mathbb{Z}}$ change continuously with θ .

4.8 Summary

We develop a generalized Nyquist stability criterion that is applicable to open-loop systems with infinite-dimensional input-output spaces and unbounded infinitesimal generators. We use this to verify the stability of spatially periodic systems, and in particular, systems governed by PDEs with periodic coefficients.

Part II

Perturbation Methods in the Analysis of Spatially Periodic Systems

Chapter 5

Perturbation Analysis of the \mathcal{H}^2 Norm of Spatially Periodic Systems

God does not care about our mathematical difficulties. He integrates empirically.
A. Einstein

5.1 Introduction

In Chapter 3 we showed that the \mathcal{H}^2 -norm of a spatially periodic system can be found by solving a family of operator-valued algebraic Lyapunov equations. We also gave conditions under which the norm can be approximated arbitrarily-well by solving the algebraic Lyapunov equations for finite but large-enough truncations of the system operators. But even such approximation schemes can be numerically expensive as the truncation size becomes increasingly large.

In this chapter we take an analytic perturbation approach to approximating the \mathcal{H}^2 -norm. Section 5.2 describes the general perturbation setup, and Section 5.3 contains the main results. We finish the chapter with many examples in Section 5.4.

Notation: To avoid clutter, we henceforth drop the “ $\hat{\cdot}$ ” from the representation of frequency domain functions. For example, we use $A_0(\cdot)$ [instead of $\hat{A}_0(\cdot)$] to represent the Fourier symbol of the spatially invariant operator A° . ■

5.2 The Perturbation Setup

Let us now consider a system of the form

$$\begin{aligned}\partial_t \psi(t, x) &= A \psi(t, x) + B u(t, x) \\ &= (A^\circ + B^\circ \epsilon F C^\circ) \psi(t, x) + B u(t, x), \\ y(t, x) &= C \psi(t, x),\end{aligned}\tag{5.1}$$

where $t \in [0, \infty)$ and $x \in \mathbb{R}$ with the following assumptions. The (possibly unbounded) operators $A^\circ, B^\circ, C^\circ$ are spatially invariant, and the bounded operators B, C are spatially periodic. $F(x) = 2L \cos(\Omega x)$ with L a constant matrix, and ϵ is a complex scalar. $A^\circ, B^\circ, C^\circ$ and $E := B^\circ F C^\circ$ are all defined on a common dense domain $\mathcal{D} \subset L^2(\mathbb{R})$, and $A = A^\circ + \epsilon E$ is closed.

Remark 15 *We point out that since $\psi(t, \cdot) \in L^2(\mathbb{R})$ for all $t \geq 0$, it follows that $\psi(t, \pm\infty) = 0$ for all t . Thus the domain \mathcal{D} only contains information about the differentiability (in x) of the functions $\psi \in \mathcal{D}$. ■*

As shown in Chapter 2, the system can be represented in the (spatial) Fourier domain by the family of systems

$$\begin{aligned}\partial_t \psi_\theta(t) &= \mathcal{A}_\theta \psi_\theta(t) + \mathcal{B}_\theta u_\theta(t) \\ &= (\mathcal{A}_\theta^\circ + \epsilon \mathcal{B}_\theta^\circ \mathcal{F} \mathcal{C}_\theta^\circ) \psi_\theta(t) + \mathcal{B}_\theta u_\theta(t) \\ y_\theta(t) &= \mathcal{C}_\theta \psi_\theta(t),\end{aligned}\tag{5.2}$$

parameterized by $\theta \in [0, \Omega)$. Here \mathcal{B}_θ and \mathcal{C}_θ have the general form of the operator in (2.12) [i.e. can possess any number of nonzero subdiagonals], \mathcal{F} has the form given in Example 1 of Section 2.5 with $\frac{1}{2}$ replaced by L , and

$$\begin{aligned}\mathcal{A}_\theta^\circ &= \begin{bmatrix} \ddots & & & \\ & A_0(\theta_n) & & \\ & & \ddots & \\ & & & \ddots \end{bmatrix}, \quad \mathcal{B}_\theta^\circ = \begin{bmatrix} \ddots & & & \\ & B^\circ(\theta_n) & & \\ & & \ddots & \\ & & & \ddots \end{bmatrix}, \quad \mathcal{C}_\theta^\circ = \begin{bmatrix} \ddots & & & \\ & C^\circ(\theta_n) & & \\ & & \ddots & \\ & & & \ddots \end{bmatrix}, \\ \mathcal{E}_\theta &:= \mathcal{B}_\theta^\circ \mathcal{F} \mathcal{C}_\theta^\circ = \begin{bmatrix} \ddots & \ddots & & & \\ \ddots & 0 & A_{-1}(\theta_n) & & \\ & A_1(\theta_{n+1}) & 0 & \ddots & \\ & & & \ddots & \ddots \end{bmatrix}\end{aligned}\tag{5.3}$$

with $\theta_n := \theta + \Omega n$, $n \in \mathbb{Z}$, and

$$A_1(\cdot) := B^\circ(\cdot) L C^\circ(\cdot - \Omega), \quad A_{-1}(\cdot) := B^\circ(\cdot) L C^\circ(\cdot + \Omega).\tag{5.4}$$

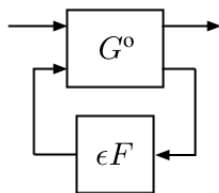


Figure 5.1: G° has a spatially invariant infinitesimal generator A° . The LFT of G° and the spatially periodic multiplication operator ϵF yields a system which has a spatially periodic infinitesimal generator A .

We emphasize that the convention used in the representation of \mathcal{E}_θ in (5.3) is the same as that used in (2.12); for example the n^{th} row of \mathcal{E}_θ is

$$\{\cdots, 0, A_1(\theta_n), 0, A_{-1}(\theta_n), 0, \cdots\}.$$

Remark 16 *We note that taking $F(x)$ to be a pure cosine is not restrictive. The results obtained here can be easily extended to problems where $F(x)$ is any periodic function with absolutely convergent Fourier series coefficients. The inclusion of higher harmonics of Ω in $F(x)$, namely functions of frequency 2Ω , 3Ω , etc, would not reveal new interesting phenomena and would only complicate the algebra. ■*

Remark 17 *Recall from Chapter 2 that the system (5.1) can be considered as the LFT (linear fractional transformation [27]) of a spatially periodic system G° with spatially invariant infinitesimal generator A° ,*

$$G^\circ = \left[\begin{array}{c|cc} A^\circ & B & B^\circ \\ \hline C & 0 & 0 \\ C^\circ & 0 & 0 \end{array} \right]$$

and the (memoryless and bounded) spatially periodic pure multiplication operator $\epsilon F(x) = \epsilon 2L \cos(\Omega x)$, see Figure 5.1. ■

5.3 Perturbation Analysis of the \mathcal{H}^2 -Norm

In the rest of this chapter we assume that the system (5.1) is exponentially stable and has finite \mathcal{H}^2 -norm for small enough values of ϵ .

Now the difficulty in calculating the \mathcal{H}^2 -norm using Theorem 3, is that unless \mathcal{A}_θ , \mathcal{B}_θ and \mathcal{C}_θ are diagonal (i.e., G is a spatially invariant system), the operators \mathcal{P}_θ and \mathcal{Q}_θ are “full”, meaning that they possess *all* of their (infinite number of) subdiagonals. This makes the computation of the \mathcal{H}^2 -norm numerically intensive. Namely, one has to solve an *infinite-dimensional* algebraic Lyapunov equation to

find the operator \mathcal{P}_θ (or \mathcal{Q}_θ) for every value of $\theta \in [0, \Omega)$. In this chapter we will see how one can use analytic perturbation techniques to compute the \mathcal{H}^2 -norm in a simple and numerically efficient way, and without having to explicitly find the full \mathcal{P}_θ and \mathcal{Q}_θ operators. Such a perturbation analysis is very useful in predicting general trends and extracting valuable information about the \mathcal{H}^2 -norm.

Let us now consider the general setup of (5.1), with ϵ a small *real* scalar. We also assume that both A° and $A = A^\circ + \epsilon E$ define exponentially stable strongly continuous semigroups (also known as C_0 -semigroups) on $L^2(\mathbb{R})$ [3], and that B and C are spatially invariant operators. We are interested in the changes in the \mathcal{H}^2 -norm of this system for small magnitudes of ϵ and different values of the frequency Ω .

Let us define

$$\mathcal{P}_\theta(\epsilon) := \mathcal{P}_\theta^{(0)} + \epsilon \mathcal{P}_\theta^{(1)} + \epsilon^2 \mathcal{P}_\theta^{(2)} + \dots,$$

with $\mathcal{P}_\theta^*(\epsilon) = \mathcal{P}_\theta(\epsilon)$. Notice that this implies $\mathcal{P}_\theta^{(m)*} = \mathcal{P}_\theta^{(m)}$ for all $m = 0, 1, 2, \dots$, i.e., $\mathcal{P}_\theta^{(m)}$ are selfadjoint operators for all m . The issue of convergence of the above series is addressed in the Appendix to this chapter. Our aim is to find $\mathcal{P}_\theta^{(m)}$ by solving the Lyapunov equation

$$\mathcal{A}_\theta(\epsilon) \mathcal{P}_\theta(\epsilon) + \mathcal{P}_\theta(\epsilon) \mathcal{A}_\theta^*(\epsilon) \equiv -\mathcal{B}_\theta \mathcal{B}_\theta^* \quad (5.5)$$

$$\begin{aligned} & \downarrow \\ & (\mathcal{A}_\theta^\circ + \epsilon \mathcal{E}_\theta) (\mathcal{P}_\theta^{(0)} + \epsilon \mathcal{P}_\theta^{(1)} + \epsilon^2 \mathcal{P}_\theta^{(2)} + \dots) + \\ & (\mathcal{P}_\theta^{(0)} + \epsilon \mathcal{P}_\theta^{(1)} + \epsilon^2 \mathcal{P}_\theta^{(2)} + \dots) (\mathcal{A}_\theta^\circ + \epsilon \mathcal{E}_\theta)^* \equiv -\mathcal{B}_\theta \mathcal{B}_\theta^*, \end{aligned} \quad (5.6)$$

and compute the \mathcal{H}^2 -norm of the system using Theorem 3

$$\|G\|_{\mathcal{H}^2}^2 = \frac{1}{2\pi} \int_0^\Omega \text{trace}[\mathcal{C}_\theta \mathcal{P}_\theta(\epsilon) \mathcal{C}_\theta^*] d\theta.$$

It is easy to see from (5.6) that

$$\mathcal{A}_\theta^\circ \mathcal{P}_\theta^{(0)} + \mathcal{P}_\theta^{(0)} \mathcal{A}_\theta^{\circ*} = -\mathcal{B}_\theta \mathcal{B}_\theta^*, \quad (5.7)$$

$$\mathcal{A}_\theta^\circ \mathcal{P}_\theta^{(1)} + \mathcal{P}_\theta^{(1)} \mathcal{A}_\theta^{\circ*} = -(\mathcal{E}_\theta \mathcal{P}_\theta^{(0)} + \mathcal{P}_\theta^{(0)} \mathcal{E}_\theta^*), \quad (5.8)$$

$$\mathcal{A}_\theta^\circ \mathcal{P}_\theta^{(2)} + \mathcal{P}_\theta^{(2)} \mathcal{A}_\theta^{\circ*} = -(\mathcal{E}_\theta \mathcal{P}_\theta^{(1)} + \mathcal{P}_\theta^{(1)} \mathcal{E}_\theta^*), \quad (5.9)$$

\vdots

Now since \mathcal{A}_θ° and $\mathcal{B}_\theta \mathcal{B}_\theta^*$ are diagonal in (5.7), so is $\mathcal{P}_\theta^{(0)}$. In (5.8), the right hand side operator has the structure of being nonzero only on the first upper and lower subdiagonals, and hence $\mathcal{P}_\theta^{(1)}$ inherits the same structure (since \mathcal{A}_θ° is diagonal). In the same manner, one can show that $\mathcal{P}_\theta^{(2)}$ is only nonzero on the main diagonal

and the second upper and lower subdiagonals, and so on for other $\mathcal{P}_\theta^{(m)}$. We have

$$\mathcal{P}_\theta^{(0)} = \begin{bmatrix} \ddots & & & & \\ & P_0(\theta_n) & & & \\ & & \ddots & & \\ & & & \ddots & \\ & & & & \ddots \end{bmatrix}, \quad \mathcal{P}_\theta^{(1)} = \begin{bmatrix} \ddots & \ddots & & & \\ & \ddots & 0 & P_1^*(\theta_n) & \\ & & P_1(\theta_n) & 0 & \ddots \\ & & & \ddots & \ddots \\ & & & & \ddots \end{bmatrix},$$

$$\mathcal{P}_\theta^{(2)} = \begin{bmatrix} \ddots & \ddots & \ddots & & & \\ & \ddots & \ddots & 0 & P_2^*(\theta_n) & \\ & & \ddots & 0 & Q_0(\theta_n) & 0 & \ddots \\ & & & 0 & Q_0(\theta_n) & 0 & \ddots \\ & & & P_2(\theta_n) & 0 & \ddots & \ddots \\ & & & & \ddots & \ddots & \ddots \\ & & & & & \ddots & \ddots \end{bmatrix}, \quad \dots$$

where we have used the selfadjointness of these operators in representing their subdiagonals.

Remark 18 *It is important to realize that, not only is $\mathcal{P}_\theta^{(m)}$ not a “full” operator, it has at most m nonzero upper and lower subdiagonals. Also, all $\mathcal{P}_\theta^{(m)}$ for odd m have zero diagonal and are thus trace-free operators. ■*

Remark 19 *Note that even though $\mathcal{A}_\theta = \mathcal{A}_\theta^0 + \epsilon \mathcal{E}_\theta$ has only one nonzero subdiagonal [see (5.3)], $\mathcal{P}_\theta(\epsilon) = \mathcal{P}_\theta^{(0)} + \epsilon \mathcal{P}_\theta^{(1)} + \dots$ possesses all of its subdiagonals. This is precisely the reason why direct calculation of \mathcal{P}_θ in Theorem 3 is computationally difficult. ■*

Now returning to (5.7)-(5.9), $\mathcal{P}_\theta^{(0)}$, $\mathcal{P}_\theta^{(1)}$ and $\mathcal{P}_\theta^{(2)}$ are found by equating, element by element, the bi-infinite matrices on both sides of these equations. For example, (5.7) leads to

$$A_0(\theta + \Omega n) P_0(\theta + \Omega n) + P_0(\theta + \Omega n) A_0^*(\theta + \Omega n) = -B(\theta + \Omega n) B^*(\theta + \Omega n)$$

for every $n \in \mathbb{Z}$, and $\theta \in [0, \Omega)$. But notice that as n assumes values over all integers and θ changes in $[0, \Omega)$, $k = \theta + \Omega n$ takes all real values, and one can rewrite the above equation as

$$A_0(k) P_0(k) + P_0(k) A_0^*(k) = -B(k) B^*(k),$$

for all $k \in \mathbb{R}$. Applying the same procedure to (5.8)-(5.9), one arrives at

$$A_0(k) P_0(k) + P_0(k) A_0^*(k) = -B(k) B^*(k), \quad (5.10)$$

$$A_0(k) P_1(k) + P_1(k) A_0^*(k - \Omega) = -\left(A_1(k) P_0(k - \Omega) + P_0(k) A_{-1}^*(k - \Omega)\right), \quad (5.11)$$

$$A_0(k) Q_0(k) + Q_0(k) A_0^*(k) = -\left(A_1(k) P_1^*(k) + P_1(k) A_1^*(k) + A_{-1}(k) P_1(k + \Omega) + P_1^*(k + \Omega) A_{-1}^*(k)\right), \quad (5.12)$$

and so on for all nonzero diagonals of $\mathcal{P}_\theta^{(m)}$, $m = 3, 4, \dots$.

Remark 20 Notice that from the above equations, one first finds $P_0(\cdot)$ from (5.10), then $P_1(\cdot)$ from (5.11), and so on. In other words, computing the subdiagonals of \mathcal{P}_θ becomes “decoupled” in one direction. This decoupling would not have been possible had we not employed a perturbation approach and had attempted to solve (5.5) directly. \blacksquare

Returning to the calculation of the \mathcal{H}^2 -norm, let us first separate the diagonal part of $\mathcal{P}_\theta^{(2)}$ by rewriting it as $\mathcal{P}_\theta^{(2)} = \overline{\mathcal{P}}_\theta^{(2)} + \widetilde{\mathcal{P}}_\theta^{(2)}$, where

$$\overline{\mathcal{P}}_\theta^{(2)} := \begin{bmatrix} \ddots & & & \\ & Q_0(\theta_n) & & \\ & & \ddots & \\ & & & \ddots \end{bmatrix},$$

and $\widetilde{\mathcal{P}}_\theta^{(2)}$ contains the rest of $\mathcal{P}_\theta^{(2)}$. Clearly $\text{trace}[\mathcal{C}_\theta \widetilde{\mathcal{P}}_\theta^{(2)} \mathcal{C}_\theta^*] = 0$. Also, recall that

$$\text{trace}[\mathcal{C}_\theta \mathcal{P}_\theta^{(2m+1)} \mathcal{C}_\theta^*] = 0, \quad m = 0, 1, 2, \dots \quad (5.13)$$

Now one can write the following

$$\begin{aligned} \|G\|_{\mathcal{H}^2}^2 &= \frac{1}{2\pi} \int_0^\Omega \text{trace}[\mathcal{C}_\theta \mathcal{P}_\theta(\epsilon) \mathcal{C}_\theta^*] d\theta \\ &= \frac{1}{2\pi} \int_0^\Omega \text{trace}[\mathcal{C}_\theta \mathcal{P}_\theta^{(0)} \mathcal{C}_\theta^* + \epsilon^2 \mathcal{C}_\theta \mathcal{P}_\theta^{(2)} \mathcal{C}_\theta^*] d\theta + O(\epsilon^4) \\ &= \frac{1}{2\pi} \int_0^\Omega \text{trace}[\mathcal{C}_\theta \mathcal{P}_\theta^{(0)} \mathcal{C}_\theta^* + \epsilon^2 \mathcal{C}_\theta \overline{\mathcal{P}}_\theta^{(2)} \mathcal{C}_\theta^*] d\theta + O(\epsilon^4), \end{aligned}$$

where the absence of odd powers of ϵ is due to (5.13), and the last equation follows from the fact that $\text{trace}[\mathcal{C}_\theta \widetilde{\mathcal{P}}_\theta^{(2)} \mathcal{C}_\theta^*] = 0$. Next, using the unitaryness of the lifting

transform we have

$$\begin{aligned}\int_0^\Omega \text{trace}[\mathcal{C}_\theta \mathcal{P}_\theta^{(0)} \mathcal{C}_\theta^*] d\theta &= \int_{-\infty}^\infty \text{trace}[C(k) P_0(k) C^*(k)] dk, \\ \int_0^\Omega \text{trace}[\mathcal{C}_\theta \overline{\mathcal{P}}_\theta^{(2)} \mathcal{C}_\theta^*] d\theta &= \int_{-\infty}^\infty \text{trace}[C(k) Q_0(k) C^*(k)] dk,\end{aligned}$$

and we arrive at the final result

$$\|G\|_{\mathcal{H}^2}^2 = \frac{1}{2\pi} \int_{-\infty}^\infty \text{trace}[C(k)P_0(k)C^*(k) + \epsilon^2 C(k)Q_0(k)C^*(k)] dk + O(\epsilon^4). \quad (5.14)$$

Remark 21 *Let us stress again the important advantage of the above perturbation analysis in comparison to the method of Theorem 3. In the direct method of computing the \mathcal{H}^2 -norm proposed in Theorem 3, one has to solve a family of infinite-dimensional (operator) algebraic Lyapunov equations, whereas the perturbation method reduces the \mathcal{H}^2 -norm computation to that of solving a family of finite-dimensional (matrix) Lyapunov/Sylvester equations (5.10)-(5.12). ■*

In summary, we have the following.

Main Result of Perturbation Analysis of \mathcal{H}^2 -Norm Consider the exponentially stable spatially periodic LTI system G , with spatial period $X = 2\pi/\Omega$ and state-space realization (5.1). Then for small values of $|\epsilon|$ the \mathcal{H}^2 -norm of the system (5.1) can be computed from (5.14), where $P_0(\cdot)$ and $Q_0(\cdot)$ are solutions of the family of finite-dimensional Lyapunov/Sylvester equations described by (5.10)-(5.12). ■

5.4 Examples

As an application of the perturbation results of the previous section, we first investigate the occurrence of ‘parametric resonance’ for a class of spatially periodic systems. Parametric resonance occurs when a specific frequency Ω_{res} of the periodic perturbation resonates with some ‘natural frequency’ \varkappa of the unperturbed system, leading to a local (in Ω) change in system behavior [7]. In the systems we consider in this section, this change in behavior is captured by the value of the \mathcal{H}^2 -norm.

Example 4 *Let us consider the periodic PDE*

$$\begin{aligned}\partial_t \psi &= -(\partial_x^2 + \varkappa^2)^2 \psi - c \psi + \epsilon \cos(\Omega x) \psi + u \\ y &= \psi,\end{aligned} \quad (5.15)$$

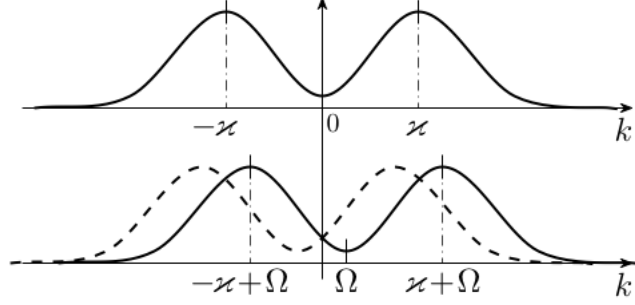


Figure 5.2: Above: Plot of $P_0(\cdot)$. Below: Plot of $P_0(\cdot - \Omega)$ and $P_0(\cdot + \Omega)$ (dashed).

with $0 \neq \varkappa \in \mathbb{R}$ and $c > 0$. Comparing (5.15) and (5.1) we have

$$A_0(k) = -(k^2 - \varkappa^2)^2 - c, \quad B^o(k) = 1, \quad C^o(k) = 1, \quad B(k) = 1, \quad C(k) = 1, \quad L = \frac{1}{2}.$$

For this system, the functions $P_0(k)$ and $Q_0(k)$ of the previous section simplify to¹

$$P_0(k) = \frac{-1}{2A_0(k)}, \quad (5.16)$$

$$\begin{aligned} Q_0(k) &= \frac{1}{(A_0(k))^2} \left(\frac{-1}{2A_0(k - \Omega)} + \frac{-1}{2A_0(k + \Omega)} \right) \\ &= 4(P_0(k))^2 (P_0(k - \Omega) + P_0(k + \Omega)), \end{aligned} \quad (5.17)$$

and it is our aim to find the \mathcal{H}^2 -norm

$$\|G\|_{\mathcal{H}^2}^2 = \frac{1}{2\pi} \int_{-\infty}^{\infty} (P_0(k) + \epsilon^2 Q_0(k)) dk + O(\epsilon^4), \quad (5.18)$$

for different values of the parameter $\Omega > 0$. More specifically, we are interested in the values of Ω for which the \mathcal{H}^2 -norm is maximized.

From (5.16), $P_0(k) = \frac{1}{2(k^2 - \varkappa^2)^2 + c}$. The first plot of Figure 5.2 shows $P_0(\cdot)$, while the second shows $P_0(\cdot - \Omega)$ and $P_0(\cdot + \Omega)$ (dashed), for a given value of $\Omega \neq 0$. As Ω is increased, $P_0(\cdot - \Omega)$ slides to the right and $P_0(\cdot + \Omega)$ to the left. From (5.17) it is clear that to find $Q_0(\cdot)$ for any Ω , one would sum the two functions in the second plot and multiply the result by the square of the first plot. The interesting question now is, for what value(s) of $\Omega \in (0, \infty)$ would the \mathcal{H}^2 -norm in (5.18) be maximized.

One can easily see that as $\Omega \rightarrow 0$, the peaks of $P_0(\cdot - \Omega)$ and $P_0(\cdot + \Omega)$ merge

¹To find $Q_0(k)$ one needs to first find $P_1(k)$, but we have omitted the details for brevity.

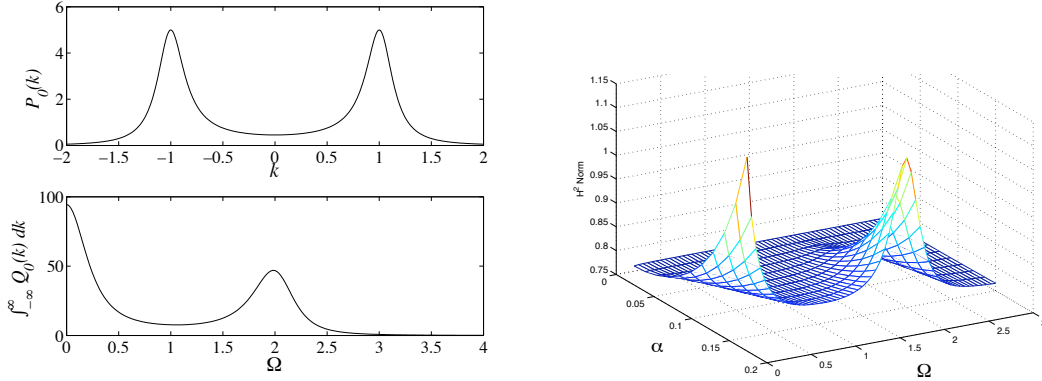


Figure 5.3: Left: Plots of Example 4 for $\varkappa = 1$ and $c = 0.1$. Notice that the first graph is plotted against k and the second against Ω . Right: The plot of \mathcal{H}^2 -norm of the same example, but calculated by taking large truncations of the \mathcal{A}_θ , \mathcal{B}_θ , \mathcal{C}_θ matrices and using Theorem 3.

toward those of $(P_0(\cdot))^2$, thus $\int_{-\infty}^{\infty} Q_0(k) dk$ grows and hence $\|G\|_{\mathcal{H}^2}^2$ grows.² This is not surprising; as $\Omega \rightarrow 0$, the perturbation is tending toward a constant function $F(x) = \cos(\Omega x) \rightarrow 1$. This results in shifting the whole spectrum of A° toward the right-half of the complex plane, thus increasing the \mathcal{H}^2 -norm of the perturbed system.

But we are more interested in frequencies $\Omega \gg 0$ that lead to a local (in Ω) increase in the \mathcal{H}^2 -norm. Now notice that a different alignment of the peaks can also occur, which leads to another local maximum of the \mathcal{H}^2 -norm as a function of Ω . This happens when the peak of $P_0(\cdot - \Omega)$ at $k = -\varkappa + \Omega$ becomes aligned with the peak of $(P_0(\cdot))^2$ at $k = \varkappa$, and, simultaneously, the peak of $P_0(\cdot + \Omega)$ at $k = \varkappa - \Omega$ becomes aligned with the peak of $(P_0(\cdot))^2$ at $k = -\varkappa$. Clearly this occurs when

$$-\varkappa + \Omega_{res} = \varkappa \implies \Omega_{res} = 2\varkappa.$$

This result agrees exactly with that obtained in [26], where in the analysis of the same problem it is shown that the part of the spectrum of A closest to the imaginary axis ‘resonates’ with perturbations whose frequency satisfies the relation $\Omega = 2\varkappa$.

Consider (5.15) with $\varkappa = 1$ and $c = 0.1$. For this system $\int_{-\infty}^{\infty} P_0(k) dk \approx 4.74$. Figure 5.3 (left) shows the graphs of $P_0(\cdot)$ (plotted against k) and $\int_{-\infty}^{\infty} Q_0(k) dk$ (plotted against Ω). The peak at $\Omega = 2$ in the lower plot verifies the result $\Omega_{res} = 2\varkappa$ obtained above.

Figure 5.3 (right) shows the \mathcal{H}^2 -norm of this system computed by taking large

²Remember that $P_0(k)$ is independent of Ω , and thus $\int_{-\infty}^{\infty} P_0(k) dk$ remains constant for different Ω .

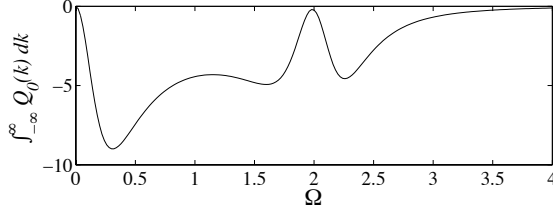


Figure 5.4: The plot of Example 4 with $\varkappa = 1$ and $c = 0.1$ and a purely imaginary perturbation.

enough truncations of the \mathcal{A}_θ , \mathcal{B}_θ , \mathcal{C}_θ matrices and then applying Theorem 3. The figure shows that the trends were indeed correctly predicted by the perturbation analysis; the peaks at $\Omega = 0, 2$ correspond to those of $\int_{-\infty}^{\infty} Q_0(k) dk$.

Now consider (5.15) with $\varkappa = 1$ and $c = 0.1$, but with ϵ replaced by ϵj ; this would correspond to $L = j/2$ in that example. Obviously the unperturbed system remains the same as before and hence $\int_{-\infty}^{\infty} P_0(k) dk \approx 4.74$. Figure 5.3 shows the graph of $\int_{-\infty}^{\infty} Q_0(k) dk$, which demonstrates that for this system the purely imaginary perturbation reduces the \mathcal{H}^2 -norm at all frequencies. We address the physical interpretation of such a perturbation in the Appendix. ■

We continue with more examples to demonstrate that by appropriately choosing the frequency of the perturbation, one can *decrease* or (as in the previous example) *increase* the \mathcal{H}^2 -norm of the unperturbed system.

Example 5 *Let us consider the periodic PDE [34]*

$$\begin{aligned} \partial_t \psi &= -(\partial_x^2 + \varkappa^2)^2 \psi - c\psi + \epsilon \cos(\Omega x) \partial_x \psi + u \\ y &= \psi. \end{aligned} \tag{5.19}$$

Comparing (5.19) and (5.1) we have

$$A_0(k) = -(k^2 - \varkappa^2)^2 - c, \quad B^o(k) = 1, \quad C^o(k) = jk, \quad B(k) = 1, \quad C(k) = 1, \quad L = \frac{1}{2}.$$

The difference between this system and (5.15) is that here C^o is a spatial derivative. The plot of Figure 5.5 demonstrates $\int_{-\infty}^{\infty} Q_0(k) dk$ for $\varkappa = 1$ and $c = 0.1$. Notice that the peak at $\Omega_{\text{res}} = 2$ remains the same as in Figure 5.3, but we now have a decrease at small frequencies. This is due to the derivative operator $C^o = \partial_x$. Finally, notice the agreement of the perturbation analysis here with the (non-perturbation) calculations for the same system in the First Example of Section 3.6. Our perturbation methods correctly predict the increase at $\Omega = 2$ and the decrease around $\Omega \approx 0.4$ of the \mathcal{H}^2 -norm. ■

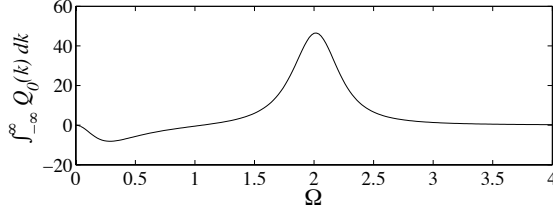


Figure 5.5: Plot of Example 5 for $\varkappa = 1$ and $c = 0.1$.

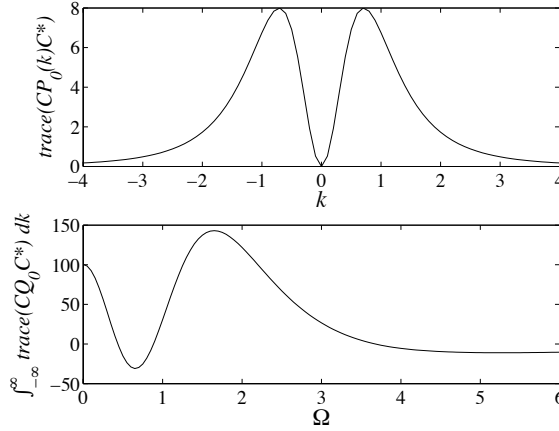


Figure 5.6: Graphs of Example 6 for $R = 6$ and $c = 1$.

Example 6 *The following system is motivated by channel flow problems*

$$A_0(k) = \begin{bmatrix} -\frac{1}{R}(k^2 + c) & 0 \\ jk & -\frac{1}{R}(k^2 + c) \end{bmatrix}$$

$$B^o(k) = \begin{bmatrix} 1 & 0 \\ 0 & 1 \end{bmatrix}, \quad C^o(k) = \begin{bmatrix} 1 & 0 \\ 0 & 1 \end{bmatrix}, \quad B(k) = \begin{bmatrix} 1 & 0 \\ 0 & 0 \end{bmatrix}, \quad C(k) = \begin{bmatrix} 0 & 0 \\ 0 & 1 \end{bmatrix}, \quad L = \frac{1}{2} \begin{bmatrix} 0 & -1 \\ 1 & 0 \end{bmatrix}.$$

We perform numerical calculations for $R = 6$, $c = 1$. We have

$$\int_{-\infty}^{\infty} \text{trace}[C(k)P_0(k)C^*(k)] dk \approx 20.72.$$

Figure 5.6 shows that the \mathcal{H}^2 -norm can be decreased by the application of periodic perturbations with frequency $\Omega \approx 0.7$. It is interesting that if one uses the locations of the peaks in the first plot of Figure 5.6 to find $\varkappa = 0.75$, then from the peak at $\Omega_{\text{res}} = 1.6$ in the second plot it seems that the relationship $\Omega_{\text{res}} \approx 2\varkappa = 1.5$ still holds with an acceptable error even for this non-scalar example. ■

5.5 Appendix to Chapter 5

Convergence of the Perturbation Series

For the series expansion

$$\mathcal{P}_\theta(\epsilon) = \mathcal{P}_\theta^{(0)} + \epsilon \mathcal{P}_\theta^{(1)} + \epsilon^2 \mathcal{P}_\theta^{(2)} + \dots$$

to be valid, we must show that all elements of $\mathcal{P}_\theta(\epsilon)$ converge for ϵ contained in some small enough domain. Let us assume that B° and C° are bounded operators, and (without loss of generality) that $\sup_{k \in \mathbb{R}} \|B(k)\| = 1$. Assume $\|e^{A_0(k)t}\| \leq M_k e^{\varrho_k t}$, and define

$$\begin{aligned} M &:= \sup_{k \in \mathbb{R}} M_k < \infty, & -\alpha_0 &:= \sup_{k \in \mathbb{R}} \varrho_k < 0, \\ \alpha_1 &:= \max\{\sup_{k \in \mathbb{R}} \|A_1(k)\|, \sup_{k \in \mathbb{R}} \|A_{-1}(k)\|\}. \end{aligned}$$

Notice that the finiteness of M and the negativity of $-\alpha_0$ follow from the exponential stability of the unperturbed system. Now from (5.10) we have

$$P_0(k) = \int_0^\infty e^{A_0(k)t} B(k) B^*(k) e^{A_0^*(k)t} dt,$$

and therefore

$$\sup_{k \in \mathbb{R}} \|P_0(k)\| \leq \frac{M^2}{2\alpha_0} =: \mu.$$

Similarly, from (5.11) we have

$$P_1(k) = \int_0^\infty e^{A_0(k)t} (A_1(k) P_0(k - \Omega) + P_0(k) A_{-1}^*(k - \Omega)) e^{A_0^*(k - \Omega)t} dt,$$

and therefore

$$\sup_{k \in \mathbb{R}} \|P_1(k)\| \leq \frac{M^2}{2\alpha_0} (2\alpha_1 \mu) \leq \mu (4\alpha_1 \mu) = 4\alpha_1 \mu^2.$$

From (5.12) we have

$$Q_0(k) = \int_0^\infty e^{A_0(k)t} (A_1(k) P_1^*(k) + \dots + P_1^*(k + \Omega) A_{-1}^*(k)) e^{A_0^*(k)t} dt,$$

and therefore

$$\sup_{k \in \mathbb{R}} \|Q_0(k)\| \leq \frac{M^2}{2\alpha_0} (4\alpha_1 (4\alpha_1 \mu^2)) \leq \mu (4\alpha_1)^2 \mu^2 = (4\alpha_1)^2 \mu^3.$$

In fact it is possible to show that any element of $\mathcal{P}_\theta^{(m)}$ is bounded by

$$(4\alpha_1)^m \mu^{(m+1)}.$$

Thus for all $|\epsilon| < 4\alpha_1\mu = 2M^2\alpha_1/\alpha_0$ the series expansion of $\mathcal{P}_\theta(\epsilon)$ converges.

5.6 Summary

We use perturbation analysis to find a computationally efficient way of revealing trends in the \mathcal{H}^2 -norm of spatially periodic systems. We show that the basic frequency of the periodic perturbation can be chosen so as to increase (by inducing parametric resonance) or decrease the \mathcal{H}^2 -norm. We demonstrate that for certain scalar systems, the value of the spatial period that achieves the desired increase/decrease of the \mathcal{H}^2 -norm can be characterized exactly, based on the description of the nominal system.

Chapter 6

Stability and the Spectrum Determined Growth Condition for Spatially Periodic Systems

Everything should be made as simple as possible, but not simpler. *A. Einstein*

6.1 Introduction

As mentioned briefly in Section 4.2, in the literature on semigroups there exist examples in which $\Sigma(A)$ lies entirely inside \mathbb{C}^- but $\|e^{At}\|$ does not decay exponentially [14] [15]. In such cases it is said that the semigroup does not satisfy the *spectrum-determined growth condition* [16]. The determining factor in the examples presented in [14] and [15] can be interpreted as the accumulation of the eigenvalues of \mathcal{A}_θ around $\pm j\infty$ in the form of Jordan blocks of ever-increasing size (i.e. as the eigenvalues tend to $\pm j\infty$ their algebraic multiplicity increases while their geometric multiplicity stays finite). But such cases are ruled out when one deals with holomorphic semigroups, which is the reason we consider these semigroups in this chapter.

Our ultimate aim in this chapter is to verify exponential stability. In Section 6.3 we describe a class of infinitesimal generators A for which $\Sigma(A) \subset \mathbb{C}^-$ yields exponential stability. Section 6.4 then gives conditions under which our spatially periodic infinitesimal generators belong to this class. And in Section 6.5 we find sufficient conditions which guarantee $\Sigma(A) \subset \mathbb{C}^-$.

The setup is the same as that in Section 5.2 with ϵ a small complex scalar. In addition, assume that $A_0(k) \in \mathbb{C}^{q \times q}$ is diagonalizable for every $k \in \mathbb{R}$. As in the previous chapter, to avoid clutter we drop the “ $\hat{}$ ” from the representation of frequency domain functions.

6.2 Spectrum of Spatially Invariant Operators

Recall that for a general spatially periodic operator A we have

$$\Sigma(A) = \overline{\bigcup_{\theta \in [0, \Omega)} \Sigma(\mathcal{A}_\theta)}. \quad (6.1)$$

In the case where A is spatially invariant [and thus $\mathcal{A}_\theta = \text{diag} \{ \dots, A_0(\theta_n), \dots \}$], (6.1) further simplifies to

$$\Sigma(A) = \overline{\bigcup_{k \in \mathbb{R}} \Sigma_p(A_0(k))}. \quad (6.2)$$

Example 7 Let $A = -(\partial_x^2 + \varkappa^2)^2$ with domain

$$\mathcal{D} = \{ \phi \in L^2(\mathbb{R}) \mid \phi, \frac{d\phi}{dx}, \frac{d^2\phi}{dx^2}, \frac{d^3\phi}{dx^3} \text{ absolutely continuous, } \frac{d^4\phi}{dx^4} \in L^2(\mathbb{R}) \}. \quad (6.3)$$

An integration by parts shows that A is a self-adjoint operator and thus closed. $A_0(k) = -(k^2 - \varkappa^2)^2$ is the Fourier symbol of A , see Figure 6.1 (top). Since $A_0(\cdot)$ is scalar, $\Sigma_p(A_0(k)) = A_0(k)$ for every k . It is easy to see that $A_0(\cdot)$ takes every real negative value and thus from (6.2) A has continuous spectrum $\Sigma(A) = (-\infty, 0]$, see Figure 6.1 (center). ■

Remark 22 When A is spatially invariant, a helpful way to think about $\Sigma(A)$ in terms of the symbol $A_0(\cdot)$ of A is suggested by the previous example. First plot $\Sigma_p(A_0(\cdot))$ in the ‘complex-plane \times spatial-frequency’ space, as in Figure 6.1 (top) of Example 7. Then the orthogonal projection onto the complex plane of this plot would give $\Sigma(A)$, as in Figure 6.1 (center). This can be considered as a geometric interpretation of (6.2). In Example 7, since $A_0(\cdot)$ is real scalar and takes only negative values, this projection yields only the negative real axis. But in general if $A_0(\cdot) \in \mathbb{C}^{q \times q}$, this projection would lead to q curves in the complex plane. Notice also that in this setting, $\Sigma(\mathcal{A}_\theta)$ is the projection onto the complex plane of samples of $\Sigma_p(A_0(\cdot))$ taken at $k = \theta_n = \theta + \Omega n$, $n \in \mathbb{Z}$, in the ‘complex-plane \times spatial-frequency’ space. This can be considered as a geometric interpretation of (6.1). Figure 6.1 (bottom) shows these samples in the ‘complex-plane \times spatial-frequency’ space for a scalar A . ■

6.3 Sectorial Operators

We next introduce a special subclass of *holomorphic* (or *analytic*) semigroups. The reader is referred to [17–19] for a detailed discussion. Suppose A is densely

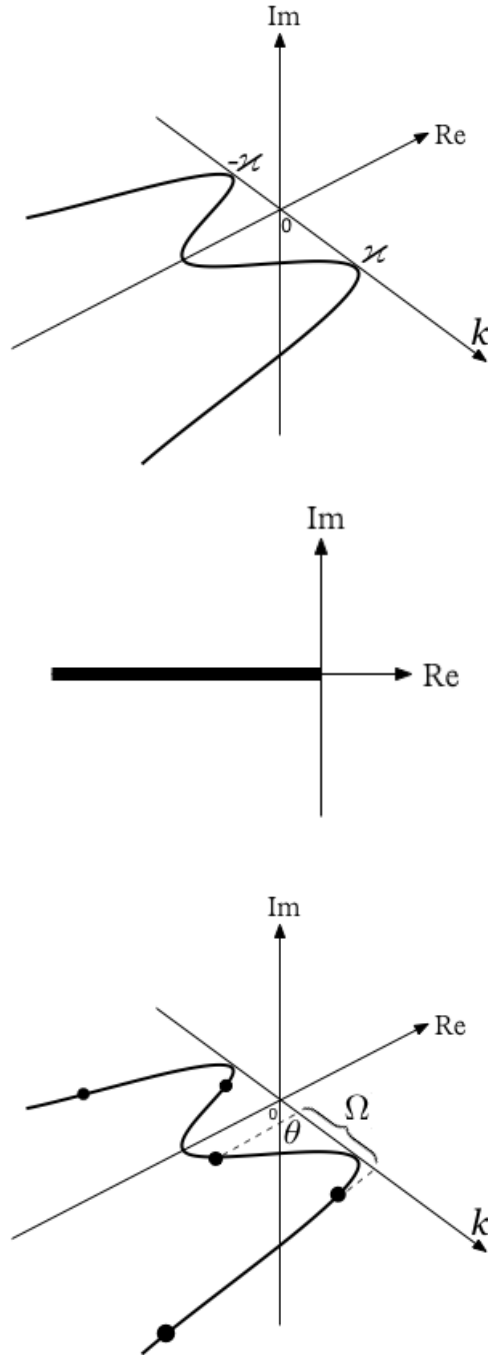


Figure 6.1: Top: Representation of the symbol $A_0(\cdot)$ of Example 7 in ‘complex-plane \times spatial-frequency’ space. Center: $\Sigma(A)$ in the complex plane. Bottom: For spatially invariant A , the (diagonal) elements of \mathcal{A}_θ are samples of the Fourier symbol $A_0(\cdot)$.

defined, $\rho(A)$ contains a sector of the complex plane $|\arg(z - \alpha)| \leq \frac{\pi}{2} + \gamma$, $\gamma > 0$, $\alpha \in \mathbb{R}$, and there exists some $M > 0$ such that

$$\|(zI - A)^{-1}\| \leq \frac{M}{|z - \alpha|} \quad \text{for} \quad |\arg(z - \alpha)| \leq \frac{\pi}{2} + \gamma. \quad (6.4)$$

Then A generates a holomorphic semigroup and we write $A \in \mathcal{H}(\gamma, \alpha, M)$ [19] [17]. We say that A is *sectorial* if A belongs to some $\mathcal{H}(\gamma, \alpha, M)$.

Theorem 19 *Assume that A is sectorial. Then if $\Sigma(A) \subset \mathbb{C}^-$, A generates an exponentially stable semigroup.*

Proof: *If A is sectorial it defines a holomorphic semigroup, and thus e^{At} is differentiable for $t > 0$ [18]. Then [16] shows that this is sufficient for the spectrum-determined growth condition to hold. Since $\Sigma(A) \subset \mathbb{C}^-$ and A is sectorial, then $\Sigma(A)$ is bounded away from the imaginary axis. Let $\omega_\sigma := \sup_{z \in \Sigma(A)} \operatorname{Re}(z)$. Then $\omega_\sigma < 0$ and A generates an exponentially stable semigroup. ■*

6.4 Conditions for Infinitesimal Generator to be Sectorial

To find conditions under which A in (5.1) will define a holomorphic semigroup we have to check the condition (6.4). Since the Fourier transform preserves norms, (6.4) is equivalent to checking $\|(zI - \hat{A})^{-1}\| \leq M/|z - \alpha|$ for z belonging to some sector of \mathbb{C} . This involves finding the inverse of the operator $zI - \hat{A}$ and then calculating its norm. Such a computation can be very difficult since $(zI - \hat{A})^{-1}$ has the form (2.9) [also depicted in Figure 2.2 (right)], i.e., it has an infinite number of impulse sheets. On the other hand, finding $\|(zI - \hat{A}^\circ)^{-1}\|$ is very easy, due to the diagonal structure of \hat{A}° . Indeed $\|(zI - \hat{A}^\circ)^{-1}\| = \sup_{k \in \mathbb{R}} \|(zI - A_0(k))^{-1}\|$.

Thus to establish conditions for A to be sectorial, we again use perturbation theory. We first find conditions under which A° is sectorial. We then show that $A = A^\circ + \epsilon E$ remains sectorial if E is ‘weaker’ than A° in a certain sense we will describe, and if ϵ is small enough.

In the next theorem we present a condition for a spatially invariant A° with Fourier symbol $A_0(\cdot)$ to be sectorial.

Theorem 20 *Let $A_0(k)$ be diagonalizable for every $k \in \mathbb{R}$, and let $U(k)$ be the transformation that diagonalizes $A_0(k)$, i.e., $A_0(k) = U(k) \Lambda(k) U^{-1}(k)$ with $\Lambda(k)$ diagonal. Let $\kappa(k) := \|U(k)\| \|U^{-1}(k)\|$ denote the condition number of $U(k)$. If $\sup_{k \in \mathbb{R}} \kappa(k) < \infty$, and for every $k \in \mathbb{R}$ the resolvent set $\rho(A_0(k))$ contains a sector of the complex plane $|\arg(z - \alpha)| < \frac{\pi}{2} + \gamma$ with $\gamma > 0$ and $\alpha \in \mathbb{R}$ both independent of k , then A° is sectorial.*

Proof: See Appendix. ■

This theorem has a particularly simple interpretation when $A_0(\cdot)$ is scalar. In this case $\kappa(k) = 1$ for all $k \in \mathbb{R}$. Now since $A_0(\cdot)$ traces a curve in the complex plane, by Theorem 20 if this curve stays outside some sector $|\arg(z - \alpha)| \leq \frac{\pi}{2} + \gamma$, $\gamma > 0$, of the complex plane then A° is sectorial.

The following theorem is the main result of this section and uses the notion of *relative boundedness* of one unbounded operator with respect to another unbounded operator [17] to prove that $A = A^\circ + \epsilon E$ is sectorial.

Theorem 21 *Let A° with domain \mathcal{D} be a closed operator, and $A^\circ \in \mathcal{H}(\gamma, \alpha, M)$. Let $E = B^\circ F C^\circ$ with domain $\mathcal{D}' \supset \mathcal{D}$ be relatively bounded with respect to A° such that*

$$\|E\psi\| \leq a\|\psi\| + b\|A^\circ\psi\|, \quad \psi \in \mathcal{D}, \quad (6.5)$$

with $0 \leq a < \infty$ and $0 \leq b|\epsilon| < 1/(1 + M)$. Then $A = A^\circ + \epsilon E$ is a closed and sectorial operator.

Proof: From (6.5) we have

$$\|\epsilon E\psi\| \leq a|\epsilon|\|\psi\| + b|\epsilon|\|A^\circ\psi\|$$

Then from [19, Thm 4.5.7] it follows that $A = A^\circ + \epsilon E$ is sectorial for $0 \leq b|\epsilon| < 1/(1 + M)$. Also since $M > 0$, then $b|\epsilon| < 1$ and [17, Thm IV.1.1] gives that A is closed. ■

This theorem says that if A° is sectorial and closed, then so is $A = A^\circ + \epsilon E$ if E is weaker than A° in the sense of (6.5) and if $|\epsilon|$ is small enough. Notice that at this point, condition (6.5) can not be reduced to a condition in terms of Fourier symbols (i.e. a condition that can be checked pointwise in k) as in Theorem 20. This is because E is not spatially invariant. But once the exact form of the operators B° and C° is known, (6.5) can be simplified to a condition on the symbols of A° , B° and C° . Let us clarify this statement with the aid of an example.

Example 8 *Consider the periodic PDE*

$$\begin{aligned} \partial_t \psi &= -(\partial_x^2 + \varkappa^2)^2 \psi - c\psi + \epsilon \partial_x \cos(\Omega x) \psi + u \\ y &= \psi, \end{aligned}$$

where $\psi \in \mathcal{D}$, and \mathcal{D} is defined as in (6.3). It is easy to see that $A^\circ = -(\partial_x^2 + \varkappa^2)^2 - c$ is sectorial by Theorem 20 and closed by Example 7, $B^\circ = \partial_x$, and $C^\circ = \delta(x)$ [the identity convolution operator]. By formal differentiation we have

$$E\psi = \partial_x \cos(\Omega x) \psi = -\Omega \sin(\Omega x) \psi + \cos(\Omega x) \partial_x \psi.$$

Using the triangle inequality and $\|\sin(\Omega x)\| = \|\cos(\Omega x)\| = 1$ we have

$$\|E\psi\| \leq |\Omega| \|\psi\| + \|\partial_x \psi\|. \quad (6.6)$$

Thus we have effectively ‘commuted out’ the bounded spatially periodic component of E , and are left with only spatially invariant operators on the right of (6.6). Hence, after applying a Fourier transformation to the right side of (6.6), a sufficient condition for (6.5) to hold is that

$$|\Omega| + |k| \leq a + b|(k^2 - \varkappa^2)^2 + c|, \quad k \in \mathbb{R},$$

which can be shown to be satisfied for large enough $a > |\Omega|$ and $b > 0$. Using Theorem 21, A is sectorial and closed for small enough $|\epsilon|$. ■

Remark 23 The above example makes clear the notion of E being ‘weaker’ than A° that we mentioned at the beginning of this section. If in Example 8 we had $B^\circ = \partial_x^\nu$ and $C^\circ = \partial_x^\mu$ and $\nu + \mu = 5$, then E would contain a 5th order derivative, whereas the highest order of ∂_x in A° is 4. This would mean that (6.5) can not be satisfied for any choice of a and b . ■

6.5 Conditions for Infinitesimal Generator to have Spectrum in \mathbb{C}^-

The final step in establishing exponential stability is to show that $\Sigma(A) \subset \mathbb{C}^-$. Unfortunately it is in general very difficult to find the spectrum of an infinite-dimensional operator. Thus we proceed as follows. We consider the (block) diagonal operators \mathcal{A}_θ° , $\theta \in [0, \Omega)$. This allows us to extend Geršgorin-type methods (existing for finite-dimensional matrices) to find bounds on the location of $\Sigma(\mathcal{A}_\theta)$, $\mathcal{A}_\theta = \mathcal{A}_\theta^\circ + \epsilon \mathcal{E}_\theta$. In turn, we use this to find conditions under which $\Sigma(\mathcal{A}_\theta) \subset \mathbb{C}^-$, and thus $\Sigma(A) \subset \mathbb{C}^-$.

In locating the spectrum of a finite-dimensional matrix $T \in \mathbb{C}^{q \times q}$, the theory of Geršgorin circles [42] provides us with a region of the complex plane that contains the eigenvalues of T . This region is composed of the union of q disks, the centers of which are the diagonal elements of T , and their radii depend on the magnitude of the off-diagonal elements [42]. This theory has also been extended to the case of finite-dimensional block matrices (i.e., matrices whose elements are themselves matrices) in [43]. Next, we further extend this theory to include bi-infinite (block) matrices \mathcal{A}_θ .

For the operator $A = A^\circ + \epsilon E$, take \mathfrak{B}_k to be the set of complex numbers z that satisfy

$$\sigma_{\min}(zI - A_0(k)) \leq |\epsilon| (\|A_{-1}(k)\| + \|A_1(k)\|), \quad (6.7)$$

where $\sigma_{\min}(zI - A_0(k))$ denotes the smallest singular value of the matrix $zI - A_0(k)$.

Lemma 22 For every θ we have $\Sigma(\mathcal{A}_\theta) \subseteq \mathfrak{S}_\theta$, where

$$\mathfrak{S}_\theta = \overline{\bigcup_{n \in \mathbb{Z}} \mathfrak{B}_{\theta_n}}.$$

Proof: See Appendix. ■

Example 9 Let us consider the periodic PDE [34]

$$\begin{aligned} \partial_t \psi &= -(\partial_x^2 + \varkappa^2)^2 \psi - c\psi + \epsilon \cos(\Omega x) \partial_x \psi + u \\ y &= \psi. \end{aligned} \tag{6.8}$$

where $\psi \in \mathcal{D}$, and \mathcal{D} defined as in (6.3). Comparing (6.8) and (5.1) we have

$$A_0(k) = -(k^2 - \varkappa^2)^2 - c, \quad B^o(k) = 1, \quad C^o(k) = jk, \quad B(k) = 1, \quad C(k) = 1, \quad L = \frac{1}{2}.$$

From (5.4), $A_1(k) = \frac{j}{2}(k - \Omega)$, $A_{-1}(k) = \frac{j}{2}(k + \Omega)$, and thus $\|A_{-1}(k)\| + \|A_1(k)\| = \frac{1}{2}(|k - \Omega| + |k + \Omega|)$. Hence (6.7) leads to

$$\sigma_{\min}(zI - A_0(k)) = |zI - A_0(k)| \leq \frac{|\epsilon|}{2} (|k - \Omega| + |k + \Omega|) = \begin{cases} \Omega |\epsilon| & |k| \leq \Omega \\ |k| |\epsilon| & |k| \geq \Omega \end{cases},$$

which means that the set \mathfrak{S}_θ is composed of the union of disks with centers at $A_0(\theta_n)$ and radii $\frac{|\epsilon|}{2}(|\theta_n - \Omega| + |\theta_n + \Omega|)$. This is nothing but an extension of the classical Geršgorin disks to bi-infinite matrices. Figure 6.2 (top & center) show \mathfrak{S}_θ in the complex-plane \times spatial-frequency space and in \mathbb{C} respectively.¹ ■

Remark 24 The set

$$\begin{aligned} \Sigma_\varepsilon(T) &:= \{z \in \mathbb{C} \mid \sigma_{\min}(zI - T) \leq \varepsilon\} \\ &= \{z \in \mathbb{C} \mid \|(zI - T)\varphi\| \leq \varepsilon \text{ for some } \|\varphi\| = 1\} \\ &= \{z \in \mathbb{C} \mid z \in \Sigma_p(T + Z) \text{ for some } \|Z\| \leq \varepsilon\} \end{aligned} \tag{6.9}$$

is called the ε -pseudospectrum of the matrix T [44]. Clearly $\Sigma_{\varepsilon'}(T) \subseteq \Sigma_\varepsilon(T)$ if $\varepsilon' \leq \varepsilon$, and $\Sigma_\varepsilon(T) = \Sigma_p(T)$ for $\varepsilon = 0$. The pseudospectrum is composed of small sets around the eigenvalues of T . For instance if T has simple eigenvalues, then for small enough values of ε the pseudospectrum consists of disjoint compact and convex neighborhoods of each eigenvalue [45]. ■

¹We would like to point out that Figure 6.2 (top) is technically incorrect; once the spatially invariant system is perturbed by a spatially periodic perturbation it is no longer spatially invariant and thus can not be represented by a Fourier symbol. Hence its spectrum can no longer be demonstrated in the complex-plane \times spatial-frequency space. Figure 6.2 (center) demonstrates the correct representation of the Geršgorin disks for \mathcal{A}_θ .

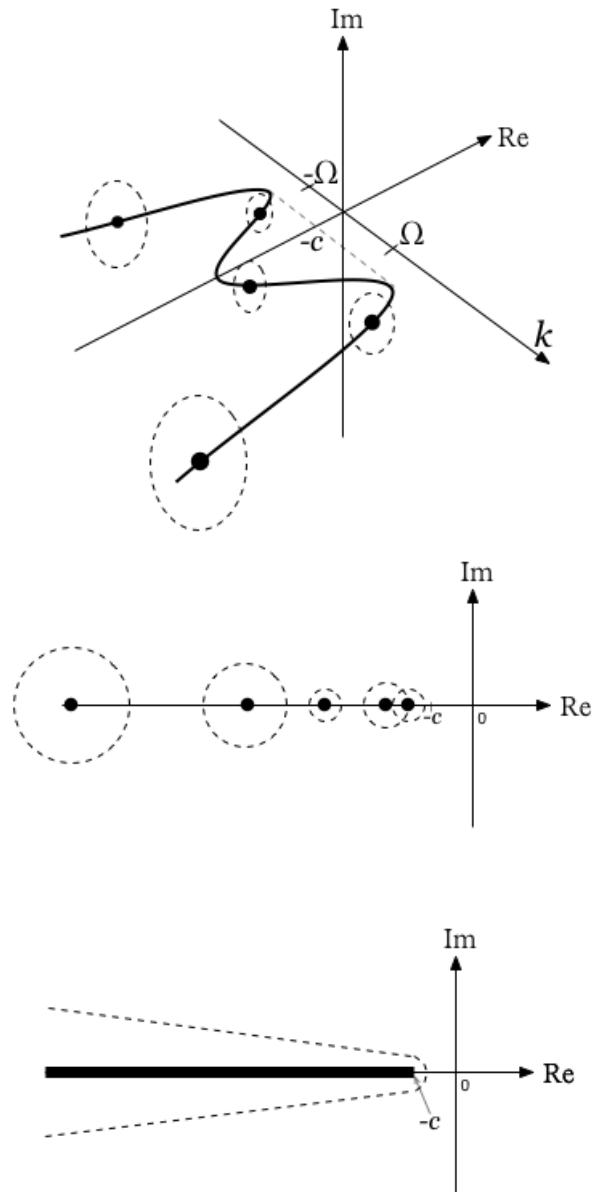


Figure 6.2: Top: The \mathfrak{B}_{θ_n} regions viewed in the ‘complex-plane \times spatial-frequency’ space (the disks are parallel to the complex plane). Center: $\Sigma(\mathcal{A}_\theta)$ is contained inside the union of the regions \mathfrak{B}_{θ_n} . Bottom: The bold line shows $\Sigma(A^\circ)$ and the dotted region contains $\Sigma(A)$, $A = A^\circ + \epsilon E$.

Remark 25 Comparing (6.9) and the definition of \mathfrak{B}_k in (6.7), it is clear that $\mathfrak{B}_k = \Sigma_\varepsilon(A_0(k))$ with $\varepsilon = |\varepsilon| (\|A_{-1}(k)\| + \|A_1(k)\|)$. Thus for every $k \in \mathbb{R}$, (6.7) defines a closed region of \mathbb{C} that includes the eigenvalues of $A_0(k)$. ■

We now employ Lemma 22 to determine whether $\Sigma(A)$ resides completely inside \mathbb{C}^- , as needed to assess system stability. Take \mathfrak{D}_ε to be the closed disk of radius ε and center at the origin, and \mathfrak{B}_k to be the region described by (6.7). Define the sum of sets by $\mathfrak{U}_1 + \mathfrak{U}_2 = \{z \mid z = z_1 + z_2, z_1 \in \mathfrak{U}_1, z_2 \in \mathfrak{U}_2\}$. Also, for every $k \in \mathbb{R}$ let $\lambda_{\max}(k)$ represent the eigenvalue of $A_0(k)$ with the maximum real part, and let $\kappa(k)$ be defined as in Theorem 20.

Theorem 23 For every k , \mathfrak{B}_k is contained inside $\Sigma_p(A_0(k)) + \mathfrak{D}_{r(k)}$ with

$$r(k) = |\varepsilon| (\|A_{-1}(k)\| + \|A_1(k)\|) \kappa(k).$$

In particular, if $\Sigma(A^\circ) \subset \mathbb{C}^-$ and

$$r(k) < |\operatorname{Re}(\lambda_{\max}(k))| + \beta \tag{6.10}$$

for every $k \in \mathbb{R}$ and some $\beta < 0$ independent of k , then $\Sigma(A) \subset \mathbb{C}^-$.

Proof: See Appendix. ■

Example 10 Once again we use the scalar system of Example 9. $\kappa(k) = 1$ since $A_0(k)$ is scalar, $|\operatorname{Re}(\lambda_{\max}(k))| = |(k^2 - \varkappa^2)^2 + c|$, and

$$\|A_{-1}(k)\| + \|A_1(k)\| = \frac{1}{2} (|k - \Omega| + |k + \Omega|).$$

Thus condition (6.10) becomes

$$\frac{|\varepsilon|}{2} (|k - \Omega| + |k + \Omega|) < |(k^2 - \varkappa^2)^2 + c| + \beta.$$

If this condition is satisfied for some $\beta < 0$, the dotted region in Figure 6.2 (bottom) will remain inside \mathbb{C}^- and thus $\Sigma(A) \subset \mathbb{C}^-$. ■

6.6 Appendix to Chapter 6

Proof of Theorem 20

It is shown in [46] that a sufficient condition for A° to be sectorial is that $\rho(A^\circ)$ contain some right half plane $\{z \in \mathbb{C} \mid \operatorname{Re}(z) \geq \mu\}$, and

$$\|z(zI - A^\circ)^{-1}\| \leq M \quad \text{for } \operatorname{Re}(z) \geq \mu,$$

for some $\mu \geq 0$ and $M \geq 1$.

Now since $A_0(k) \in \mathbb{C}^{q \times q}$ is diagonalizable for every k , there exists a matrix $U(k)$ such that $A_0(k) = U(k) \Lambda(k) U^{-1}(k)$ with $\Lambda(k)$ a diagonal matrix. Let $\lambda_i(k)$, $i = 1, \dots, q$ denote the diagonal elements of $\Lambda(k)$. Clearly these are also the eigenvalues of $A_0(k)$. Thus we have

$$\begin{aligned} \|z(zI - A^0)^{-1}\| &\leq \sup_{k \in \mathbb{R}} \left(\|z(zI - A_0(k))^{-1}\| \right) \\ &\leq \sup_{k \in \mathbb{R}} \left(\|U(k)\| \|U^{-1}(k)\| \|z(zI - \Lambda(k))^{-1}\| \right) \\ &= \sup_{k \in \mathbb{R}} \left(\kappa(k) \frac{|z|}{\text{dist}[z, \Sigma_p(A_0(k))]} \right) \\ &\leq \kappa_{\max} \sup_{k \in \mathbb{R}} \left(\frac{|z|}{\text{dist}[z, \Sigma_p(A_0(k))]} \right), \end{aligned}$$

where $\kappa_{\max} := \sup_{k \in \mathbb{R}} \kappa(k)$.

Let us now choose the positive scalar $M' = (1 + \kappa_{\max})M$, $M > 1$, and consider for a given k the region of the complex plane where

$$\kappa_{\max} \frac{|z|}{\text{dist}[z, \Sigma_p(A_0(k))]} \geq M'.$$

This region (which contains the eigenvalues $\lambda_i(k)$) is contained inside the union of the circles

$$\kappa_{\max} \frac{|z|}{|z - \lambda_i(k)|} \geq M', \quad i = 1, \dots, q,$$

which are themselves contained inside the larger circles

$$|z - \lambda_i(k)| \leq \frac{|\lambda_i(k)|}{M}, \quad i = 1, \dots, q. \quad (6.11)$$

Notice that (6.11) describes circles whose radii increase like $|\lambda_i(k)|/M$, $M > 1$, as their centers $\lambda_i(k)$ become distant from the origin. Clearly a sufficient condition for these circles to belong to some open half plane $\{z \in \mathbb{C} \mid \text{Re}(z) < \mu\}$ for all $k \in \mathbb{R}$ and large enough M is that $\Sigma_p(A_0(k))$, $k \in \mathbb{R}$, reside outside some sector $|\arg(z - \alpha)| \leq \frac{\pi}{2} + \gamma$, $\gamma > 0$, of the complex plane.

Finally, if the circles (6.11) are contained in some open half plane $\{z \in \mathbb{C} \mid \text{Re}(z) < \mu\}$ for all $k \in \mathbb{R}$, then for $\text{Re}(z) \geq \mu$, $z \in \rho(A_0(k))$ and we have

$$\kappa_{\max} \sup_{k \in \mathbb{R}} \left(\frac{|z|}{\text{dist}[z, \Sigma_p(A_0(k))]} \right) \leq M$$

and thus $\|z(zI - A^0)^{-1}\| \leq M$ for $\text{Re}(z) \geq \mu$.

Proof of Lemma 22

We use $\Pi_N T \Pi_N$ to denote the $(2N + 1) \times (2N + 1)$ [block] truncation of an operator T on ℓ^2 , as defined in Section 3.5. We now form the finite-dimensional matrix $\Pi_N \mathcal{A}_\theta \Pi_N|_{\Pi_N \ell^2}$ by restricting $\Pi_N \mathcal{A}_\theta \Pi_N$ to the finite-dimensional space $\Pi_N \ell^2$. Clearly $\Pi_N \mathcal{A}_\theta \Pi_N|_{\Pi_N \ell^2}$ has pure point spectrum. Hence using a generalized form of the Geršgorin Circle Theorem [43] for finite-dimensional (block) matrices, we conclude that

$$\Sigma(\Pi_N \mathcal{A}_\theta \Pi_N|_{\Pi_N \ell^2}) \subset \bigcup_{|n| \leq N} \mathfrak{B}_{\theta_n} \subseteq \overline{\bigcup_{n \in \mathbb{Z}} \mathfrak{B}_{\theta_n}}$$

where \mathfrak{B}_{θ_n} are regions of \mathbb{C} defined by (6.7). Since this holds for all $N \geq 0$, we have $\Sigma(\mathcal{A}_\theta) \subseteq \mathfrak{S}_\theta$.

Proof of Theorem 23

If $U(k)$ diagonalizes $A_0(k)$, i.e.

$$A_0(k) = U(k) \Lambda(k) U^{-1}(k),$$

and $\kappa(k) = \|U(k)\| \|U^{-1}(k)\|$ denotes the condition number of $U(k)$, then from [47] the pseudospectrum of $A_0(k)$ satisfies

$$\Sigma_p(A_0(k)) + \mathfrak{D}_\varepsilon \subseteq \Sigma_\varepsilon(A_0(k)) \subseteq \Sigma_p(A_0(k)) + \mathfrak{D}_{\varepsilon \kappa(k)} \quad (6.12)$$

for all $\varepsilon \geq 0$. Thus the first statement of the Theorem follows immediately from (6.12) and the fact that $\mathfrak{B}_k = \Sigma_\varepsilon(A_0(k))$ with $\varepsilon = |\varepsilon| (\|A_{-1}(k)\| + \|A_1(k)\|)$ [see Remark 25]. To prove the second statement, let \mathbb{C}_β^- denote all complex numbers with real part less than $\beta \in \mathbb{R}$. It follows from $\Sigma(A^\theta) \subset \mathbb{C}^-$ that $\Sigma(\mathcal{A}_\theta^0) \subset \mathbb{C}^-$ for every θ . If (6.10) holds then

$$\mathfrak{B}_{\theta_n} \subseteq \Sigma_p(A_0(\theta_n)) + \mathfrak{D}_{r(\theta_n)} \subset \mathbb{C}_\beta^-$$

for every $n \in \mathbb{Z}$, and from Lemma 22 we have $\Sigma(\mathcal{A}_\theta) \subseteq \mathfrak{S}_\theta = \overline{\bigcup_{n \in \mathbb{Z}} \mathfrak{B}_{\theta_n}} \subset \mathbb{C}_{\beta'}^-$ for some $\beta < \beta' < 0$ and every θ . Thus $\Sigma(A) \subset \mathbb{C}^-$.

6.7 Summary

We study the problem of checking the exponential stability of a spatially periodic system. To this end, we first find sufficient conditions under which A is a sectorial operator and thus the semigroup it generates satisfies the spectrum-determined growth condition. We then find sufficient conditions for A to have \mathbb{C}^- spectrum.

We do this by extending the notion of Geršgorin circles to bi-infinite (block) matrices.

Chapter 7

Conclusions and Future Directions

We are usually convinced more easily by reasons we have found ourselves than by those which have occurred to others.

B. Pascal

We use spatial-frequency lifting to represent spatially periodic systems as infinite-dimensional multivariable systems. This allows us to extend many existing tools from linear systems theory to such systems, such as the Nyquist stability criterion, \mathcal{H}^2 and \mathcal{H}^∞ norms, and Geršgorin-like spectral bounds.

The infinite dimensionality of these problems can make numerical computations expensive. Hence we employ a variety of perturbation methods, which essentially helps remove this infinite dimensionality at the cost of conservative results or results that are only accurate within certain parameter domains.

Future work in the stability analysis of spatially periodic systems would include finding larger classes of semigroups for which the spectrum-determined growth condition is satisfied. Also, one would like to characterize all spatially periodic operators that would stabilize a given unstable spatially periodic system.

Future research in the perturbation analysis of spatially periodic systems would include an exact (analytical) characterization of the spatial-frequencies for which the \mathcal{H}^2 -norm of the system is most increased/decreased for the general case of a matrix-valued Fourier symbol $A_0(\cdot)$. The perturbation methods presented in this work could also be generalized to bi-infinite Sylvester equations which arise frequently in problems of fluid mechanics. Finally, the developed tools can be applied to problems of practical significance, particularly in the area of fluid mechanics and sensor-less flow control.

Bibliography

- [1] J. L. Lions, *Optimal Control of Systems Governed by Partial Differential Equations*. Springer-Verlag, 1971.
- [2] A. Bensoussan, G. D. Prato, M. C. Delfour, and S. K. Mitter, *Representation and Control of Infinite Dimensional Systems*. Boston: Birkhauser, 1992.
- [3] R. F. Curtain and H. J. Zwart, *An Introduction to Infinite-Dimensional Linear Systems Theory*. New York: Springer-Verlag, 1995.
- [4] S. P. Banks, *State-Space and Frequency-Domain Methods in the Control of Distributed Parameter Systems*. London, UK: Peter Peregrinus Ltd., 1983.
- [5] B. Bamieh, F. Paganini, and M. A. Dahleh, “Distributed control of spatially invariant systems,” *IEEE Transactions on Automatic Control*, vol. 47, pp. 1091–1107, July 2002.
- [6] S. M. Meerkov, “Principle of vibrational control: Theory and applications,” *IEEE Transactions on Automatic Control*, vol. 25, pp. 755–762, August 1980.
- [7] V. Arnold, *Mathematical Methods of Classical Mechanics*. Springer-Verlag, 1989.
- [8] N. Wereley, *Analysis and Control of Linear Periodically Time Varying Systems*. PhD thesis, Dept. of Aeronautics and Astronautics, MIT, 1991.
- [9] M. Araki, Y. Ito, and T. Hagiwara, “Frequency response of sampled-data systems,” *Automatica*, vol. 32, no. 4, pp. 483–497, 1996.
- [10] G. Dullerud, *Control of Uncertain Sampled-Data Systems*. Birkhauser, 1996.
- [11] E. Moellerstedt, *Dynamic Analysis of Harmonics in Electrical Systems*. PhD Thesis, Dept. Automatic Control, Lund Institute of Technology, 2000.
- [12] W. A. Gardner, *Introduction to Random Processes with Applications to Signals and Systems*. McGraw-Hill, 1990.

- [13] A. Bensoussan, J. Lions, and G. Papanicolaou, *Asymptotic Analysis for Periodic Structures*. North-Holland, 1978.
- [14] J. Zabczyk, “A note on C_0 -semigroups,” *Bull. Acad. Polon. Sci.*, vol. 23, pp. 895–898, 1975.
- [15] M. Renardy, “On the linear stability of hyperbolic PDEs and viscoelastic flows,” *Z. angew. Math. Phys. (ZAMP)*, vol. 45, pp. 854–865, 1994.
- [16] Z. Luo, B. Guo, and O. Morgul, *Stability and Stabilization of Infinite Dimensional Systems with Applications*. Springer-Verlag, 1999.
- [17] T. Kato, *Perturbation Theory for Linear Operators*. Springer-Verlag, 1995.
- [18] E. Hille and R. S. Phillips, *Functional Analysis and Semigroups*. American Mathematical Society, 1957.
- [19] M. Miklavčič, *Applied Functional Analysis and Partial Differential Equations*. World Scientific, 1998.
- [20] I. C. Gohberg and M. G. Krein, *Introduction to the Theory of Linear Non-selfadjoint Operators*. American Mathematical Society, 1969.
- [21] W. Rudin, *Fourier Analysis on Groups*. Wiley Interscience, 1962.
- [22] M. R. Jovanovic, B. Bamieh, and M. Grebeck, “Parametric resonance in spatially distributed systems,” in *Proceedings of the 2003 American Control Conference*, pp. 119–124, 2003.
- [23] M. R. Jovanović, *Modeling, Analysis, and Control of Spatially Distributed Systems*. PhD thesis, Ph.D. dissertation, University of California, Santa Barbara, 2004.
- [24] E. Wong and B. Hajek, *Stochastic Processes in Engineering Systems*. Springer-Verlag, 1985.
- [25] W. A. Gardner, “Exploitation of spectral redundancy in cyclostationary signals,” *IEEE SP Magazine*, pp. 14–36, 1991.
- [26] M. Fardad and B. Bamieh, “A perturbation analysis of parametric resonance and periodic control in spatially distributed systems,” in *Proceedings of the 43rd IEEE Conference on Decision and Control*, pp. 3786–3791, 2004.
- [27] K. Zhou, J. Doyle, and K. Glover, *Robust and Optimal Control*. Prentice Hall, 1996.
- [28] B. Bamieh and J. Pearson, “The H^2 problem for sampled-data systems,” *Systems and Control Letters*, vol. 19, no. 1, pp. 1–12, 1992.

- [29] E. VanMarcke, *Random Fields: Analysis and Synthesis*. MIT Press, 1988.
- [30] C. R. Doering, “Nonlinear parabolic stochastic differential equations with additive colored noise on $\mathbb{R}^d \times \mathbb{R}_+$: A regulated stochastic quantization,” *Commun. Math. Phys.*, vol. 109, pp. 537–561, 1987.
- [31] J. B. Walsh, “An introduction to stochastic partial differential equations,” in *École d’Été de Probabilités de Saint-Flour XIV (Lecture Notes in Mathematics 1180)*, pp. 265–439, Springer, 1984.
- [32] J. B. Conway, *A Course in Functional Analysis*. Springer-Verlag, 1990.
- [33] I. Gohberg, S. Goldberg, and M. A. Kaashoek, *Classes of Linear Operators; Vol I*. Birkhauser, 1990.
- [34] M. Fardad, M. R. Jovanović, and B. Bamieh, “Frequency analysis and norms of distributed spatially periodic systems,” *submitted to IEEE Transactions on Automatic Control*. Also available as technical report at <http://ccec.mee.ucsb.edu/Author/FARDAD-M.html>.
- [35] I. M. Gel’fand and G. E. Shilov, *Generalized Functions, Vol I: Properties and Operations*. Academic Press, 1964.
- [36] M. Reed and B. Simon, *Methods of Mathematical Physics, Vol I: Functional Analysis*. Academic Press, 1978.
- [37] A. Bottcher and B. Silbermann, *Analysis of Toeplitz Operators*. Springer-Verlag, 1990.
- [38] M. Fardad and B. Bamieh, “An extension of the argument principle and nyquist criterion to systems with unbounded generators,” *submitted to IEEE Transactions on Automatic Control*. Also available as technical report at <http://ccec.mee.ucsb.edu/Author/FARDAD-M.html>.
- [39] H. Baumgartel, *Analytic Perturbation Theory for Matrices and Operators*. Birkhauser, 1985.
- [40] C. Desoer and Y. Wang, “On the generalized nyquist stability criterion,” *IEEE Transactions on Automatic Control*, vol. 25, pp. 187–196, April 1980.
- [41] M. Reed and B. Simon, *Methods of Mathematical Physics, Vol IV: Analysis of Operators*. Academic Press, 1978.
- [42] R. Horn and C. R. Johnson, *Matrix Analysis*. Cambridge University Press, 1985.

- [43] D. G. Feingold and R. S. Varga, “Block diagonally dominant matrices and generalizations of the Gerschgorin circle theorem,” *Pacific J. Math.*, vol. 12, pp. 1241–1250, 1962.
- [44] L. N. Trefethen, “Pseudospectra of matrices,” in *Numerical Analysis 1991 (Pitman Research Notes in Mathematics Series, vol. 260)*, pp. 234–266, 1992.
- [45] J. V. Burke, A. S. Lewis, and M. L. Overton, “Optimization and pseudospectra, with applications to robust stability,” *SIAM J. Matrix Anal. Appl.*, vol. 25, no. 1, pp. 80–104, 2003.
- [46] L. Lorenzi, A. Lunardi, G. Metafune, and D. Pallara, *Analytic Semigroups and Reaction-Diffusion Problems*. Internet Seminar, 2005. http://www.fa.uni-tuebingen.de/teaching/isem/2004_05/phase1.
- [47] S. C. Reddy, P. J. Schmid, and D. S. Henningson, “Pseudospectra of the Orr-Sommerfeld operator,” *SIAM J. Appl. Math.*, vol. 53, no. 1, pp. 15–47, 1993.